Synergic green technologies for treatment of hexavalent chromium polluted waters
Project PNII-RU-TE-2014-4-0508
No. 129/1/10/2015

Scientific report

Phase 2: 01.01.2016 – 31.12.2016

Objective 1. Ensuring the necessary conditions for the research activities
Activities: The needed existent materials have been identified and prepared. Other necessary but not existent materials have been purchased (UV-VIS spectrofotometer, pH-meter, electrodes, analitical balance, laboratory furnace, laptop, desktop, micropipette). The analytical methods have been selected and prepared in order to support the research activities.

Objective 2. Investigation of the effect of sand co-presence on Cr(VI) removal with Fe^0
Activities: Column treatability experiments for Cr(VI) removal with Fe^0 in the co-presence of sand

2.1. Materials and methods

Commercially available Fe^0 from Alfa Aesar (≥ 99%, 1-2 mm) and Merck (≥ 99%, 10 μm) was used in this assay as received. Sand obtained from a local source was sieved to obtain the following grain sizes: 0.1-0.5 mm, 0.5-1.25 mm and 1.25-2 mm; the sand was then washed with distilled water and dried. The laboratory apparatus used for the flow-through column experiments consisted in polyethylene columns (inner diameter: 2 cm; height: 11 cm), an Ismatec IP08 peristaltic pump and a tank with a capacity of 60 L (Fig. 1). The columns were packed either with bare Fe^0, or with a mixture of Fe^0 + sand having various volumic ratios. Below and above the filling was a layer of 5 cm^3 sand with d = 1.25-2 mm. Cr(VI) stock solution (10 g/L) was prepared by dissolving 28.29 g $K_2Cr_2O_7$ in 1000 mL of distilled deionized water. Working solutions of the desired initial Cr(VI) concentrations (5 and 10 mg/L) were then prepared by diluting the stock solution with tap water, in order to simulate a case of natural water pollution. These concentrations were selected because they are within the range of relevant concentrations for Cr(VI) polluted groundwaters (Flury et al., 2009; Wilkin et al., 2005). The pH was adjusted to 6.9 by small addition of concentrated H_2SO_4 and measured in samples collected from column influent and effluent using an Inolab 7320 pH-meter. The Cr(VI) working solution was passed through the column, at room temperature, from the bottom to the top, and effluent samples were withdrawn at regular time intervals for the analysis of following parameters: Cr(total), Cr(VI), Cr(III), Fe(total), Fe(II), Fe(III) and pH. Chromium and iron dissolved species were determined by spectrophotometric methods, using a Specord 200 Plus spectrophotometer (Standard Methods, 1995). Cr(VI) concentration was determined by the 1,5-diphenylcarbazide method, at 540 nm. Cr(total) was analyzed by oxidizing any Cr(III) with $KMnO_4$, followed by analysis as Cr(VI). Cr(III) was determined from the difference between Cr(total) and Cr(VI). Fe(II) concentrations were determined by the 1,10-ortophenanthroline method, at 510 nm; Fe(total) was determined by reduction of any Fe(III) to Fe(II) with hydroxylamine hydrochloride followed by analysis as Fe(II). Fe(III) was determined from the difference between Fe(tot) and

Fe(II). The calibration curves of Cr(VI) and Fe(II), and the equations obtained by linear regression, are depicted in Figs.2 and 3.

Fig.1. Experimental setup for column studies

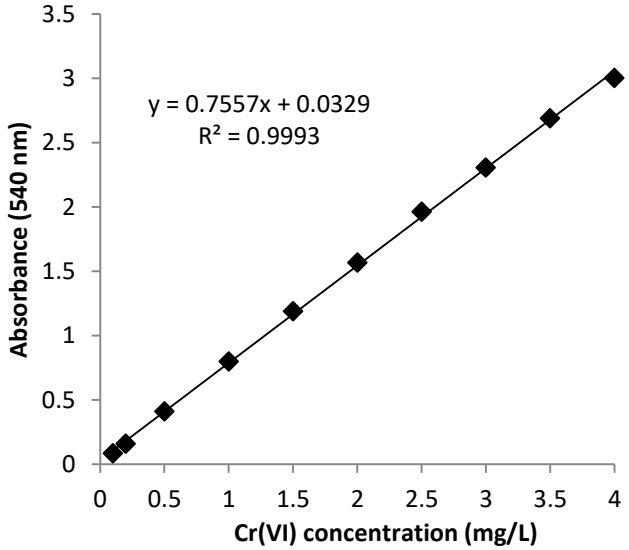

Fig.2. Cr(VI) calibration curve

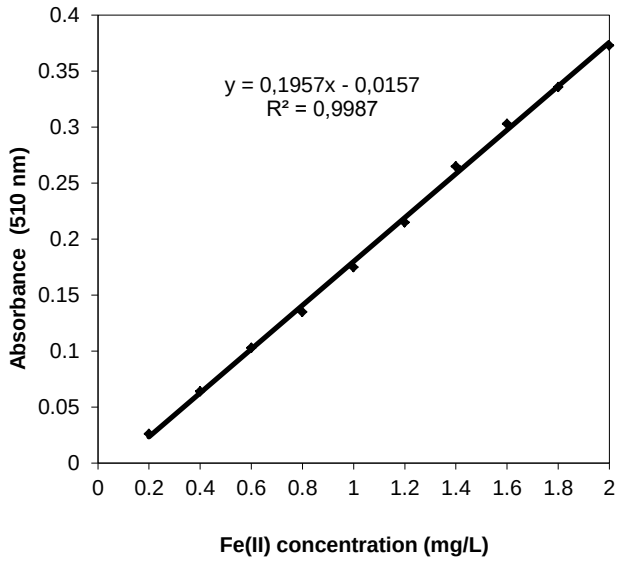

Fig.3. Fe(II) calibration curve

2.2. Results and discussion

2.2.1 The effect of Cr(VI) concentration

In order to study the effect of Cr(VI) concentration, we have conducted experiments using Fe^0 with size 1-2 mm and solutions with Cr(VI) concentration of 5 and 10 mg/L. The experimental conditions are summarized in Tables 1 and 2.

Table 1. Experiments carried out with solution Cr(VI) 10 mg/L

Column	Column filling				Cr(VI) solution		
	Fe^0 1-2 mm		Sand 0.5-1.25 mm		Concentration (mg/L)	pH	Flow (mL/h)
	(% vol.)	(cm^3)	(% vol.)	(cm^3)			
1	20	10	80	40	10	6.9	30
2	40	20	60	30	10	6.9	30
3	50	25	50	25	10	6.9	30
4	60	30	40	20	10	6.9	30
5	80	40	20	10	10	6.9	30
6	100	50	0	0	10	6.9	30
7	0	0	100	50	10	6.9	30

Table 2. Experiments carried out with solution Cr(VI) 5 mg/L

Column	Column filling				Cr(VI) solution		
	Fe^0 1-2 mm		Sand 0.5-1.25 mm		Concentration (mg/L)	pH	Flow (mL/h)
	(% vol.)	(cm^3)	(% vol.)	(cm^3)			
1	20	10	80	40	5	6.9	30
2	40	20	60	30	5	6.9	30
3	50	25	50	25	5	6.9	30
4	60	30	40	20	5	6.9	30
5	80	40	20	10	5	6.9	30
6	100	50	0	0	5	6.9	30
7	0	0	100	50	5	6.9	30

Fig.4 shows the evolution of Cr(VI) concentration in the effluent of the columns fed with solution Cr(VI) 10 mg/L. It can be seen that the smaller the percentage of Fe^0 in the column filling, the faster the appearance of Cr(VI) in column effluent. Column breakthrough occurred after one day in column with 20% Fe^0 and after 3 days in column with 100% Fe^0. During the course of the experiment with solution Cr(VI) 10 mg/L, no species of Cr(III), Fe(II) or Fe(III) were identified in the columns effluent. This can be explained by their precipitation inside the column filling, due to the high pH of the solution of Cr (VI) after it has passed through the columns (Fig. 5). The brown precipitate deposited inside the column filling consist of simple and/or mixed hydroxides and oxyhydroxides of Fe(III) and Cr(III), which precipitates at pH > 4, and which, in time, can be converted into oxides (Gheju, 2011):

$$Cr^{3+} + 3HO^- \rightarrow Cr(OH)_3 \quad (1)$$

$$Fe^{2+} + 2HO^- \rightarrow Fe(OH)_2 \quad (2)$$

$$4Fe^{2+} + O_2 + 2H_2O \rightarrow 4Fe^{3+} + 4OH^- \quad (3)$$

$$Fe^{2+} + 3HO^- \rightarrow Fe(OH)_3 \quad (4)$$

$$3Fe^{2+} + 4H_2O \rightarrow Fe_3O_4 + H_2 + 6H^+ \quad (5)$$

$$3Fe(OH)_2 \rightarrow Fe_3O_4 + H_2 + 2H_2O \quad (6)$$

$$Fe(OH)_3 \rightarrow FeOOH + H_2O \quad (7)$$

$$3FeOOH + H^+ \rightarrow Fe_3O_4 + 2H_2O \quad (8)$$

$$(1-x)Fe^{3+} + (x)Cr^{3+} + 3H_2O \rightarrow Cr_xFe_{1-x}(OH)_3 + 3H^+ \quad (9)$$

$$(1-x)Fe^{3+} + (x)Cr^{3+} + 2H_2O \rightarrow Cr_xFe_{1-x}(OOH) + 3H^+ \quad (10)$$

where x can take values from 0 to 1.

From Fig.5 it is noted that the pH of the effluent increases significantly after the first days, and then decreases gradually until the end of experiment. It is known that corrosion of Fe^0 in the co-presence of oxidants like Cr(VI), O_2 or H_2O takes place with consumption of protons and generation of hydroxyl ions, according to Eqs.11-14 (Gheju, 2011):

$$3Fe^0 + Cr_2O_7^{2-} + 14H^+ \rightarrow 3Fe^{2+} + 2Cr^{3+} + 7H_2O \quad (11)$$

$$6Fe^{2+} + Cr_2O_7^{2-} + 14H^+ \rightarrow 6Fe^{3+} + 2Cr^{3+} + 7H_2O \quad (12)$$

$$2Fe^0 + O_2 + 2H_2O \rightarrow 2Fe^{2+} + 4HO^- \quad (13)$$

$$Fe^0 + 2H_2O \rightarrow Fe^{2+} + H_2 + 2HO^- \quad (14)$$

Therefore, it is expected that, in a first phase, the effluent pH will increase. The subsequent decrease in pH is due to reduction in intensity of the Cr(VI) reduction and Fe^0 corrosion, as a result of precipitation on the surface of Fe^0 of the above-mentioned solid mineral phases.

Fig.6 depicts the evolution of Cr(VI) concentration in the effluent of columns fed with solution Cr(VI) 5 mg/L. Just like for the experiments with solution Cr(VI) 10 mg/L, also in this case the column breakthrough occurs later in columns with higher percentage of Fe^0 than in columns with lower percentage of Fe^0. Column breakthrough occurred after two days in the column with 20% Fe^0 and after 262 days the column with 100% Fe^0. In the same time, column breakthrough occurred much earlier in experiments with solution Cr(VI) 10 mg/L than in experiments with solution Cr(VI) 5 mg/L. Therefore, by decreasing the concentration of the influent solution from 10 to 5 mg/L, the operational duration of columns increased, especially for the columns with high Fe^0 percentages. Unlike the situation when columns were loaded with solution Cr(VI) 10 mg/L, in column experiments carried out with solution Cr(VI) 5 mg/L Cr(III), Fe(II) and Fe(III) were detected in column effluent. This can be explained by the fact that, when using solution Cr(VI) 5 mg/L, the increase in effluent pH was not as great as in the case of columns that have been fed with solution Cr(VI) 10 mg/L, as shown in Figure 12. Figs. 6 and 7 indicate that Cr(III) breakthrough occurred before the breakthrough of Cr(VI). Fig. 7 also shows that, after the breakthrough, concentration of Cr(III) increased up to a maximum value, after which decreased until totally disappeared from the column effluent. The highest value of Cr(III) concentration was noticed in the effluent of the column filled with 50% Fe^0.

The evolution of Fe species concentration in the effluent of columns fed with solution Cr(VI) 5 mg/L is presented in Figs. 9-11. It can be seen that highest Fe concentrations were detected as Fe(II), at the beginning of experiments; subsequently, Fe(II) concentrations continuously decreased in column effluent, until Fe(II) was not any more detected. In turn, the occurrence of Fe(III) in column effluent was noticed until the end of the experiments. The highest Fe(II) concentration, observed during the first days of the experiment, is attributable to Eq. 11, which generates Fe(II). At the beginning of experiments, the main path of Cr(VI) removal was the heterogeneous reduction of Cr(VI) at the surface of Fe^0 (Eq.11), while the homogeneous reduction with Fe(II) (Eq.12) was less important. This can explain why Fe(II) generated during the first days of the experiment was consumed only in a limited extent inside the column. However, in time, due to passivation of Fe^0 surface with precipitates, Eq.11 is increasingly inhibited and lower amounts of Fe(II) are generated. In the same time, direct reduction of Cr(VI) at the surface of Fe^0 is also increasingly hindered, while the indirect reduction with Fe(II) becomes more important. This explains the decrease in time of Fe(II) concentration in column effluent until its total disappearance, and, in the same time, the occurrence of Fe(III) in column effluent.

Fig. 13 presents the evolution of Cr(VI) breakthrough in the effluent of the columns fed with solution Cr(VI) 5 mg/L, as a function of column filling composition: bare Fe^0 or 50 cm^3 mixture Fe^0 + sand. It is clearly shown that, for the same volume of Fe^0, column breakthrough occurred later when the filling was a mixture comprised of Fe^0 + sand, than when the column was packed only with Fe^0, which has a positive influence on the efficiency of Cr(VI) removal inside the columns.

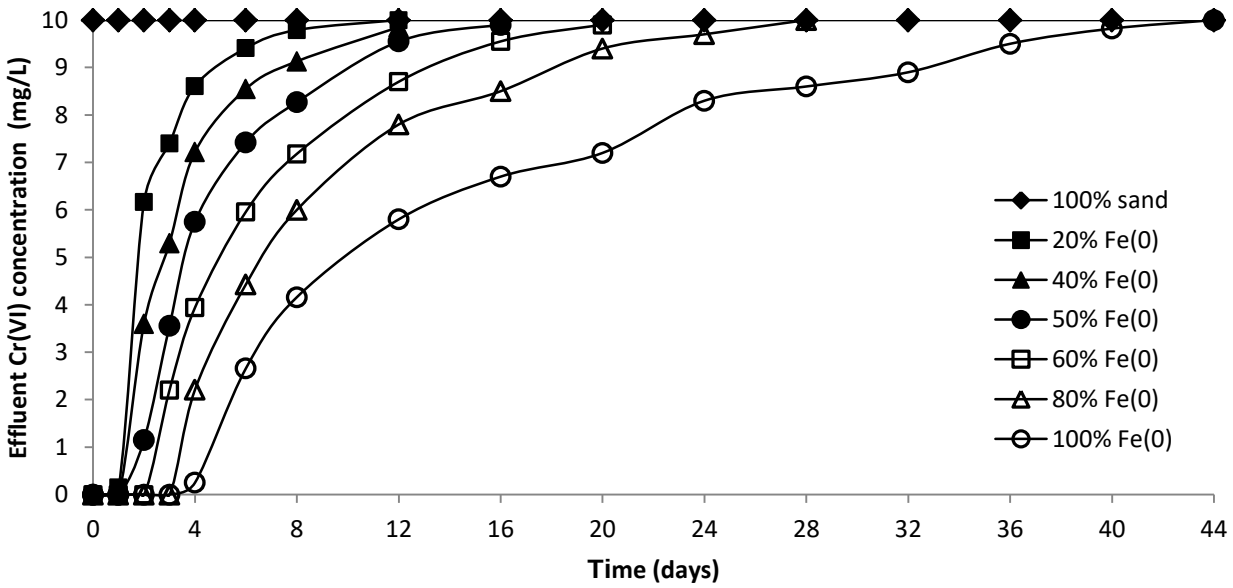

Fig.4. Cr(VI) concentration in column effluent vs. time, for columns with various Fe^0 1-2 mm percentage, fed with solution Cr(VI) 10 mg/L

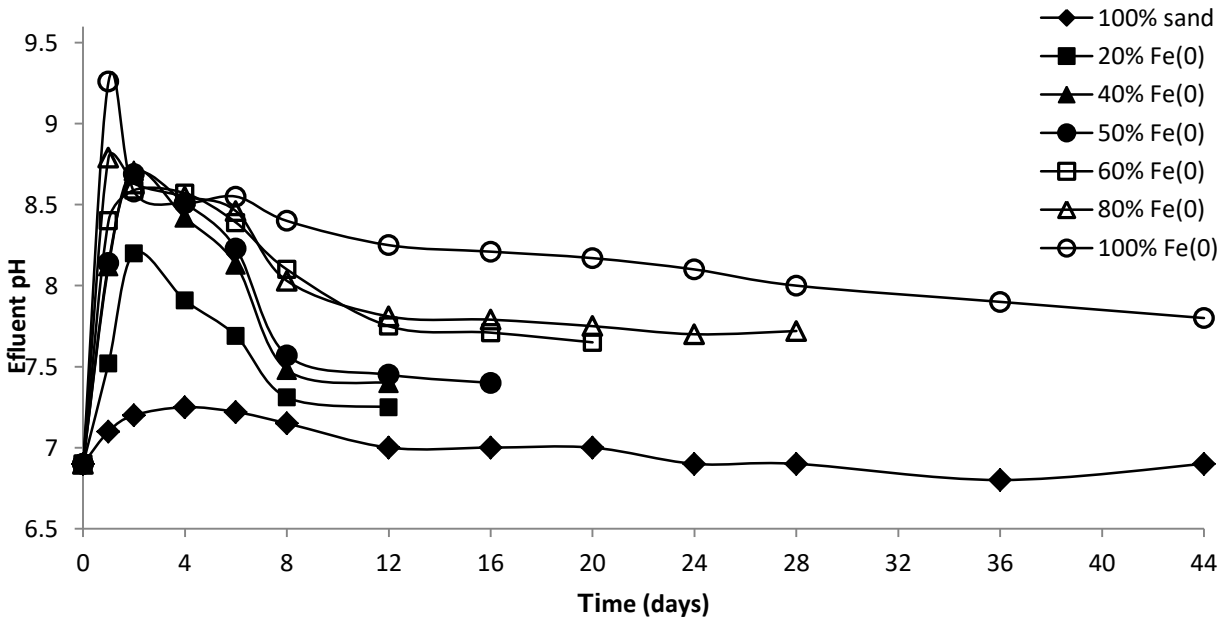

Fig.5. pH in column effluent vs. time, for columns with various Fe^0 1-2 mm percentage, fed with solution Cr(VI) 10 mg/L

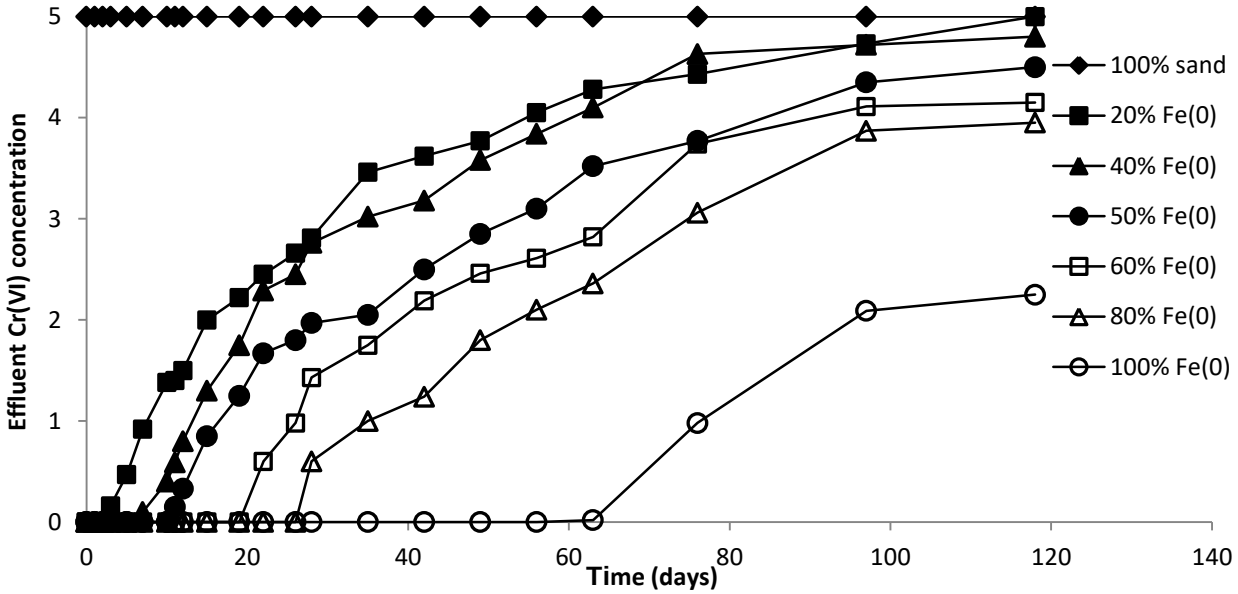

Fig.6. Cr(VI) concentration in column effluent vs. time, for columns with various Fe^0 1-2 mm percentage, fed with solution Cr(VI) 5 mg/L

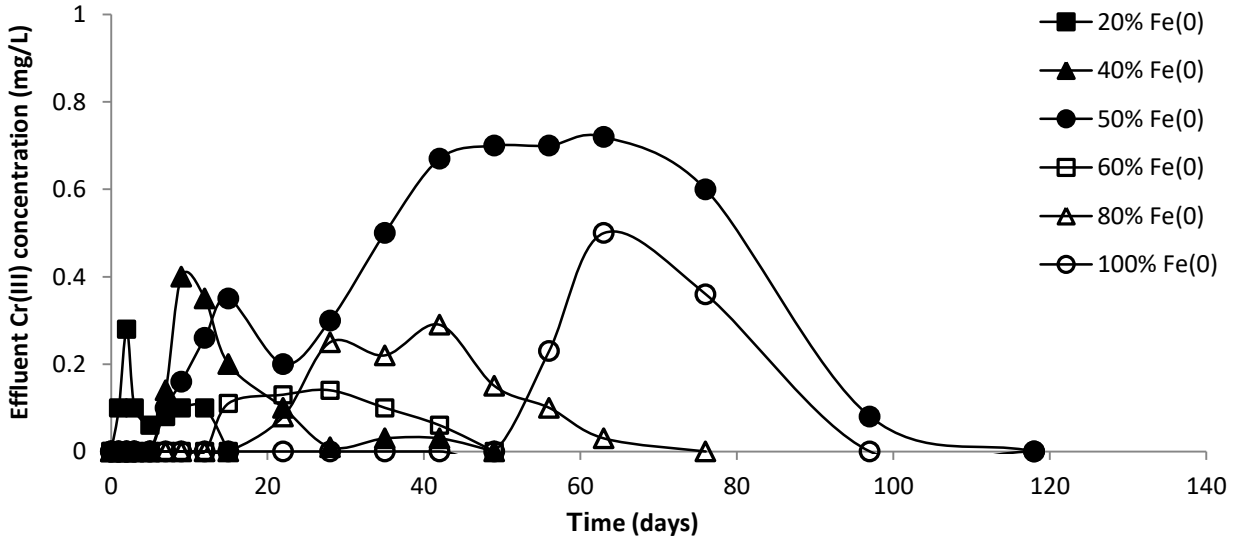

Fig.7. Cr(III) concentration in column effluent vs. time, for columns with various Fe^0 1-2 mm percentage, fed with solution Cr(VI) 5 mg/L

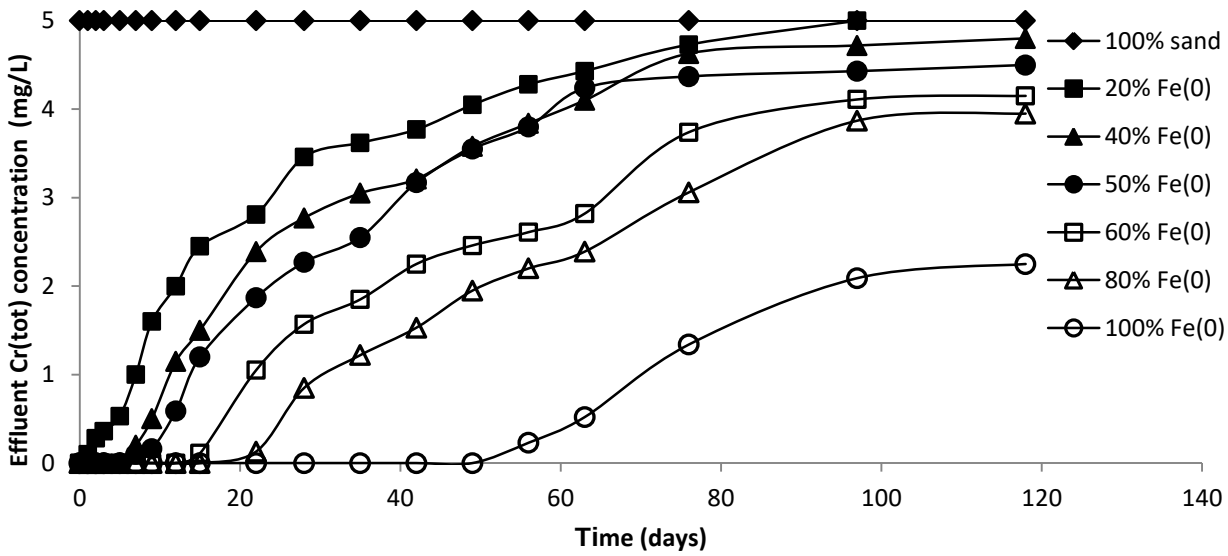

Fig.8. Cr(tot) concentration in column effluent vs. time, for columns with various Fe^0 1-2 mm, percentage fed with solution Cr(VI) 5 mg/L

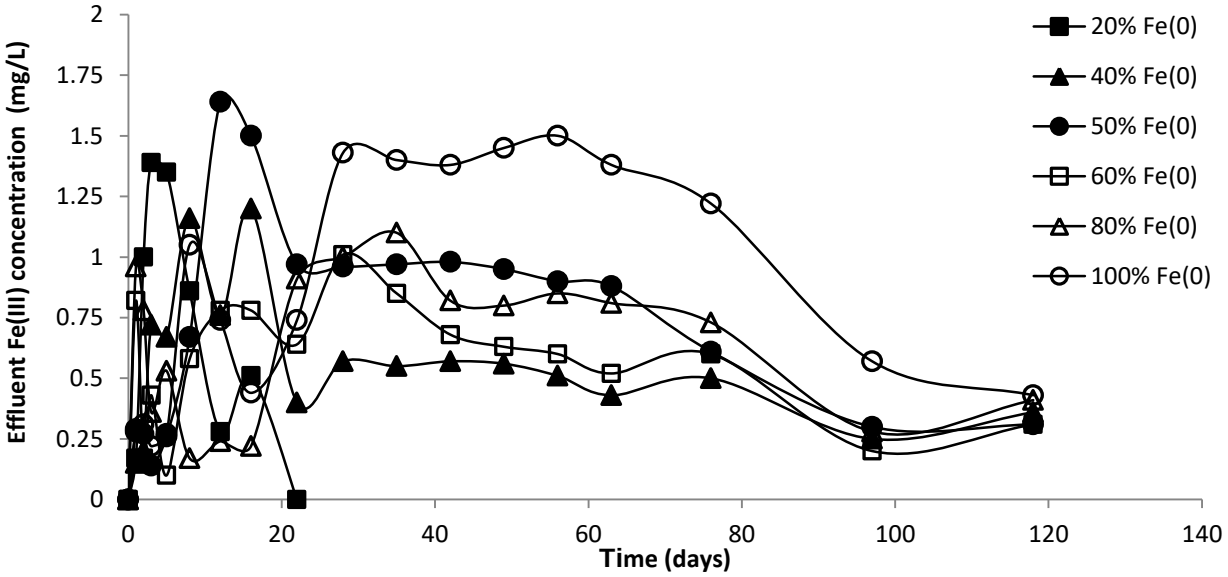

Fig.9. Fe(III) concentration in column effluent vs. time, for columns with various Fe^0 1-2 mm percentage, fed with solution Cr(VI) 5 mg/L

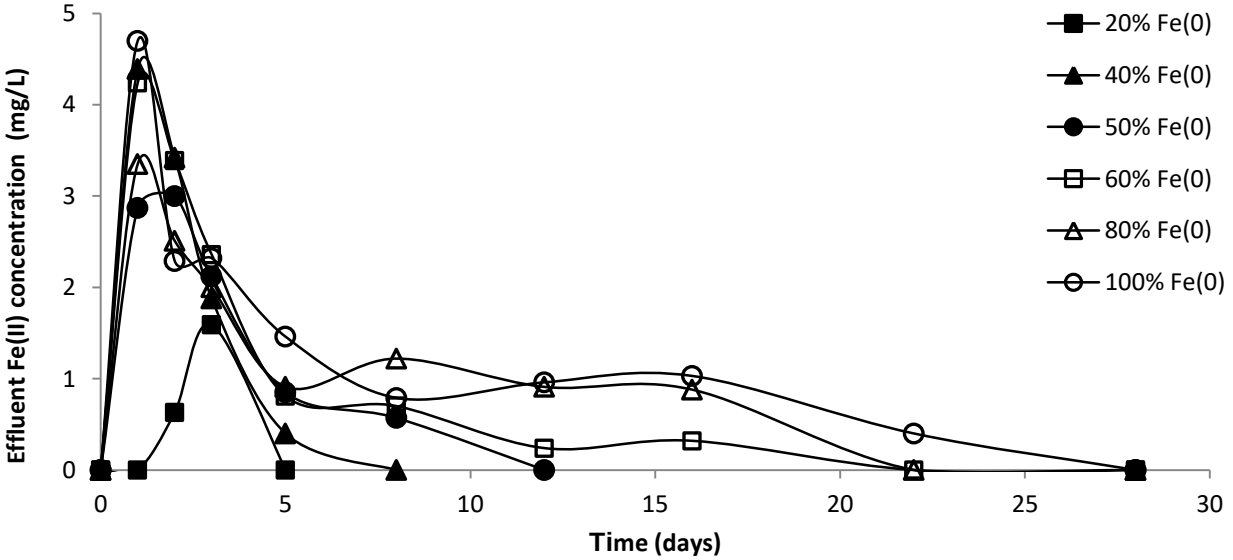

Fig.10. Fe(II) concentration in column effluent vs. time, for columns with various Fe^0 1-2 mm percentage, fed with solution Cr(VI) 5 mg/L

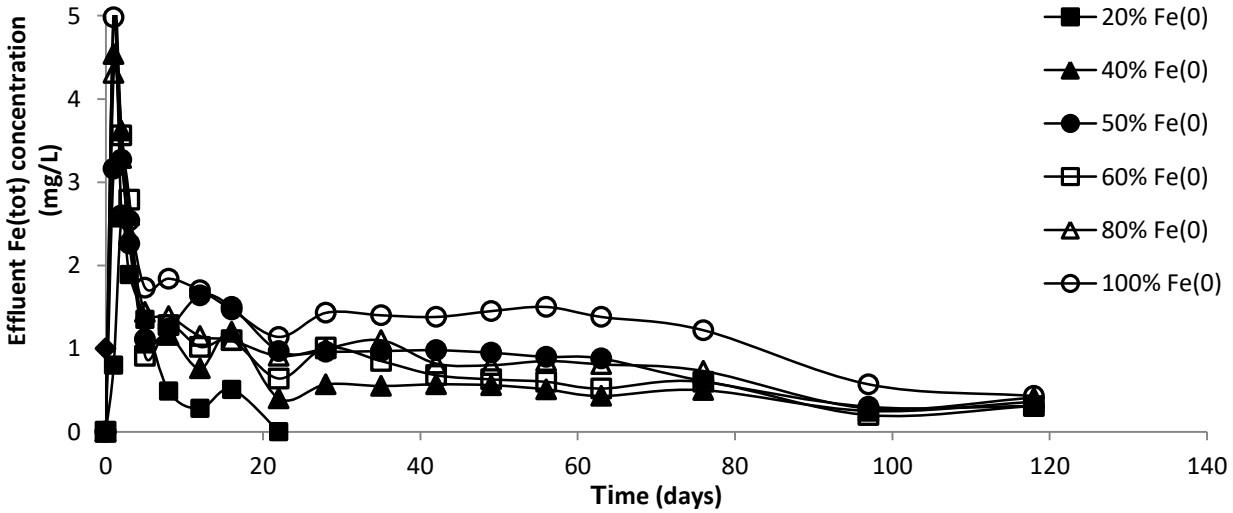

Fig.11. Fe(tot) concentration in column effluent vs. time, for columns with various Fe^0 1-2 mm percentage, fed with solution Cr(VI) 5 mg/L

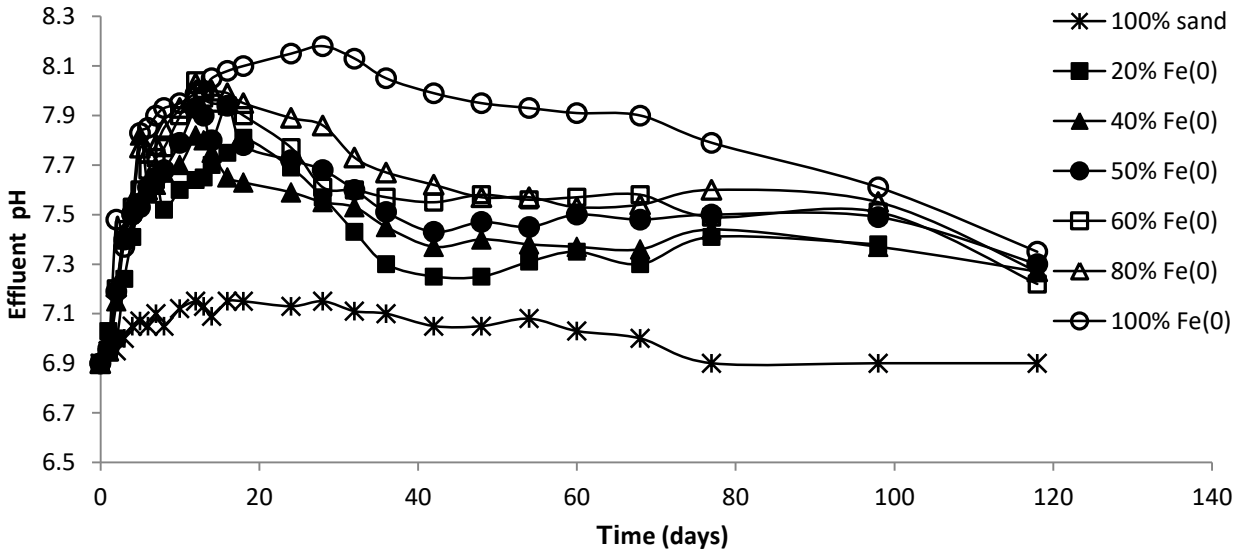

Fig.12. pH in column effluent vs. time, for columns with various Fe^0 1-2 mm percentage, fed with solution Cr(VI) 5 mg/L

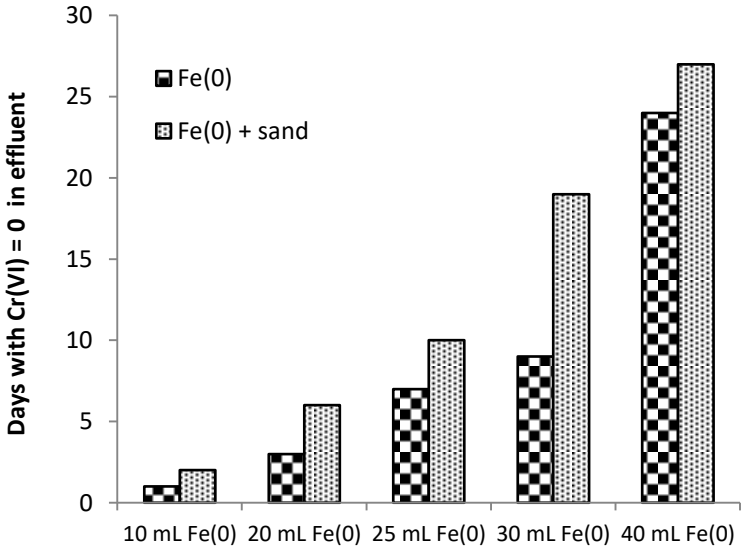

Fig.13. Evolution of Cr(VI) breakthrough in the effluent of the columns fed with solution Cr(VI) 5 mg/L, as a function of column filling composition

2.2.2. Influence of sand size

In order to study the influence of sand size, we conducted experiments using Fe^0 1-2 mm, Cr(VI) solution 5 mg/L and sand with following grain sizes: 0.1-0.5 mm, 0.5-1.25 mm and 1.25-2 mm. The experimental conditions are summarized in Table 3.

Table 3. Experimental conditions

Column	Column filling				Cr(VI) solution		
	Fe^0 1-2 mm		Sand		Concentration (mg/L)	pH	Flow (mL/h)
	(% vol.)	(cm^3)	(mm)	(cm^3)			
1	50	25	0.1-0.5	25	5	6.9	30
2	50	25	0.5-1.25	25	5	6.9	30
3	50	25	1.25-2	25	5	6.9	30

The evolution of Cr species concentration in the effluent of the three columns is shown in Figs.14-16. It can be seen that the larger the size of sand, the faster the occurrence of column breakthrough. Accordingly, the breakthrough occurred after 1, 11 and 12 days for sand with sizes of 1.25-2 mm, 0.5-1.25 mm and 0.1-0.5 mm, respectively. After the breakthrough, the evolution of Cr(VI) concentration in column effluent was similar when sand with 0.5-1.25 mm and 0.1-0.5 mm was used; nevertheless, highest efficiency of Cr(VI) removal was achieved for sand with 0.1-0.5 mm. In the same time, Cr(III) concentrations in column effluent were lowest when sand with smallest size was used, which means that, in this case, Cr(III) was better retained inside the column. This is confirmed also by the fact that effluent pH had the highest values during the first 60 days of the experiment when sand with 0.1-0.5 mm was used (Fig. 17), which has a positive influence on the precipitation of Cr(VI) inside the column.

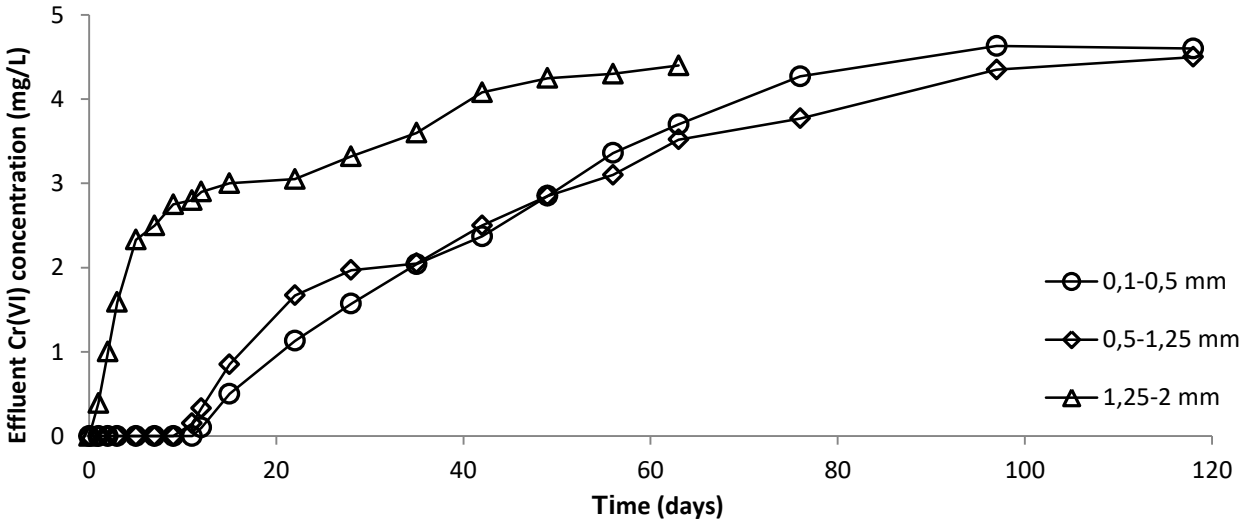

Fig.14. Evolution of Cr(VI) concentration in column effluent, for columns with 50% Fe^0 1-2 mm, fed with solution Cr(VI) 5 mg/L, as a function of sand size.

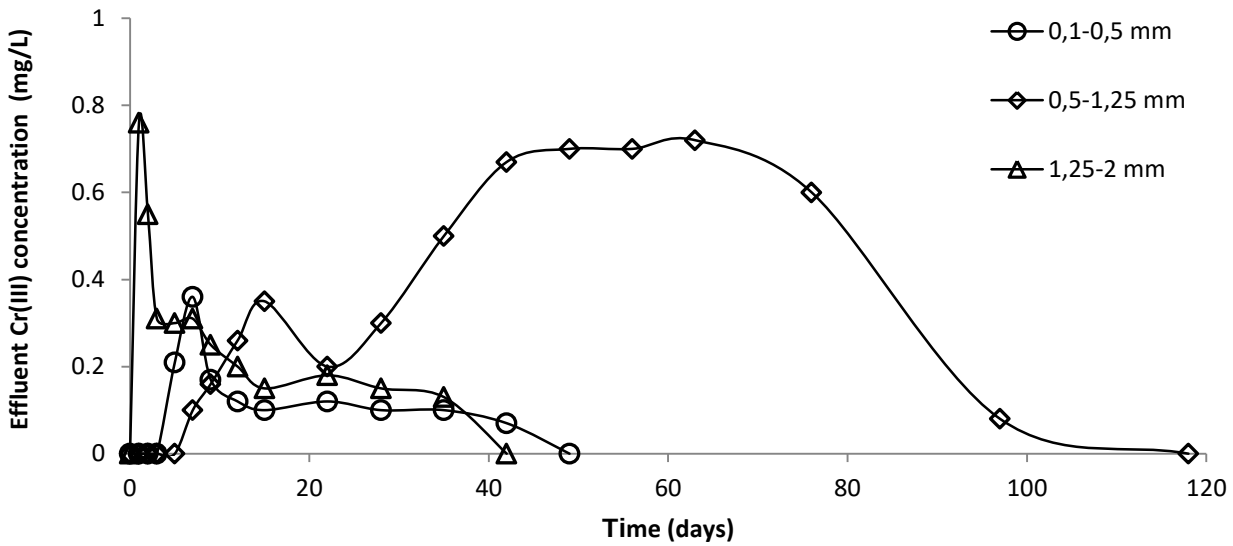

Fig.15. Evolution of Cr(III) concentration in column effluent, for columns with 50% Fe^0 1-2 mm, fed with solution Cr(VI) 5 mg/L, as a function of sand size.

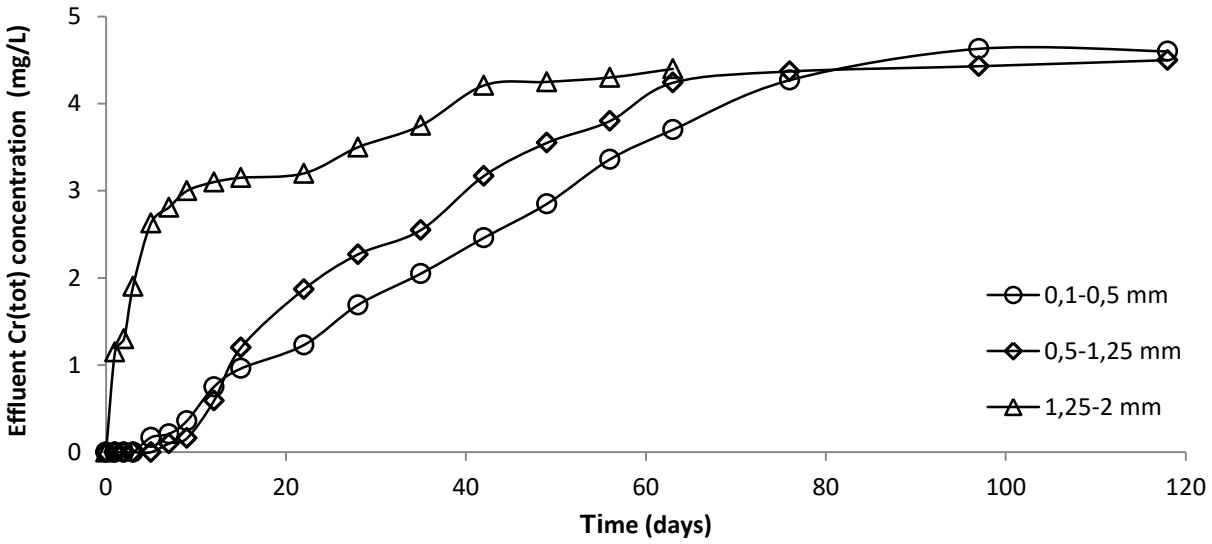

Fig.16. Evolution of Cr(tot) concentration in column effluent, for columns with 50% Fe^0 1-2 mm, fed with solution Cr(VI) 5 mg/L, as a function of sand size.

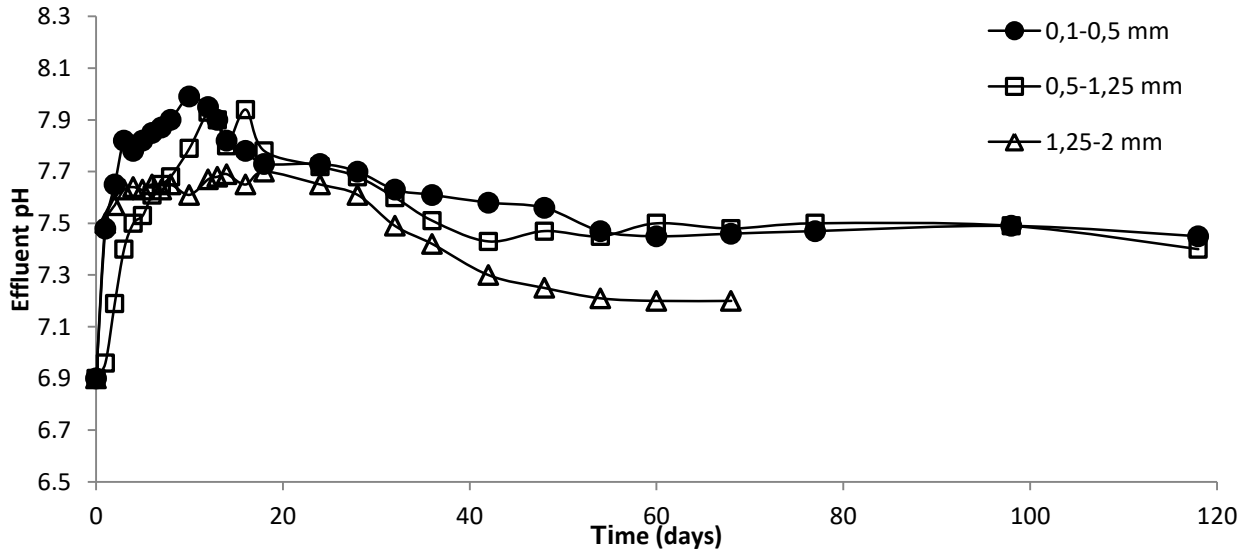

Fig.17. Evolution of pH in column effluent, for columns with 50% Fe^0 1-2 mm, fed with solution Cr(VI) 5 mg/L, as a function of sand size.

2.2.3. Influence of Fe^0 size

In order to study the influence of this parameter, we conducted experiments using Fe^0 with particle size of 10 µm and Cr(VI) solution 5 mg/L. The experimental conditions are summarized in Table 3. The result of these experiments have been compared with those of experiments carried out with Fe^0 with 1-2 mm and Cr(VI) solution 5 mg/L, described at section 2.2.1.

Table 4. Experimental conditions

Column	Column filling				Cr(VI) solution			
	$Fe^0$10 µm		Sand 0.1-0.5 mm		Concentration (mg/L)	pH	Flow (mL/h)	
	(% vol.)	(cm^3)	(% vol.)	(cm^3)			Day 1-2	Day 2-260
1	20	10	80	40	5	6.9	30	8
2	40	20	60	30	5	6.9	30	8
3	50	25	50	25	5	6.9	30	8
4	60	30	40	20	5	6.9	30	8
5	80	40	20	10	5	6.9	30	8
6	100	50	0	0	5	6.9	30	8
7	0	0	100	50	5	6.9	30	8

The evolution of Cr(VI) concentration in the effluent of the columns is presented in Fig.18. At the beginning of experiments, columns were fed with Cr(VI) solution at a flow of 30 mL/h. But, in contrast to experiments with Fe^0 1-2 mm, for $Fe^0$10 µm it was observed that Cr(VI) breakthrough occurred after the first day in effluent of all columns: Cr(VI) concentration was 5 mg/L in all effluents, excepting the effluent of column with 100% Fe(0), where it was 3.5 mg/L. The second

day, Cr(VI) concentration was the same (5 mg/L) in effluents of columns packed with mixture Fe^0 + sand, but increased to 3.9 in the effluent of column with 100% Fe^0. Therefore, in the second day, we decided to decrease the flow of Cr(VI) solution to 8 mL/h, in order to increase the contact time inside the column. This flow was maintained constant for the rest of experiment duration. Even though the flow was lowered, Cr(VI) concentration in the effluent of column with 20% Fe^0 remained constant for the rest of experiment duration: 5 mg/L. In the same time, in the effluent of column with 100% Fe(0), Cr(VI) concentration reached to zero the next day after the flow changing. Instead, Cr(VI) concentration in the effluent of all other column decreased after the flow changing. The most important decrease was observed in the effluent of column with 80% Fe^0, where Cr(VI) concentration rapidly dropped to a value of about 1.5 mg/L, which was maintained relatively constant for a long period. A similar, but, however, slower decrease was noticed also in the effluent of column with 60% Fe^0. This phenomenon may be attributed to corrosion of Fe^0 and generation of iron oxides/hydroxides. It is known that the surface of iron corrosion products is mostly positively charged under circumneutral conditions, which makes them good adsorbents for negatively charged pollutants such as Cr(VI) (Noubactep, 2015). Therefore, it may be assumed that, because of the Fe^0 with small particle size and high specific surface area that was used, adsorption on oxide layers existent at surface of Fe(0) was one of the most important pathway of Cr(VI) removal under the experimental conditions tested here. During experiments, no Fe(II), Fe(III) or Cr(III) were detected in columns effluents. This phenomenon is attributable to higher pH observed for a longer period of time in effluent of columns with Fe^0 10 μm (Fig. 19), than in effluent of columns with Fe^0 1-2 mm (Fig. 12), which favored the precipitation of Fe(II), Fe(III) and Cr(III) inside the column. In the same time, it may be ascribed to the fact that fillings containing Fe^0 10 μm had a much higher specific surface area than fillings containing Fe^0 1-2 mm, which also favored the retaining of Fe(II), Fe(III) and Cr(III) inside the column.

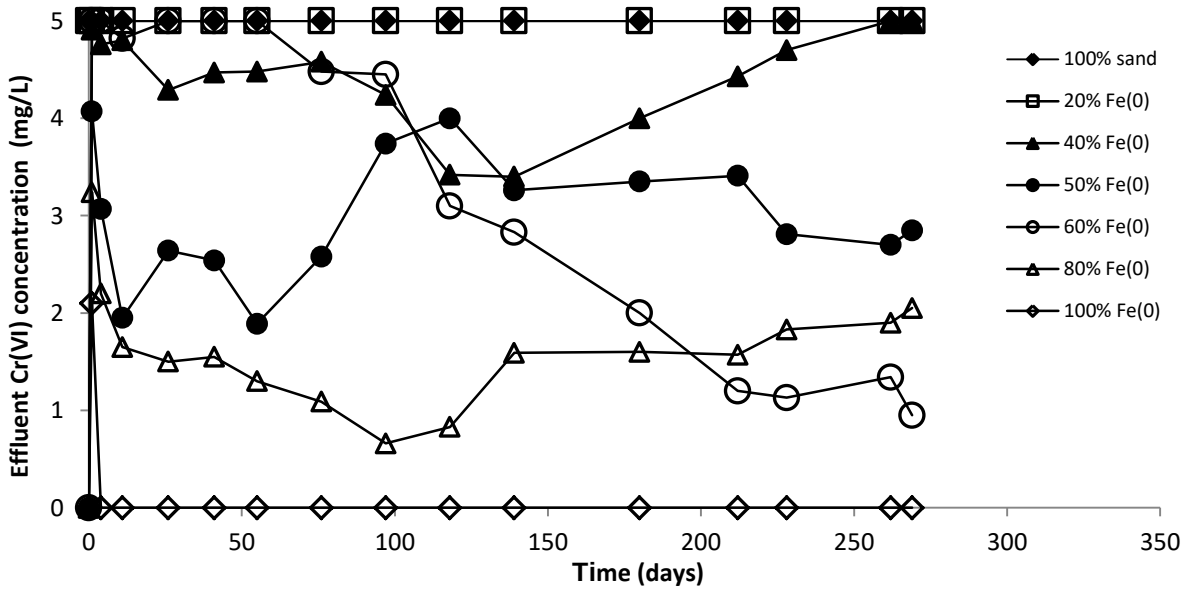

Fig.18. Evolution of Cr(VI) concentration in column effluent, for columns with various Fe^0 10 μm percentage, fed with solution Cr(VI) 5 mg/L.

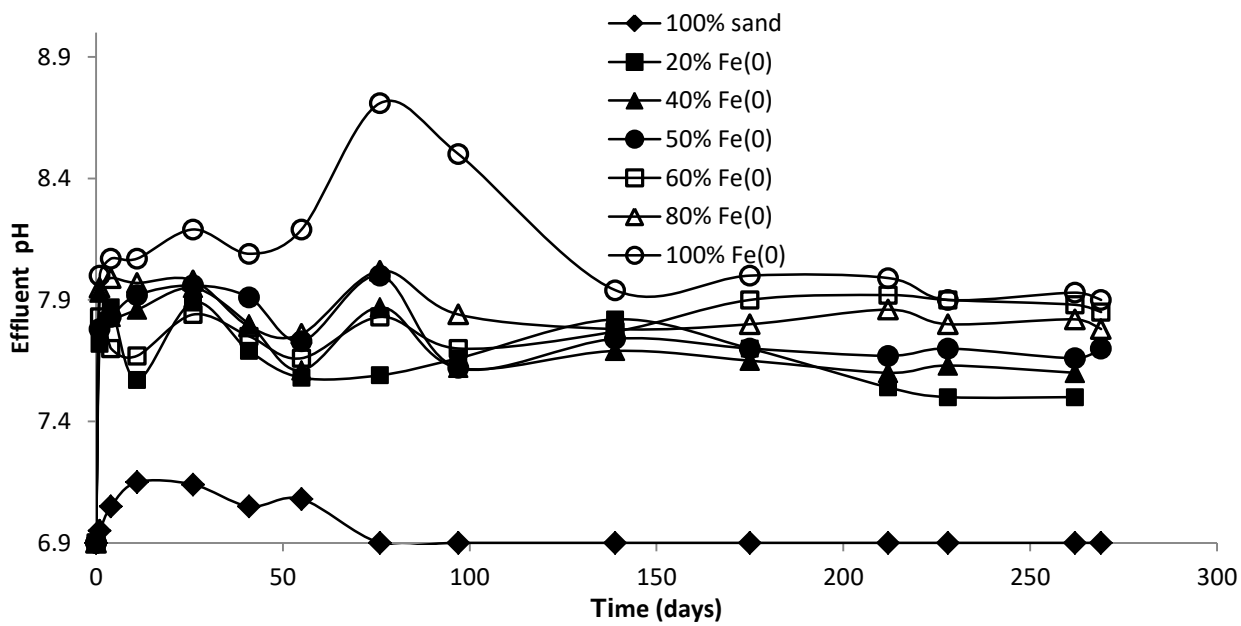

Fig.19. Evolution of pH in column effluent, for columns with various Fe^0 10 μm percentage, fed with solution Cr(VI) 5 mg/L

2.3. Conclusions

Experiments conducted to investigate the influence of sand co-presence indicated that sand has a positive effect on the removal of Cr(VI) with Fe^0. In all studied cases, the columns packed with a mixture of Fe^0 + sand had a higher Cr(VI) removal efficiency than those filled only with Fe^0, for an identical volume of Fe^0. The best results were obtained for sand with smaller size than of Fe^0. In the same time, it has been observed that the use of reactive mixtures comprised of Fe^0 + sand having Fe^0 in a millimeter size rage is more advantageous in comparison to the use of reactive mixtures comprised of Fe^0 + sand having Fe^0 in a micrometer size rage.

Objective 3. Investigation of the effect of MnO_2 co-presence on Cr(VI) removal with Fe^0

Activități: Column treatability experiments for Cr(VI) removal with Fe^0 in the co-presence of MnO_2

3.1. Materials and methods

Commercially available Fe^0 from Alfa Aesar (≥ 99%, 1-2 mm) and MnO_2 from Merck (≥ 99%, 10 μm) were used in this assay as received. The laboratory apparatus used for the flow-through column experiments consisted in polyethylene columns (inner diameter: 2 cm; height: 11 cm), an Ismatec IP08 peristaltic pump and a tank with a capacity of 60 L (Fig.1). The columns were packed with a mixture of Fe^0 + MnO_2 having various volumic ratios. Below and above the filling was a layer of 5 cm^3 sand with d = 1.25-2 mm. Cr(VI) stock solutions (10 g/L) were prepared by dissolving 28.29 g $K_2Cr_2O_7$ in 1000 mL of distilled deionized water. Working solutions of the desired initial Cr(VI) concentrations (5 mg/L) were then prepared by diluting the stock solution with tap water, in order to simulate a case of natural water pollution. This concentration was selected because it is within the range of relevant concentrations for Cr(VI) polluted groundwaters (Flury et al., 2009; Wilkin et al., 2005). The pH was adjusted to 6.9 by small addition of concentrated H_2SO_4.

The Cr(VI) working solution was passed, at room temperature, through the column from the bottom to the top, and effluent samples were withdrawn at regular time intervals for the analysis of following parameters: pH, Cr(total), Cr(VI), Cr(III), Fe(total), Fe(II), Fe(III), Mn(II). pH, chromium and iron dissolved species were determined as shown at section 2.1. Concentration of Mn(II) was also determined, by the formaldoxime spectrophotometric method, at 450 nm, using a Specord 200 Plus spectrophotometer (SR ISO 6333/1996). The calibration curve of Mn(II) and the equation obtained by linear regression, are depicted in Fig.20. The experimental conditions applied to study the influence of MnO_2 co-presence are summarized in Table 5.

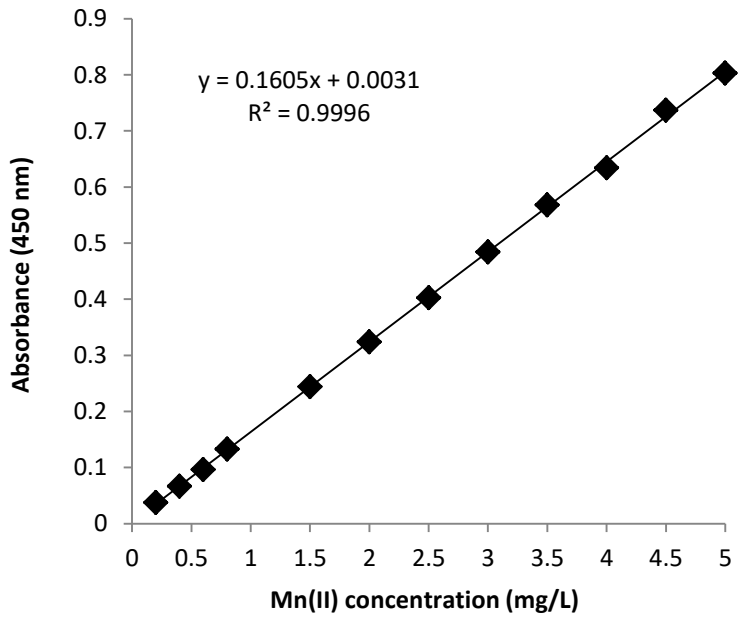

Fig.20. Mn(II) calibration curve

Table 5. Experimental conditions

Column	Column filling			Cr(VI) solution		
	MnO_2 (% vol.)	Fe^0 1-2 mm (cm^3)	MnO_2 (cm^3)	Concentration (mg/L)	pH	Flow (mL/h)
1	20	20	5	5	6.9	30
2	33.3	20	10	5	6.9	30
3	0	20	0	5	6.9	30
4	100	0	10	5	6.9	30

3.2. Results and discussion

Fig.21 depicts the evolution of Cr(VI) concentration in the effluent of the four columns presented in table 5. In addition, for comparison purposes, results of column experiments with mixture of 20 cm^3 Fe^0 1-2 mm + 30 cm^3 sand 0.5-1.25 mm, taken from section 2.2, are also plotted in Fig.21. This figure clearly shows that co-presence of MnO_2 had a detrimental effect on the efficiency of Cr(VI) removal with Fe^0. Cr(VI) breakthrough occurred after the first day in effluent of

both columns with mixture of Fe(0) + MnO_2, as can be seen from Fig. 22. By comparison, Cr(VI) breakthrough in columns with 100% MnO_2, 100% Fe^0 and with mixture Fe^0 1-2 mm + sand 0.5-1.25 mm occurred after 3, 4 and 7 days, respectively. Previous studies have suggested that, in H_2O-Fe^0 system, co-presence of MnO_2 may sustain Fe^0 oxidative dissolution (and therefore, the process of contaminant removal in H_2O-Fe^0 system) by: (1) accelerating Fe^0 oxidative dissolution (Eq.15), and (2) avoiding or delaying the formation of oxide film on the surface of Fe^0 by consuming Fe(II) and preventing thus precipitation of Fe species (Eq. 16-19) (Bafghi et al., 2008; Noubactep et al., 2011; Noubactep et al., 2012, Postma and Appelo, 2000):

$$MnO_2 + Fe^0 + 4H^+ \Leftrightarrow Mn^{2+} + Fe^{2+} + 2H_2O \quad (15)$$

$$MnO_2 + Fe^{2+} + 2H_2O \Leftrightarrow FeOOH + MnOOH + 2H^+ \quad (16)$$

$$MnOOH + Fe^{2+} \Leftrightarrow FeOOH + Mn^{2+} \quad (17)$$

$$MnO_2 + 2Fe^{2+} + 4H^+ \Leftrightarrow Mn^{2+} + 2Fe^{3+} + 2H_2O \quad (18)$$

$$MnO_2 + 2Fe^{2+} + 2H_2O \Leftrightarrow 2FeOOH + Mn^{2+} + 2H^+ \quad (19)$$

Even though from thermodynamic perspective it seems that reductive dissolution of MnO_2 with Fe^0 is much favorable than that involving Fe(II) (solid Fe^0 is a stronger reductant than dissolved Fe(II)), from a kinetic point of view, reaction of MnO^2 with Fe^{2+} is more feasible (Bafghi et al., 2008). Hence, it can be presumed that the fastest reactions of MnO_2 in our system were those with Fe(II) (Eqs. 16-19). For Cr(VI), indirect reduction with Fe(II) is one of the most important removal mechanisms in H_2O-Fe^0 systems (Gheju 2011). Therefore, the lower Cr(VI) removal efficiency of the columns packed with a mixture of Fe^0 + MnO_2 can be ascribed to the decrease of Fe(II) available for Cr(VI) reduction, as a result of Fe(II) reaction with MnO_2, according to Eqs. 16-19. This phenomenon is suggested also by the evolution of Mn(II) concentration in the effluent of columns packed with a mixture of Fe^0 + MnO_2 (Fig. 23). Mn(II) concentration increased rapidly at the beginning of experiments up to a maximal value, and then subsequently decreased gradually until the end of experiment. The initial increase could be ascribed to interactions between MnO_2 and Fe(II), which lead to generation of Mn(II). The later progressive decrease of Mn(II) concentration is attributable to declining of Fe(II) concentrations, as a result of Fe^0 passivation with layers of Fe and Cr oxide/hydroxide. Fig.23 also shows that there are no important differences between the evolution of Mn(II) concentration in the effluent of columns with 5 cm^3 and 10 cm^3 MnO_2. Similarly, with the exception of first 3 days, there are no important differences between the evolution of pH in the effluent of columns with 5 cm^3 and 10 cm^3 MnO_2 (Fig. 24). During the course of the experiments, no species of Cr(III), Fe(II) or Fe(III) were identified in the effluent of columns packed with Fe^0 + MnO_2. This can be explained by their precipitation inside the column filling, due to the high pH of the solution of Cr (VI) after it has passed through the columns.

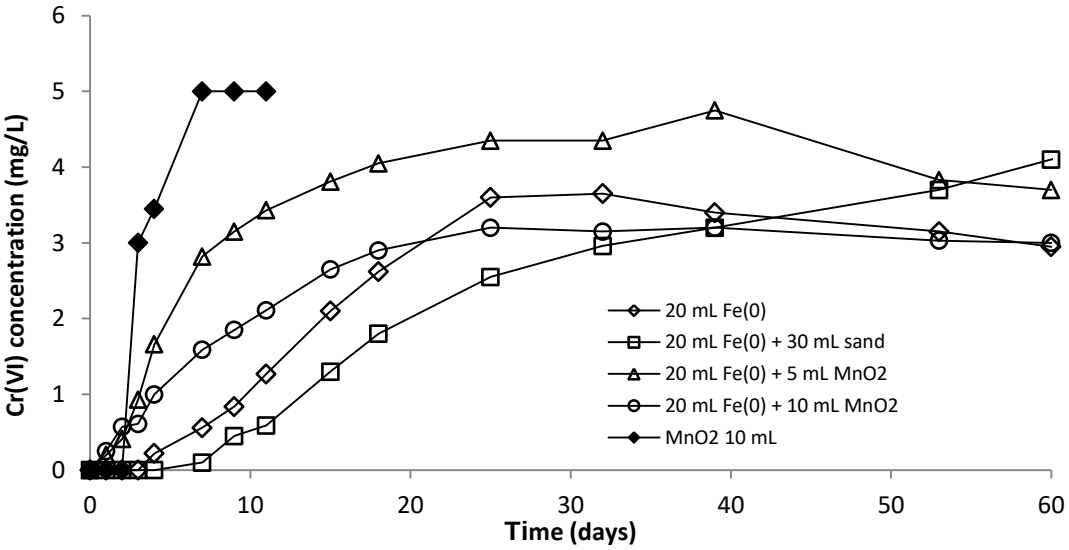

Fig.21. Evolution of Cr(VI) concentration in column effluent, for columns packed with Fe^0 1-2 mm and MnO_2, fed with solution Cr(VI) 5 mg/L, as a function of MnO_2 percentage. For comparison purposes, control experiments with bare MnO_2, bare Fe^0 1-2 mm, and mixture of Fe^0 1-2 mm + sand 0.5-1.25 mm are also plotted

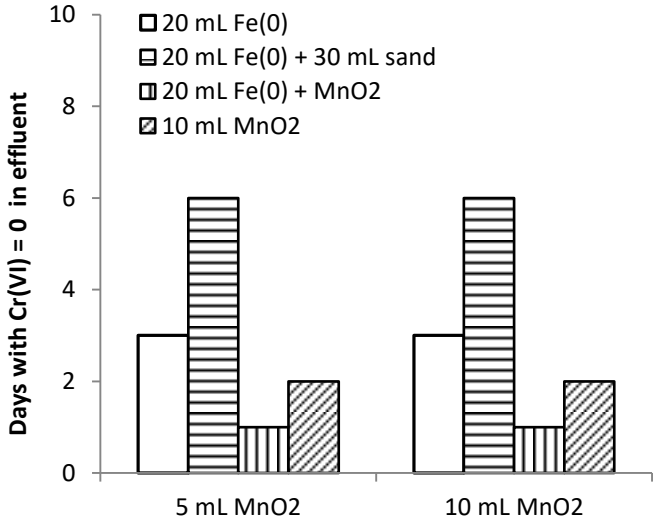

Fig.22. Evolution of Cr(VI) breakthrough in the effluent, as a function of volume of MnO_2

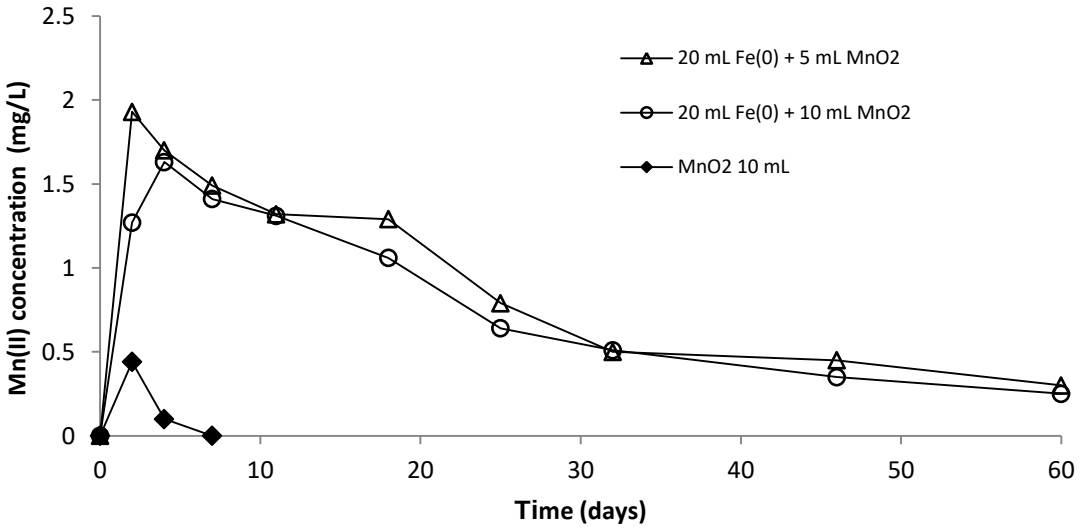

Fig.23. Evolution of Mn(II) concentration in column effluent, for columns packed with Fe^0 1-2 mm and MnO_2, fed with solution Cr(VI) 5 mg/L, as a function of MnO_2 percentage. For comparison purposes, control experiments with bare MnO_2 are also plotted

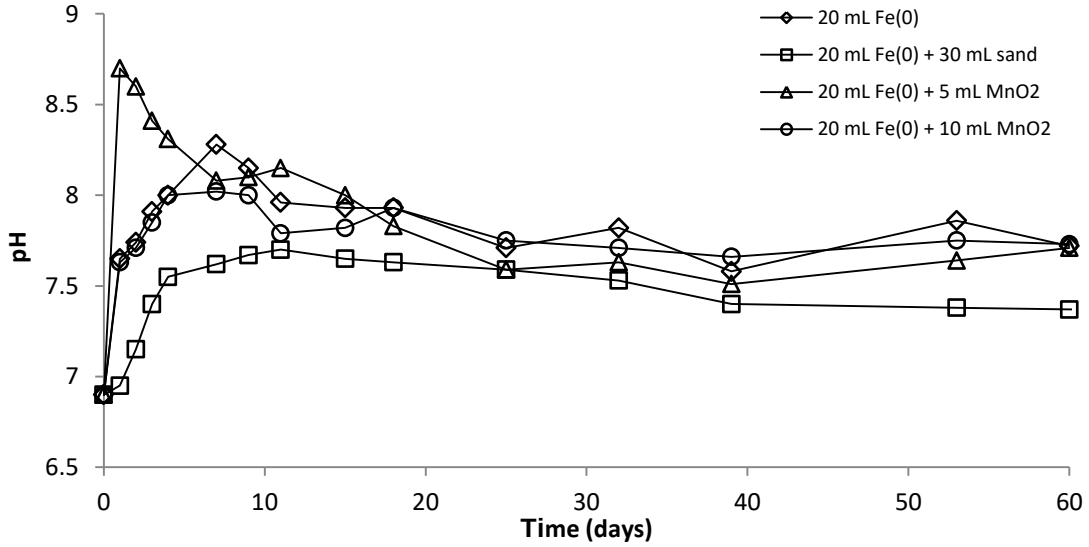

Fig.24. Evolution of pH in column effluent, for columns packed with Fe^0 1-2 mm and MnO_2, fed with solution Cr(VI) 5 mg/L, as a function of MnO_2 percentage. For comparison purposes, control experiments with bare Fe^0 1-2 mm and mixture of 20 cm^3 Fe^0 1-2 mm + 30 cm^3 sand 0.5-1.25 mm are also plotted

3.3. Conclusions

Long-term column experiments carried out here have shown that the process of Cr(VI) removal with Fe^0 was significantly inhibited in the co-presence of MnO_2. This phenomenon was ascribed to the fact that reaction between MnO_2 and Fe(II), which consumes Fe(II), was much faster than the one between MnO_2 and Fe^0, which generates Fe(II). These results endorse the importance of the indirect mechanism of Cr(VI) reduction with Fe(II) within the frame of the process of Cr(VI) removal with Fe^0.

Objective 4. Investigation of the effect of sand and MnO_2 co-presence on Cr(VI) removal with Fe^0

Activities: Batch and column treatability experiments for Cr(VI) removal with Fe^0 in the co-presence of sand and MnO_2.

4.1. Materials and methods

4.1.1. Batch experiments in co-presence of sand and MnO_2

Commercially available Fe^0 (≥ 99%, ~10 μm) and MnO_2 from Merck (≥ 99%, ~10 μm) were used in this assay as received. Sand obtained from a local source was sieved to obtain grain size ranging from 0.1 to 0.5 mm; the sand was then washed with distilled water and dried. Experiments were conducted in a 1.5 L Berzelius flask open to the atmosphere, containing 1000 mL of 2 mg/L Cr(VI) solution (Fig. 25). The reactive solids were added to the Cr(VI) solution and the flask content was mixed continuously (200 rpm) at room temperature by a Heidolph vertical agitator equipped with a polymethacrylate stirring shaft. pH 2.5 was selected because it was previously reported that experiments of Cr(VI) removal with Fe^0 in batch system can be best carried out in acidic environment (Gheju and Iovi, 2006). Additional experiments were conducted at 6 and 32 ^oC in order to study the influence of temperature, keeping all other conditions equal. Samples were collected at predetermined time intervals for the analysis of following parameters: pH, Cr(total), Cr(VI), Cr(III), Fe(total), Fe(II), Fe(III). All these parameters were determined as shown at section 2.1.

Fig.25. Experimental setup for batch studies

4.1.2. Column experiments in co-presence of sand and MnO_2

Commercially available Fe^0 from Alfa Aesar (≥ 99%, 1-2 mm) and MnO_2 from Merck (≥ 99%, ~10 μm) were used in this assay as received. Sand obtained from a local source was sieved to obtain the grain sizes of 0.5-1.25 mm and 1.25-2 mm; the sand was then washed with distilled water and dried. The laboratory apparatus used for the flow-through column experiments consisted in polyethylene columns (inner diameter: 2 cm; height: 11 cm), an Ismatec IP08 peristaltic pump and a tank with a capacity of 60 L (Fig.1). The columns were packed with a mixture of Fe^0 + sand 0.5-1.25 mm + MnO_2 having various volumic ratios. Below and above the filling was a layer of 5 cm^3 sand with d = 1.25-2 mm. Cr(VI) stock solutions (10 g/L) were prepared by dissolving 28.29 g $K_2Cr_2O_7$ in 1000 mL of distilled deionized water. Working solutions of the desired initial Cr(VI) concentration (5 mg/L) were then prepared by diluting the stock solution with tap water, in order to simulate a case of natural water pollution. This concentration was selected because it is within the range of relevant concentrations for Cr(VI) polluted groundwaters (Flury et al., 2009; Wilkin et al., 2005). The pH was adjusted to 6.9 by small addition of concentrated H_2SO_4 and measured in samples collected before and after the reaction using an Inolab 7320 pH-meter. The Cr(VI) working solution was passed, at room temperature, through the column, from the bottom to the top, and effluent samples were withdrawn at regular time intervals for the analysis of following parameters: pH, Cr(total), Cr(VI), Cr(III), Fe(total), Fe(II), Fe(III), and Mn(II). All these parameters were determined as shown at section 2.1 and 3.1. The experimental conditions applied to study the influence of sand and MnO_2 co-presence are summarized in Table 6.

Table 6. Experimental conditions

Column	Colum filling			Cr(VI) solution		
	Sand 0.5-1.25 mm (cm^3)	Fe^0 1-2 mm (cm^3)	MnO_2 (cm^3)	Concentration (mg/L)	pH	Flow (mL/h)
1	20	20	5	5	6.9	30
2	10	20	10	5	6.9	30
3	0	20	0	5	6.9	30
4	0	0	10	5	6.9	30

4.2. Results and discussion

4.2.1. Batch experiments in co-presence of sand and MnO_2

Fig. 26 illustrates the results of Cr(VI) removal experiments conducted in the presence of a mixture comprising Fe^0, MnO_2 and sand. It can be seen that this process is very similar to those carried out in H_2O-Fe^0-MnO_2-Cr(VI) and H_2O-MnO_2-Cr(VI) systems (Fig 27): very rapid at initial stages and decreases with approaching equilibrium. Just like for the H_2O-Fe^0-MnO_2-Cr(VI) system, no Cr(III) was detected at the end of experiments, and final Fe(total) concentration was much lower than for H_2O-Fe^0 system. Thus, following a similar rationale to that presented in section 3.2 of the Scientific Report 2015, the removal of Cr(VI) in H_2O-Fe^0-MnO_2-Sand-Cr(VI) system was attributed to adsorption processes of Cr(VI) on MnO_2.

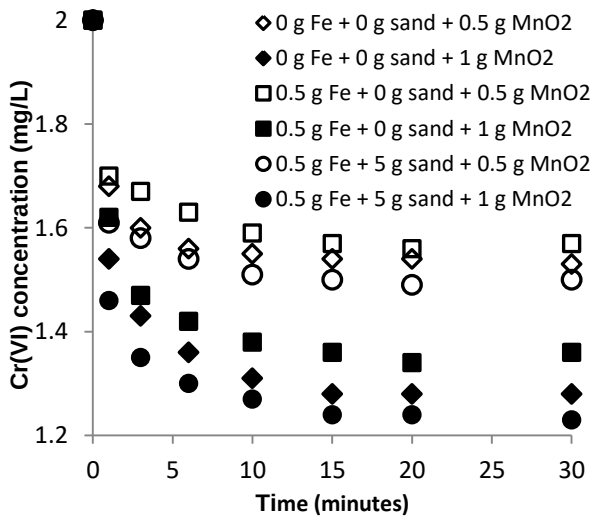

Fig.26. Cr(VI) vs. time for removal experiments with different Fe^0, sand and MnO_2 mixtures. For comparison purposes, experiments with Fe^0 + MnO_2 mixtures and control experiments with bare MnO_2 are also plotted

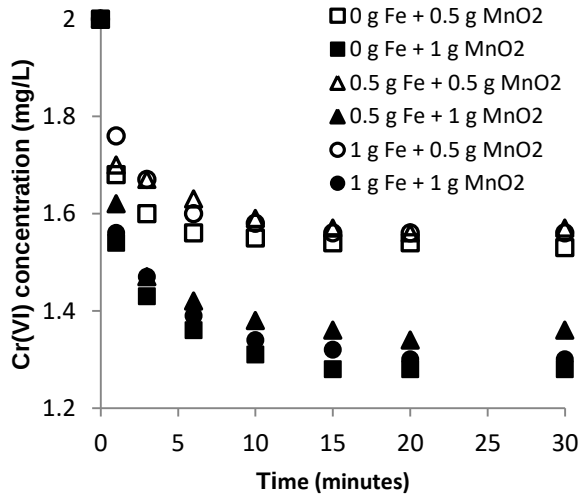

Fig.27. Cr(VI) vs. time for removal experiments with different Fe^0 and MnO_2 mixtures. For comparison purposes, control experiments with bare MnO_2 are also plotted

A slight enhancement of the removal rate was, however, observed in the H_2O-Fe^0-MnO_2-Sand-Cr(VI) system, compared to H_2O-MnO_2-Cr(VI) system, which can be ascribed to the favorable effect of sand; sand may work as an adsorbent for Cr(VI) and, in the same time, may catalyze the reduction of adsorbed Cr(VI). The effect of temperature on Cr(VI) removal in H_2O-Fe^0-MnO_2-Sand-Cr(VI) system was similar to that observed for the H_2O-Fe^0-MnO_2-Cr(VI) system: Cr(VI) removal efficiency slightly decreased as the temperature increased from 6 ^oC to 22 ^oC, while sharply increased when temperature was further raised to 32 ^oC (Fig.28). Additionally, the rate of Cr(VI) removal at 32 ^oC was faster in H_2O-Fe^0- Sand-MnO_2-Cr(VI) system than in H_2O-Fe^0-MnO_2-Cr(VI) system, being complete after about 1.5 minutes, presumably due to the catalytic effect of sand. Since

Cr(VI) removal in H_2O-Fe^0-Cr(VI) system was almost totally inhibited at 6 ^oC (Fig.9), it is obvious that adsorption was the main mechanism responsible for Cr(VI) removal in H_2O-Fe^0-Sand-MnO_2-Cr(VI) system not only at 22 ^oC, but also at 6 ^oC. Instead, the results obtained at 32 ^oC suggest that, at this temperature, the disappearance of Cr(VI) was the result of a different mechanism than at 6 and 22 ^oC. If the removal mechanism would have been the same (i.e. adsorption on MnO_2) over the entire temperature range, then Cr(VI) removal rates in H_2O-Fe^0-Sand-MnO_2-Cr(VI) system should decrease in the following order: 6 ^oC > 22 ^oC > 32 ^oC. Instead, a much efficient Cr(VI) removal was observed at 32 ^oC than at 6 and 22 ^oC. This behavior is very similar to the removal of Cr(VI) in H_2O-Fe^0-Cr(VI) system at 32 ^oC, when chemical reduction with Fe(II) was the main mechanism. Thus, at 32 ^oC, reduction of Cr(VI) with Fe(II) seems to be the main removal mechanism of Cr(VI) in H_2O-Fe^0-Sand-MnO_2-Cr(VI) system, just like in H_2O-Fe^0-Cr(VI) system. Since adsorption was the main mechanism responsible for the disappearance of Cr(VI) at 22 ^oC, the experimental data was kinetically analyzed using the pseudo first-order and the pseudo second-order kinetic models; by comparing the correlation coefficients it was found that removal of Cr(VI) in H_2O-Fe^0- Sand-MnO_2-Cr(VI) system fitted well to the pseudo second-order kinetic model (Figs.29 and 30).

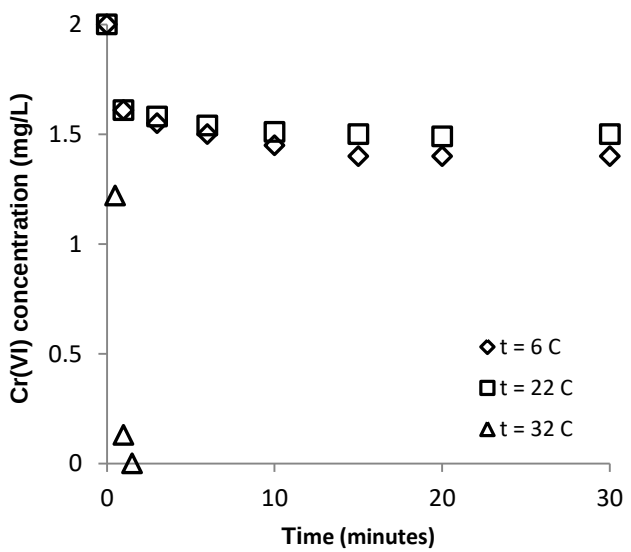

Fig.28. Effect of temperature on Cr(VI) removal in H_2O-Fe^0-MnO_2-Sand-Cr(VI) system

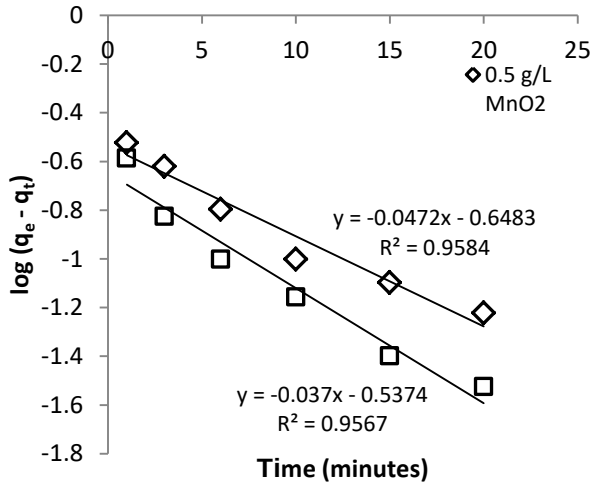

Fig.29. Linearized first-order plots for Cr(VI) removal in H_2O-Fe^0-MnO_2-Sand-Cr(VI) system

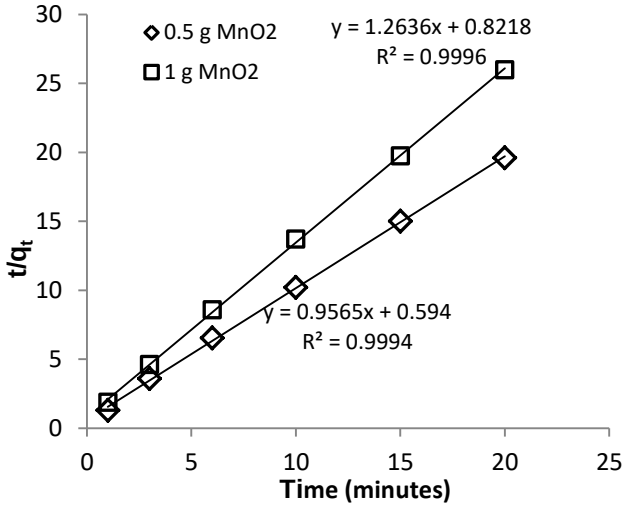

Fig.30. Linearized second-order plots for Cr(VI) removal in H_2O-Fe^0-MnO_2-Sand-Cr(VI) system

4.2.2. Column experiments in co-presence of sand and MnO_2

Fig.31 shows the evolution of Cr(VI) concentration in the effluent of the four columns presented in table 6. In addition, in Fig.31 are also plotted, for comparison purposes, the results of column experiments with mixture of 20 cm^3 Fe^0 1-2 mm + 30 cm^3 sand 0.5-1.25 mm, taken from section 2.2. This figure clearly shows that co-presence of MnO_2 and sand had a detrimental effect on the efficiency of Cr(VI) removal with Fe^0, which is similar to the effect of MnO_2 co-presence on the efficiency of Cr(VI) removal with Fe^0. Cr(VI) breakthrough occurred after the first day in effluent of both columns with mixture of Fe^0 + MnO_2 + sand (Fig.32); by comparison, Cr(VI) breakthrough in columns with 100% MnO_2, 100 Fe^0 and with mixture Fe^0 1-2 mm + sand 0.5-1.25 mm occurred after 3, 4 and 7 days, respectively (Fig.32). This phenomenon can be ascribed to the decrease of Fe(II) concentrations, as a result of reactions between Fe(II) and MnO_2 (Eqs. 16-19). This is indicated also by the evolution of Mn(II) concentration (Fig. 33) and of pH (Fig. 34) in the effluent of columns packed with a mixture of Fe^0 + sand + MnO_2. Fig. 33 shows that Mn(II) concentration increased during the first 18 days up to a value of about 1.2-1.3 mg/L, and then slowly decreased until the end

of experiment. The initial increase is attributable to reactions between MnO_2 and Fe(II), which lead to generation of Mn(II). The subsequent decrease of Mn(II) concentration can be ascribed to low Fe(II) concentrations, as a result of Fe^0 passivation with layers of Fe and Cr oxides/hydroxides. Even though there are no important differences between the evolution of Mn(II) concentration in the effluent of columns with 5 cm^3 and 10 cm^3 MnO_2 (Fig 33), however, slightly higher effluent Mn(II) concentrations were noticed for the column with 10 mL MnO_2 than for the column with 5 mL MnO_2. Similarly, there are no important differences between the evolution of pH in the effluent of columns with 5 cm^3 and 10 cm^3 MnO_2, with slightly higher values observed in the effluent of column with 5 cm^3 MnO_2 (Fig.34). During the course of the experiments, no Cr(III), Fe(II) or Fe(III) species were identified in the effluent of columns packed with Fe^0 + MnO_2 + sand. This can be explained by their precipitation inside the column filling, due to the high pH of Cr(VI) solution after passing through the columns.

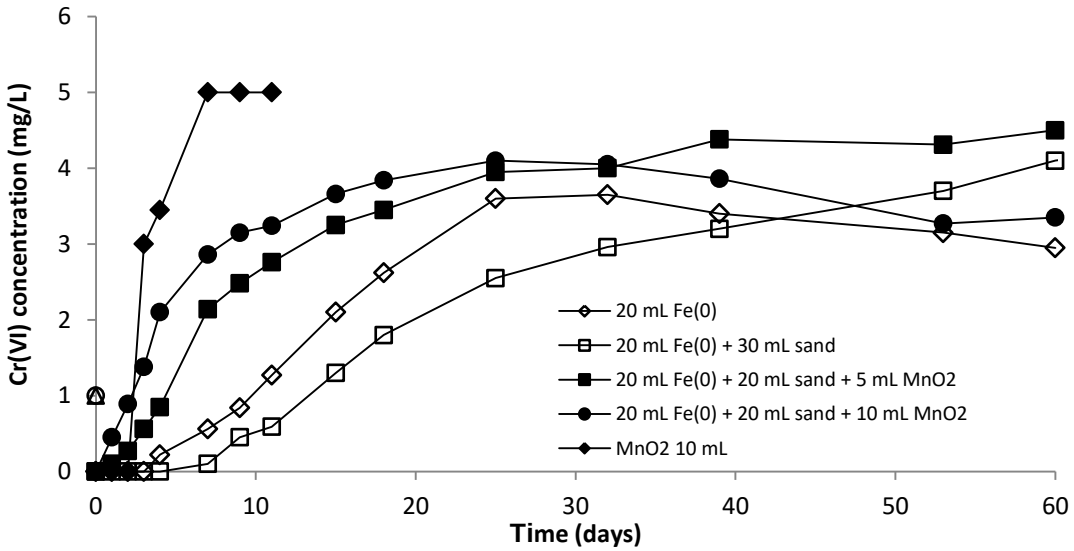

Fig.31. Evolution of Cr(VI) concentration in column effluent, for columns packed with Fe^0 1-2 mm sand 0.5-1.25 mm and MnO_2, fed with solution Cr(VI) 5 mg/L, as a function of MnO_2 percentage. For comparison purposes, control experiments with bare MnO_2, bare Fe^0 1-2 mm, and mixture of 20 cm^3 Fe^0 1-2 mm + 30 cm^3 sand 0.5-1.25 mm are also plotted.

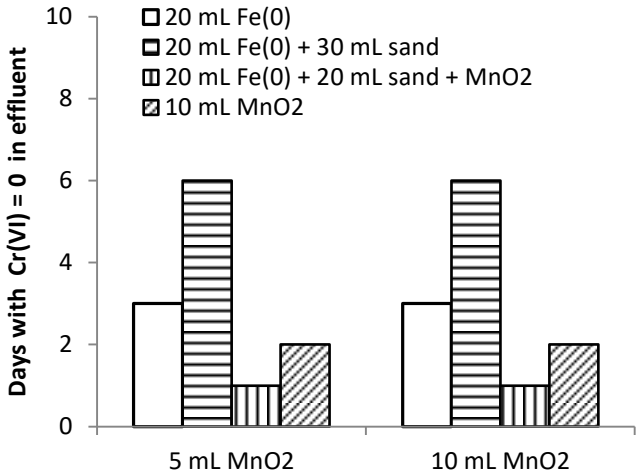

Fig.32. Evolution of Cr(VI) breakthrough in the effluent, as a function of volume of MnO_2

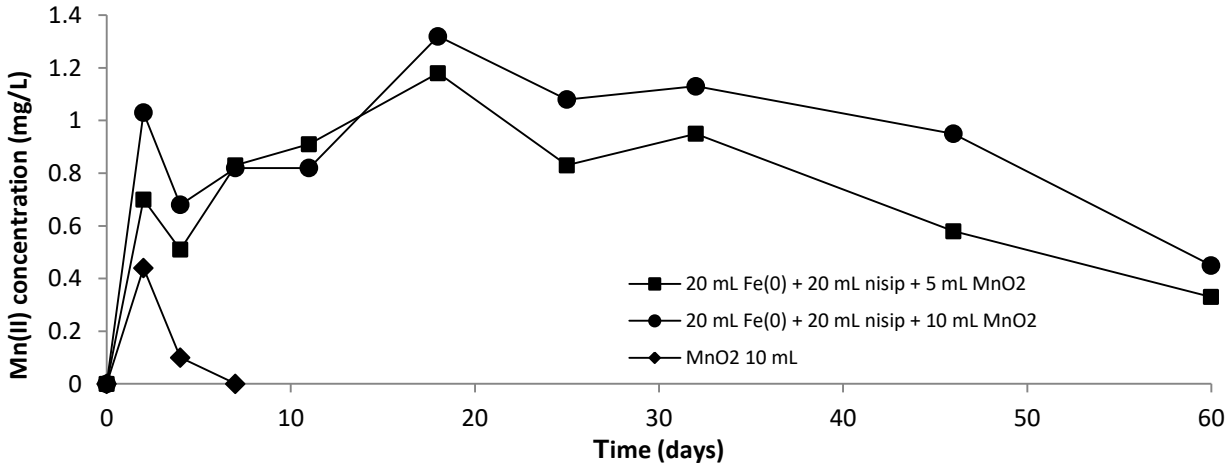

Fig.33. Evolution of Mn(II) concentration in column effluent, for columns packed with Fe^0 1-2 mm sand 0.5-1.25 mm and MnO_2, fed with solution Cr(VI) 5 mg/L, as a function of MnO_2 percentage. For comparison purposes, control experiments with bare MnO_2 are also plotted

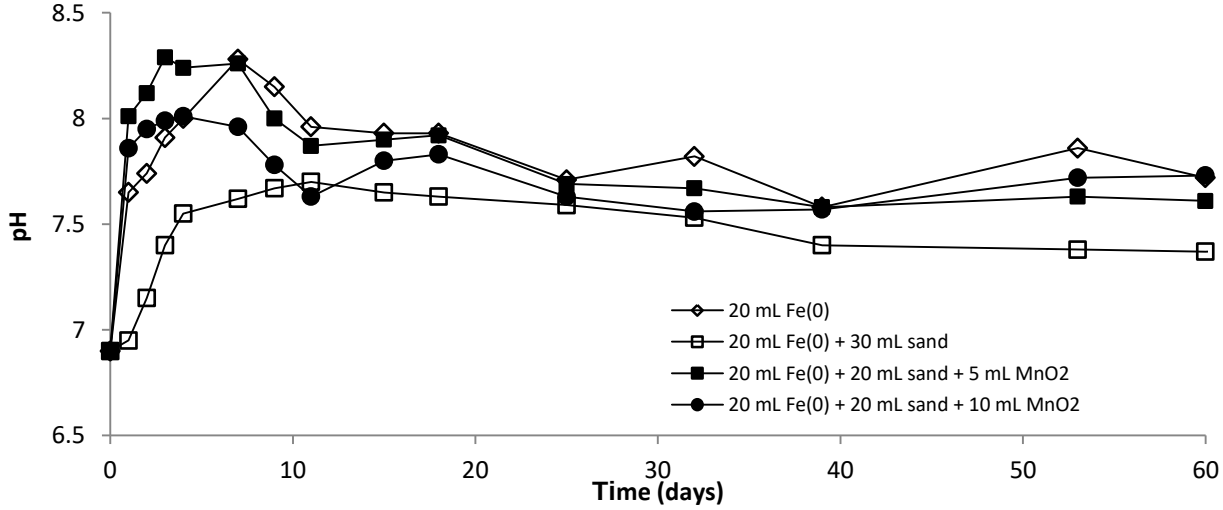

Fig.34. Evolution of pH in column effluent, for columns packed with Fe^0 1-2 mm, sand 0.5-1.25 mm and MnO_2, fed with solution Cr(VI) 5 mg/L, as a function of MnO_2 percentage. For comparison purposes, control experiments with bare Fe^0 1-2 mm and mixture of Fe^0 1-2 mm + sand 0.5-1.25 mm are also plotted.

4.3. Conclusions

Experiments carried out in batch system have shown that, in contrast with H_2O-Fe^0-Cr(VI) and H_2O-Fe^0-Sand-Cr(VI) systems, but just like for the H_2O-Fe^0-MnO_2-Cr(VI) system, the main mechanism of Cr(VI) removal in H_2O-Fe^0-Sand-MnO_2-Cr(VI) system was adsorption on the surface of MnO_2. In the co-presence of MnO_2 and sand, Cr(VI) reduction seems to be strongly inhibited. However, it should be pointed out that MnO_2 has the most important hindering effect, and not sand. The efficiency of Cr(VI) removal with Fe^0 decreased in following order: 32 ^oC >> 6 ^oC > 22 ^oC. This temperature dependence indicates that, at 32 ^oC, MnO_2 does not exert an inhibitory effect any

more. Hence, while at 6 and 22 ^{o}C the main mechanism of Cr(VI) removal in H_2O-Fe^0-Sand-MnO_2-Cr(VI) system was adsorption on the surface of MnO_2, at 32 ^{o}C the main Cr(VI) removal path was the indirect reduction of Cr(VI) to Cr(III) with Fe(II). Removal of Cr(VI) in H_2O-Fe^0-MnO_2-Sand-Cr(VI) system was very similar to that in H_2O-Fe^0-MnO_2-Cr(VI) system also in what concerns the kinetics of Cr(VI) removal, which was best modeled by the pseudo second-order kinetic model. The only difference between the two systems was a slight enhancement of the removal efficiency in the H_2O-Fe^0-MnO_2-Sand-Cr(VI) system, ascribed to the catalytic effect of sand at low Fe^0 doses.

Long-term column experiments carried out here have shown that the process of Cr(VI) removal with Fe^0 was inhibited in the co-presence of a mixture of sand + MnO_2. These results are comparable with those obtained in the co-presence of MnO_2. This phenomenon was ascribed to the fact that reaction between MnO_2 and Fe(II), which consumes Fe(II), was much faster than the one between MnO_2 and Fe^0, which generates Fe(II). Thus, the co-presence of sand does not attenuate the detrimental effect of MnO_2.

Objective 5. Investigation of the alternative to immobilize exhausted reactive mixtures in vitreous matrices.

Activities: Experiments for the synthesis and characterization of glasses from exhausted reactive mixtures

5.1 Immobilization of the retained chromium from exhausted reactive mixtures containing Fe(0) in glass matrices

The immobilization of the exhausted reactive mixtures was realized by vitrification together with two types of common glass wastes: window panes and cathode ray tubes (CRT).

5.1.1 Experimental procedure

The compositions of the precursor glass wastes, determined by X ray fluorescence using a Niton XL 3 analyzer, are presented in table 7.

Table 7. Oxidic composition of the precursor glass wastes [wt. %]

Oxide	Window pane	CRT
SiO_2	71.86	60.92
Na_2O	13.13	8.96
K_2O	0.02	7.44
CaO	9.23	0.67
MgO	5.64	0.14
BaO	-	10.80
PbO	-	8.85
Al_2O_3	0.08	2.07
Fe_2O_3	0.04	0.15

The two glass wastes were powdered by wet grinding using a Pulverisette laboratory mill than dried and sieved so that the granulometric fraction under 100 μm was kept in order to be used as glass precursor (Lazău and Vancea 2013).

The composition of the exhausted reactive mixture and the corresponding retained chromium from each column is presented in the tables 8-10.

Table 8. The composition of the exhausted reactive mixture and the corresponding retained chromium from each column from the Ist set [g].

Column	Fe^0 fraction 1-2 mm	Sand fraction 0.5-1.25 mm	Sand fraction 1.25-2 mm	Retained chromium [mg]
1	40	58.4	7.4	18.3
2	80	43.8	7.4	26.3
3	100	36.5	7.4	33.6
4	120	29.2	7.4	44.6
5	160	14.6	7.4	56.1

Table 9. The composition of the exhausted reactive mixture and the corresponding retained chromium from each column from the IInd set [g].

Column	Fe^0 fraction 1-2 mm	Sand fraction 0.5-1.25 mm	Sand fraction 1.25-2 mm	Retained chromium [mg]
1	40	58.4 (0.5-1.25 mm)	7.4	86
2	80	43.8 (0.5-1.25 mm)	7.4	138
3	100	36.5 (0.5-1.25 mm)	7.4	193
4	120	29.2 (0.5-1.25 mm)	7.4	202
5	160	14.6 (0.5-1.25 mm)	7.4	247
7	100	36.5 (0.1-0.5 mm)	7.4	177
8	100	0	43.9	81

Table 10. The composition of the exhausted reactive mixture and the corresponding retained chromium from each column from the IIIrd set [g].

Column	Fe^0 fraction 1-2 mm	Sand fraction 0.5-1.25 mm	Sand fraction 1.25-2 mm	Retained chromium [mg]
1	40	58.4 (<0.5 mm)	7.4	0
2	80	43.8 (<0.5 mm)	7.4	33
7	100	55.1 (0.5-1.25 mm)	7.4	39
8	100	14.6 (0.5-1.25 mm)	43.9	50

The exhausted reactive mixtures were dried at 105°C for 24 hours and then mixed together with the glass waste precursors.

The melting process was conducted at 1000°C for 180 minutes using a Nabertherm HTC08/16 electric furnace. The vitrification of the two types of wastes (glass and the reactive mixture containing chromium) in this economically advantageous conditions led to very viscous melts that were difficult to process. Therefore it was considered necessary to use borax as a flux in order to improve the fluidity of the melted glasses.

Three weight ratios exhausted reactive mixture-glass waste-borax were tested: 1-1-1, 1-2-1 and 1-1-2, the obtained glasses are presented in figure 35.

Fig.35. Glasses obtained using three different weight ratios exhausted reactive mixture-glass waste-borax

The initial idea was to use prevalently the two types of wastes on the expanse of the borax but, as the above picture shows, the amount of glass than can be process is low due to the high viscosity at the melting temperature. The increase of the flux amount have a positive effect upon the glass fluidity due to the fondant effect of the two oxides brought by borax: Na_2O and B_2O_3. The negative effect of the flux is the fragilization of the glass matrix due to the destructive effect of the alkaline oxide upon the vitreous structure. The samples corresponding to the weight ratio 1-1-2 were considered optimal and used in the future experiments. The composition of the glass samples is presented in table 11.

Table 11. Composition of the studied glasses

Sample	Set-column	Exhausted reactive mixture	Glass waste		Borax
			Window pane	CRT	
I.1G	I-1	1	1	-	2
I.2G	I-2	1	1	-	2
I.3G	I-3	1	1	-	2
I.4G	I-4	1	1	-	2
I.5G	I-5	1	1	-	2
I.1C	I-1	1	-	1	2
I.2C	I-2	1	-	1	2
I.3C	I-3	1	-	1	2
I.4C	I-4	1	-	1	2
I.5C	I-5	1	-	1	2
II.1G	II-1	1	1	-	2
II.2G	II-2	1	1	-	2
II.3G	II-3	1	1	-	2
II.4G	II-4	1	1	-	2
II.5G	II-5	1	1	-	2
II.7G	II-7	1	1	-	2
II.8G	II-8	1	1	-	2
II.1C	II-1	1	-	1	2

II.2C	II-2	1	-	1	2
II.3C	II-3	1	-	1	2
II.4C	II-4	1	-	1	2
II.5C	II-5	1	-	1	2
II.7C	II-7	1	-	1	2
II.8C	II-8	1	-	1	2
III.1G	III-1	1	1	-	2
III.2G	III-2	1	1	-	2
III.7G	III-7	1	1	-	2
III.8G	III-8	1	1	-	2
III.1C	III-1	1	-	1	2
III.2C	III-2	1	-	1	2
III.7C	III-7	1	-	1	2
III.8C	III-8	1	-	1	2

5.1.2 Properties of the obtained glasses

Considering the objective of this study – to immobilize the exhausted reactive mixtures containing chromium in vitreous matrices – the investigated properties for the obtained glasses were the phase composition and the chemical resistance towards chemical aggression.

5.1.2.1 Phase composition of the studied glasses

The phase composition of the studied glass samples was determined using a Rigaku Ultima 4 diffractometer.

The diffraction spectra corresponding to the samples II.8G and III.8G, containing the highest amount of coarse sand, are presented in figure 36.

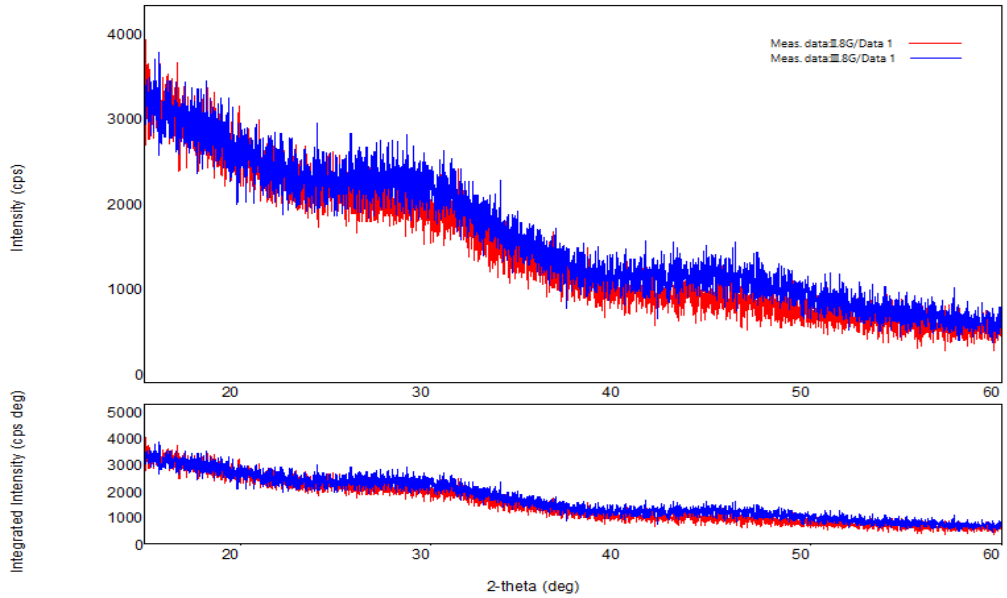

Fig.36. Diffraction spectra of the samples II.8G and III.8G

The diffuse pattern of both spectra confirm the amorphous character of the samples, confirming the purposed melting conditions.

5.1.2.2 Glasses hydrolytic stability

The hydrolytic stability of the glass ceramic samples was determined according to ISO 719-1985 (ISO 719-1985), using 2 grams of product, having particles size less than 500 µm, kept for 60 min in 50 mL de-ionized water at 98°C. A volume of 25 mL of the obtained solution was titrated against 0.01 mol/l HCl solution. The volume of HCl needed for neutralization is recorded in order to express the equivalent R_2O extracted and the corresponding stability class. The obtained results are presented in table 12 and illustrated in figure 37.

Table 12. Extracted R_2O and hydrolytic stability classes for the studied glasses

Sample	Alkali oxide leached [µg/g glass]	Stability class	Sample	Alkali oxide leached [µg/g glass]	Stability class	Sample	Alkali oxide leached [µg/g glass]	Stability class
I.1G	15.45	HGB1	II.1G	15.45	HGB1	III.1G	14.25	HGB1
I.2G	18.6	HGB1	II.2G	18.6	HGB1	III.2G	15.05	HGB1
I.3G	22.25	HGB1	II.3G	22.25	HGB1	III.7G	17.85	HGB1
I.4G	25.8	HGB1	II.4G	25.8	HGB1	III.8G	18.95	HGB1
I.5G	30.55	HGB1	II.5G	30.55	HGB1	III.1C	13.35	HGB1
I.1C	13.95	HGB1	II.7G	21.75	HGB1	III.2C	15.4	HGB1
I.2C	16.05	HGB1	II.8G	35.5	HGB2	III.7C	16.8	HGB1
I.3C	20.15	HGB1	II.1C	13.95	HGB1	III.8C	18.25	HGB1
I.4C	23.25	HGB1	II.2C	16.05	HGB1			
I.5C	27.65	HGB1	II.3C	20.15	HGB1			
			II.4C	23.25	HGB1			
			II.5C	27.65	HGB1			
			II.7C	20.2	HGB1			
			II.8C	33.55	HGB2			

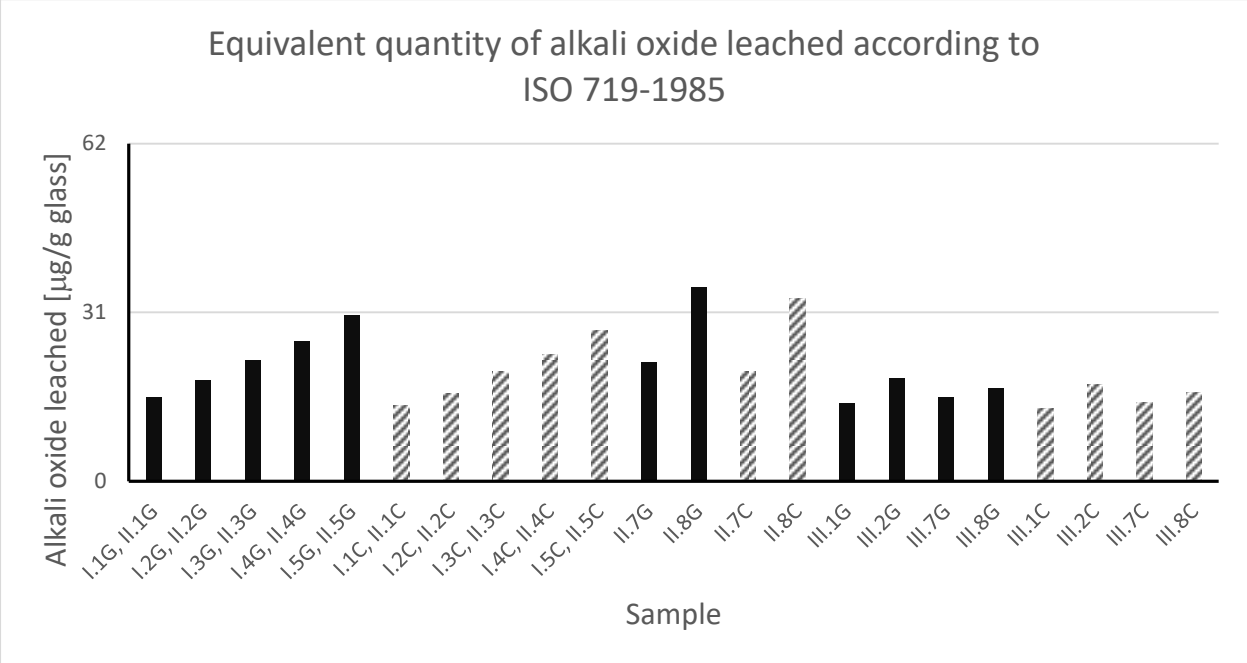

Fig.37. Evolution of alkali oxide losses in the investigated samples

The studied glasses excepting II.8G and II.8C belongs to the most stable class of glasses HGB1. The two exceptions correspond to HGB2 stability class, common to most of the industrial types of glasses.

A major influence upon the hydrolytic stability of the synthesized glasses is that of the SiO_2 amount brought as sand within the exhausted reactive mixture as it is presented in figure 38.

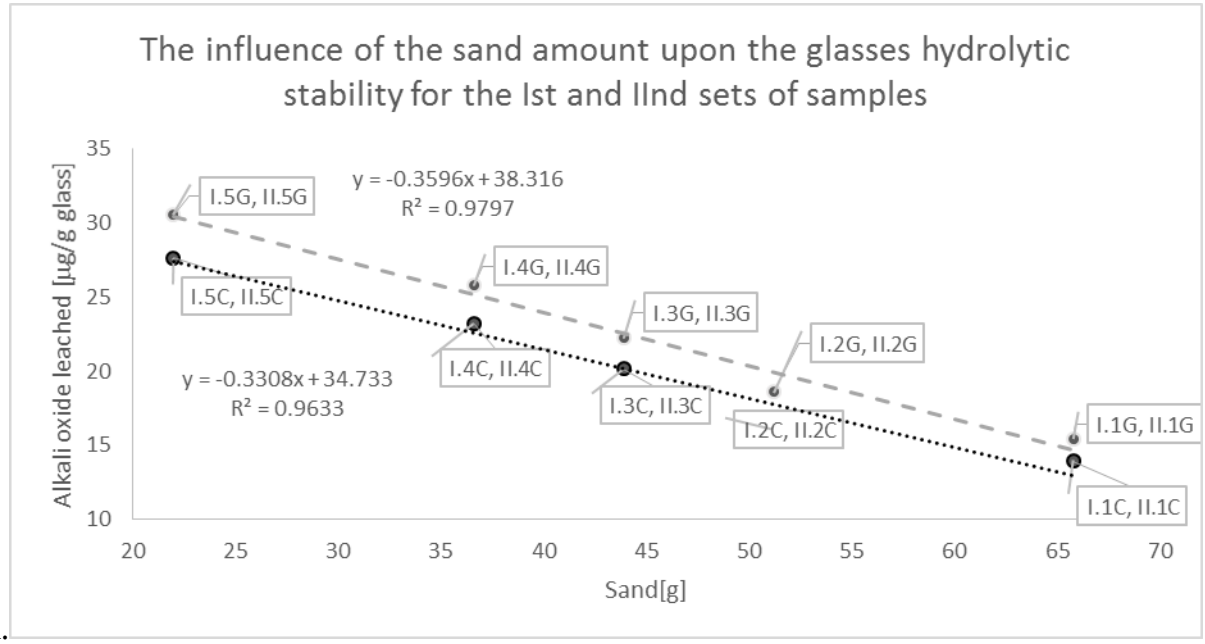

a.

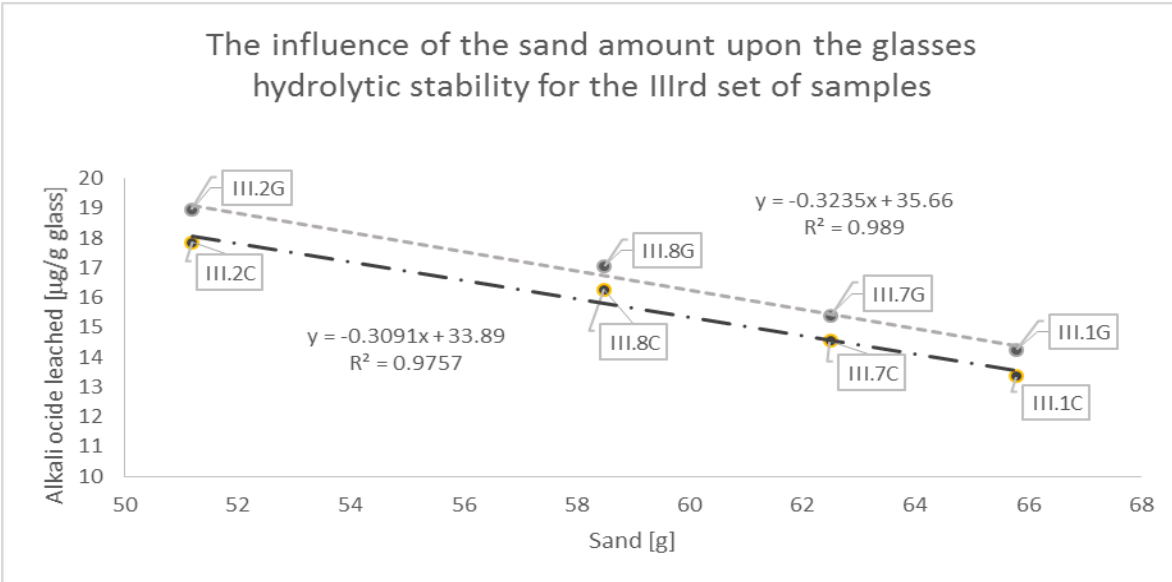

b.

Fig.38. The influence of the sand amount upon the hydrolytic stability of the glasses containing exhausted reactive mixtures from: a - Ist and IInd set of columns; b - IIIrd set of columns.

All the studied glasses show a quasilinear dependence of their hydrolytic stability upon the quantity of sand from the exhausted reactive mixture used as precursor. The explanation of this behavior is based on the stabilization effect of SiO_2 upon the vitreous matrix knowing that this oxide is a glass network former.

5.1.2.3. Chemical stability of the studied glasses

The chemical stability of the glasses was investigated by measuring the dissolution rate of the samples immersed in three extraction mediums having pH 5.5, 7.0 and 8.5 respectively for 28 days. The volume of the utilized solutions of 100 mL was maintained constant during the considered determination time at a constant temperature of 20 ± 2°C. After 28 days the samples were dried for 6 hours at 110°C until they reach constant mass. The dissolution rate of the glass samples is expressed as weight loss in time as it is presented in equation 20.

$$\mathrm{Dr} = \frac{\Delta \mathrm{m}}{t} = \frac{m_i - m_f}{t} \quad [\mu g/h] \qquad (20)$$

where: m_i is the initial sample mass, m_f the final sample mass and t represents the considered experimental time of 28 days.

The calculated values for the dissolution rate of the investigated samples are presented in the table 13 and illustrated in the figure 39.

Table 13. Dissolution rates of the studied glasses

Sample	Dissolution rate [µg/h]			Sample	Dissolution rate [µg/h]			Sample	Dissolution rate [µg/h]		
	pH				pH				pH		
	pH=5.5	pH=7.0	pH=8.5		pH=5.5	pH=7.0	pH=8.5		pH=5.5	pH=7.0	pH=8.5
I.1G	0.013	0.013	0.143	II.1G	0.013	0.013	0.143	III.1G	0.012	0.013	0.155
I.2G	0.015	0.016	0.153	II.2G	0.015	0.016	0.153	III.2G	0.017	0.014	0.212
I.3G	0.030	0.034	0.208	II.3G	0.030	0.034	0.208	III.7G	0.013	0.014	0.185
I.4G	0.030	0.037	0.291	II.4G	0.030	0.037	0.291	III.8G	0.014	0.015	0.200
I.5G	0.058	0.059	0.414	II.5G	0.058	0.059	0.414	III.1C	0.013	0.013	0.149

I.1C	0.015	0.013	0.158	II.7G	0.029	0.028	0.206	III.2C	0.016	0.017	0.234
I.2C	0.022	0.022	0.195	II.8G	0.035	0.035	0.331	III.7C	0.014	0.015	0.174
I.3C	0.030	0.032	0.232	II.1C	0.015	0.013	0.158				
I.4C	0.033	0.034	0.316	II.2C	0.022	0.022	0.195				
I.5C	0.043	0.038	0.492	II.3C	0.030	0.032	0.232				
				II.4C	0.033	0.034	0.316				
				II.5C	0.043	0.038	0.492				
				II.7C	0.022	0.022	0.201				
				II.8C	0.031	0.030	0.286				

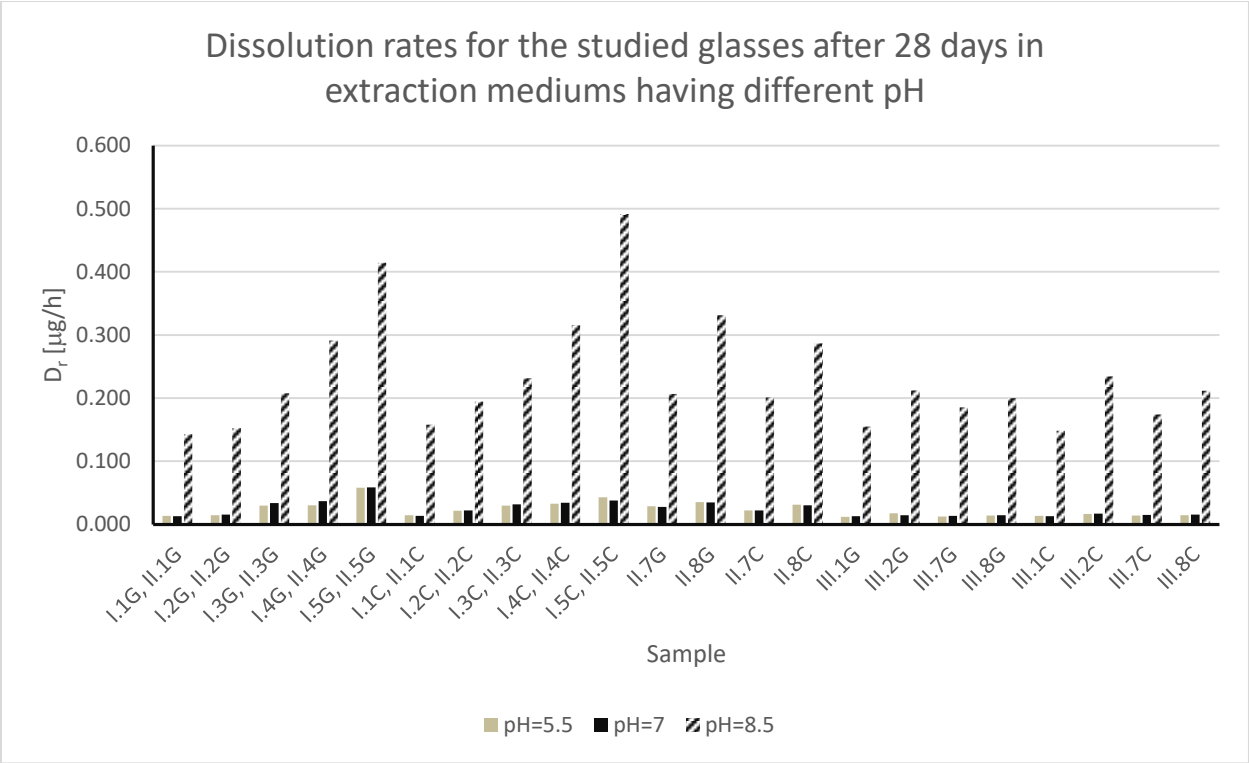

Fig.39. Dissolution rates of the studied glasses

Two different behaviors can be observed, one for acidic and neutral mediums and another for alkaline medium. At pH = 5.5 and pH = 7.0 the glasses dissolution rates are very low, between 0.013-0.059 µg/h. This can be explain by the leaching of the alkali oxides from the glass surface in acidic and neutral mediums that lead to an enrichment in SiO_2 at the surface level. This oxide has an acidic character and therefore it is insoluble in the considered mediums. Consequently it creates a passivation effect that causes the lower dissolution rates values.

The alkaline environment leach SiO_2 and B_2O_3, both network former oxides, generating a continuous aggressive attack on the vitreous matrix. Without the passive layer the glasses are more sensitive to the alkaline medium and therefore the dissolution rate values are higher than in the previous case, between 0.143-0.492 µg/h.

5.1.2.4. Chromium and iron ions immobilization in glasses

The chromium and iron immobilization capacity of the studied glasses was investigated by measuring the chromium ions extraction using leaching tests performed according to the American Extraction Procedure Toxicity Test (US EPA625/6-89/022). Three extraction mediums having pH 5.5, 7.0 and 8.5 respectively were used, analysis being performed after 1, 14 and 28 days. The buffer solutions from 5.5, 7.0 and 8.5 pH were prepared by taking 2.5% v/v glacial acetic acid in water and by adding concentrated ammonia solution until the desired pH value was reached. The pH of the solution was measured using a digital pH meter (Type E-500). Two grams of each sample were taken and shaken with 250 mL of ammonia–acetate buffer solution for different time periods at a constant temperature of 20 ± 2°C. The chromium and iron concentration in the extraction mediums was measured using a Bruker Aurora M90 Inductively Coupled Plasma Mass Spectrometer.

The chromium ions leached from the studied glasses in the three chemical aggressive environments for the three considered periods of time are presented in the table 14 and illustrated in the figure 40.

Table 14. Chromium ions leached from the investigated glasses

Sample	Chromium ions leached [%]								
	7 days			14 days			28 days		
	pH=5.5	pH=7.0	pH=8.5	pH=5.5	pH=7.0	pH=8.5	pH=5.5	pH=7.0	pH=8.5
I.1G	0.0000	0.0000	0.0000	0.0000	0.0000	0.0000	0.0000	0.0000	0.0016
I.2G	0.0000	0.0000	0.0000	0.0000	0.0000	0.0000	0.0000	0.0000	0.0020
I.3G	0.0000	0.0000	0.0000	0.0021	0.0018	0.0076	0.0042	0.0043	0.0061
I.4G	0.0000	0.0000	0.0000	0.0035	0.0036	0.0080	0.0054	0.0051	0.0071
I.5G	0.0000	0.0000	0.0000	0.0039	0.0039	0.0083	0.0069	0.0064	0.0091
I.1C	0.0000	0.0000	0.0000	0.0000	0.0000	0.0000	0.0000	0.0000	0.0018
I.2C	0.0000	0.0000	0.0000	0.0000	0.0000	0.0000	0.0000	0.0000	0.0021
I.3C	0.0000	0.0000	0.0000	0.0000	0.0000	0.0000	0.0000	0.0000	0.0046
I.4C	0.0000	0.0000	0.0000	0.0031	0.0042	0.0088	0.0045	0.0051	0.0096
I.5C	0.0000	0.0000	0.0000	0.0032	0.0046	0.0092	0.0054	0.0061	0.0104
II.1G	0.0000	0.0000	0.0000	0.0042	0.0041	0.0098	0.0044	0.0043	0.0107
II.2G	0.0000	0.0000	0.0000	0.0047	0.0044	0.0104	0.0048	0.0045	0.0112
II.3G	0.0000	0.0000	0.0000	0.0051	0.005	0.0111	0.0053	0.0051	0.0125
II.4G	0.0000	0.0000	0.0000	0.0051	0.0051	0.0117	0.0055	0.0055	0.0133
II.5G	0.0000	0.0000	0.0000	0.0055	0.0057	0.0121	0.0056	0.0058	0.0148
II.7G	0.0000	0.0000	0.0000	0.0049	0.0049	0.0125	0.005	0.0051	0.0122
II.8G	0.0000	0.0000	0.0000	0.0041	0.0042	0.0093	0.0041	0.0044	0.0108
II.1C	0.0000	0.0000	0.0000	0.0040	0.0041	0.0089	0.004	0.0041	0.0105
II.2C	0.0000	0.0000	0.0000	0.0044	0.0044	0.0091	0.0045	0.0044	0.0118
II.3C	0.0000	0.0000	0.0000	0.0048	0.0047	0.0101	0.0049	0.0048	0.1210
II.4C	0.0000	0.0000	0.0000	0.0050	0.0050	0.0109	0.0052	0.0051	0.0129
II.5C	0.0000	0.0000	0.0000	0.0055	0.0052	0.0117	0.0055	0.0052	0.0130
II.7C	0.0000	0.0000	0.0000	0.0049	0.0051	0.0110	0.0051	0.0052	0.0150
II.8C	0.0000	0.0000	0.0000	0.0042	0.0040	0.0103	0.0042	0.0040	0.0105

III.1G	0.0000	0.0000	0.0000	0.0000	0.0000	0.0000	0.0000	0.0000	0.0000
III.2G	0.0000	0.0000	0.0000	0.0000	0.0000	0.0000	0.0000	0.0000	0.0011
III.7G	0.0000	0.0000	0.0000	0.0020	0.0018	0.0064	0.0022	0.0020	0.0085
III.8G	0.0000	0.0000	0.0000	0.0029	0.0025	0.0071	0.0030	0.0025	0.0097
III.1C	0.0000	0.0000	0.0000	0.0000	0.0000	0.0000	0.0000	0.0000	0.0000
III.2C	0.0000	0.0000	0.0000	0.0000	0.0000	0.0000	0.0000	0.0000	0.0010
III.7C	0.0000	0.0000	0.0000	0.0020	0.0015	0.0058	0.0020	0.0017	0.0078
III.8C	0.0000	0.0000	0.0000	0.0031	0.0022	0.0069	0.0031	0.0023	0.0085

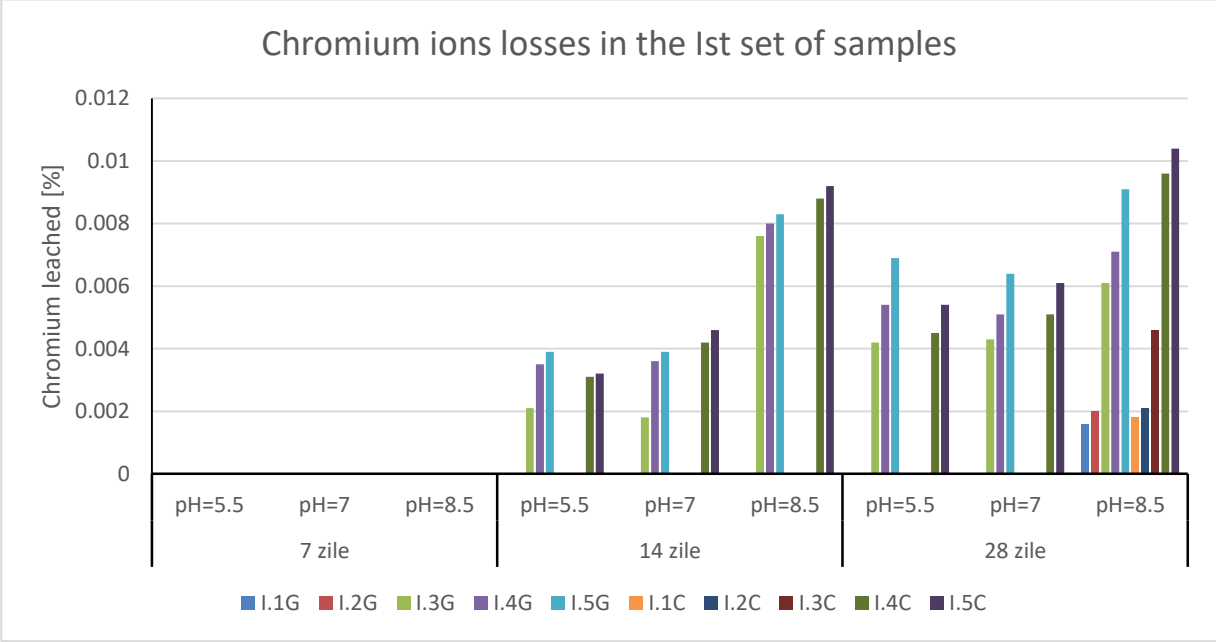

a.

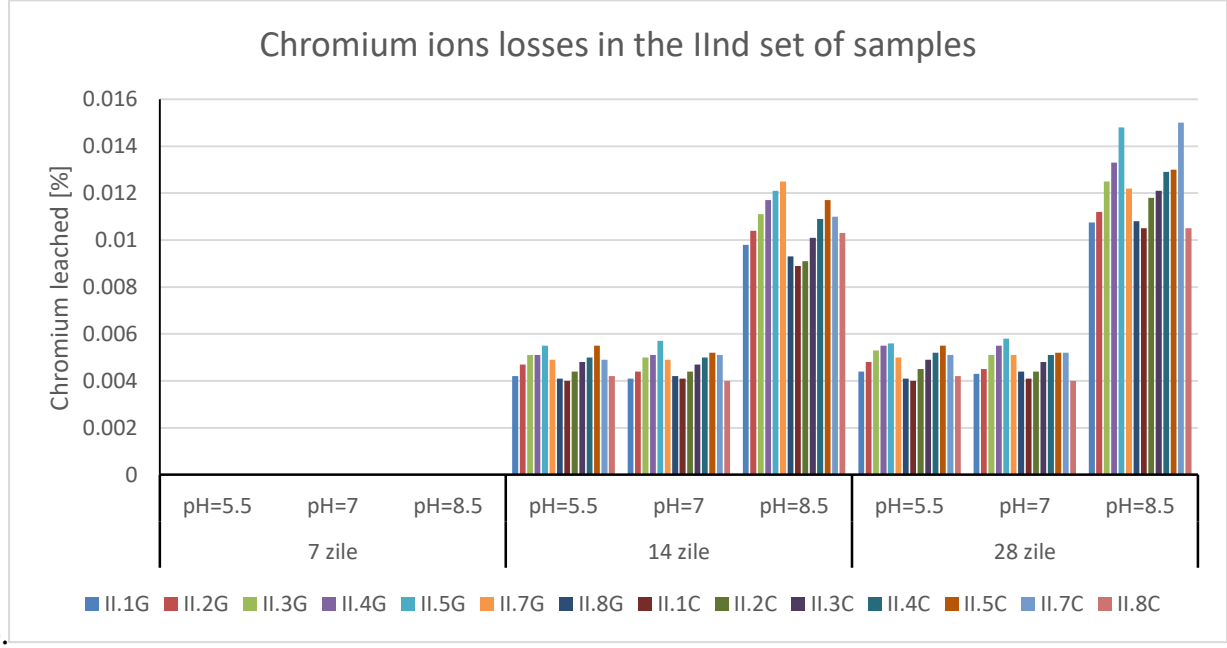

b.

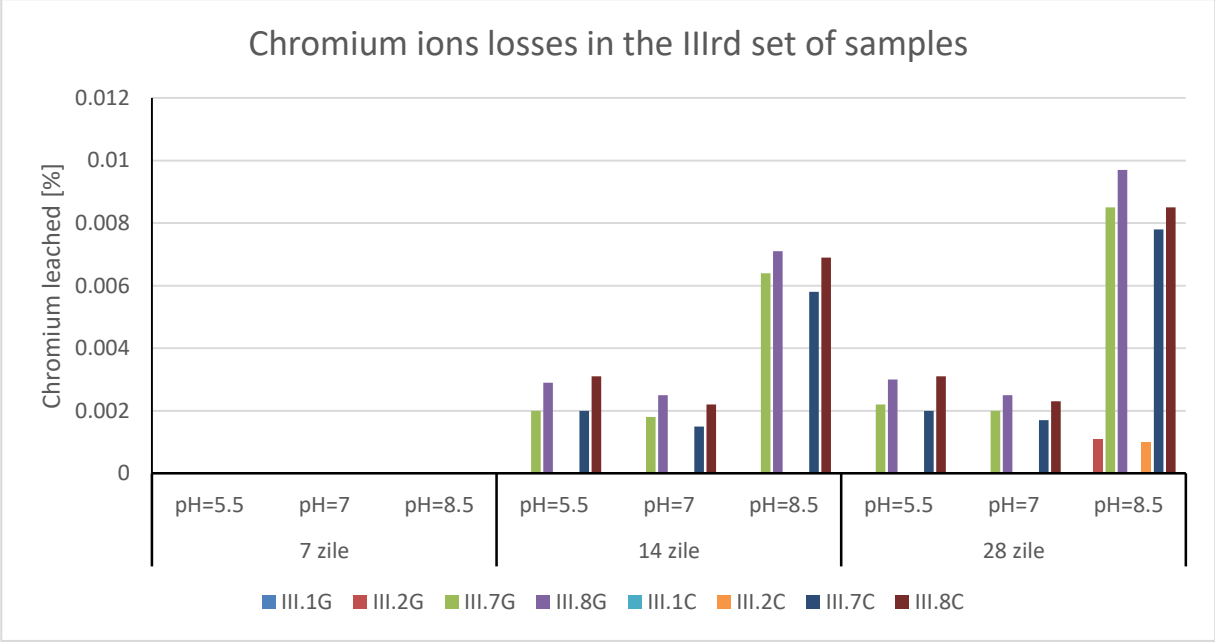

c.

Fig.40. Cromium ions losses from the glasses containing exhausted reactive mixtures from: a - Ist set of columns; b - IInd set of columns; c - IIIrd set of columns.

The amount of chromium ions leached from all the investigated glasses regardless the environment's pH and the considered time is very low, between 0-0.0148% of the total chromium brought by the exhausted reactive mixtures.

The vitrification of the exhausted reactive mixtures from the first set of columns leads to glass with no discernable losses of chromium after 7 days, regardless of the environment's pH. At the 14 days term, the samples I.1G and I.2.G containing window panes glass wastes and I.1C-I.3C containing CRT glass wastes show no chromium losses. With increasing the amount of exhausted reactive mixture amount more chromium ions are leached since the mixture is the ion bearing vector. The corresponding decrease of the SiO_2 amount generates a lower encapsulation of the chromium ions in the glass network. The CRT glass generates at the synthesizing temperature more fluid melts comparing to window pane glass and therefore increase the chromium immobilization.

All the obtained glasses show higher chromium losses in alkaline environment compared to acid and neutral environments, due to the passivation effect discussed in chapter 5.1.2.3.

The glasses obtained based on the second set of columns exhausted reactive mixtures don't present discernable chromium ions losses after 7 days, regardless the environment's pH. After 14 and 28 days, the losses in acidic and neutral mediums are comparable and both are lower than those recorded in alkaline environment due to the lower resistance of glass towards this last medium. Comparing to the previous set of samples, chromium losses are higher in the second set due to a higher amount of chromium introduced with the exhausted reactive mixtures.

The samples synthesized using exhausted reactive mixtures from the third set of columns don't present any discernable chromium losses after 7 days, regardless the mediums' pH. The sample III.1 has no chromium adsorbed in the column and therefore were no chromium losses. The sample III.2 is stable towards the three aggressive environments after 14 days. Similarly to the previous sets of samples, all glasses are more sensitive to the alkaline environment as it was explained before.

The iron ions losses for all the investigated samples are presented in the table 15 and illustrated in the figure 41.

Table 15. Iron ions leached from the investigated glasses

Sample	Iron ions leached [%]								
	7 days			14 days			28 days		
	pH=5.5	pH=7	pH=8.5	pH=5.5	pH=7	pH=8.5	pH=5.5	pH=7	pH=8.5
I.1G	0.0000	0.0000	0.0000	0.0000	0.0000	0.0000	0.0000	0.0000	0.0015
I.2G	0.0000	0.0000	0.0000	0.0000	0.0000	0.0000	0.0000	0.0000	0.0023
I.3G	0.0000	0.0000	0.0000	0.0010	0.0011	0.0022	0.0011	0.0011	0.0029
I.4G	0.0011	0.0011	0.0025	0.0011	0.0012	0.0031	0.0011	0.0012	0.0038
I.5G	0.0015	0.0014	0.0031	0.0016	0.0014	0.0036	0.0014	0.0015	0.0042
I.1C	0.0000	0.0000	0.0000	0.0000	0.0000	0.0000	0.0000	0.0000	0.0010
I.2C	0.0000	0.0000	0.0000	0.0000	0.0000	0.0000	0.0000	0.0000	0.0015
I.3C	0.0000	0.0000	0.0000	0.0010	0.0010	0.0018	0.0010	0.0010	0.0025
I.4C	0.0010	0.0010	0.0018	0.0011	0.0010	0.0023	0.0011	0.0011	0.0029
I.5C	0.0013	0.0014	0.0025	0.0014	0.0014	0.0031	0.0014	0.0014	0.0040
II.1G	0.0000	0.0000	0.0000	0.0000	0.0000	0.0000	0.0000	0.0000	0.0015
II.2G	0.0000	0.0000	0.0000	0.0000	0.0000	0.0000	0.0000	0.0000	0.0023
II.3G	0.0000	0.0000	0.0000	0.0010	0.0011	0.0022	0.0011	0.0011	0.0029
II.4G	0.0011	0.0011	0.0025	0.0011	0.0012	0.0031	0.0011	0.0012	0.0038
II.5G	0.0015	0.0014	0.0031	0.0016	0.0014	0.0036	0.0014	0.0015	0.0042
II.7G	0.0000	0.0000	0.0000	0.0010	0.0010	0.0021	0.0010	0.0011	0.0028
II.8G	0.0000	0.0000	0.0000	0.0013	0.0011	0.0025	0.0014	0.0012	0.0032
II.1C	0.0000	0.0000	0.0000	0.0000	0.0000	0.0000	0.0000	0.0000	0.0010
II.2C	0.0000	0.0000	0.0000	0.0000	0.0000	0.0000	0.0000	0.0000	0.0015
II.3C	0.0000	0.0000	0.0000	0.0010	0.0010	0.0018	0.0010	0.0010	0.0025
II.4C	0.0010	0.0010	0.0018	0.0011	0.0010	0.0023	0.0011	0.0011	0.0029
II.5C	0.0013	0.0014	0.0025	0.0014	0.0014	0.0031	0.0014	0.0014	0.0040
II.7C	0.0000	0.0000	0.0000	0.0010	0.0010	0.0015	0.0010	0.0010	0.0020
II.8C	0.0000	0.0000	0.0000	0.0013	0.0012	0.0021	0.0013	0.0013	0.0031
III.1G	0.0000	0.0000	0.0000	0.0000	0.0000	0.0012	0.0000	0.0000	0.0018
III.2G	0.0000	0.0000	0.0000	0.0000	0.0000	0.0019	0.0000	0.0000	0.0023
III.7G	0.0000	0.0000	0.0000	0.0000	0.0000	0.0022	0.0000	0.0000	0.0026
III.8G	0.0000	0.0000	0.0000	0.0010	0.0010	0.0024	0.0010	0.0011	0.0029
III.1C	0.0000	0.0000	0.0000	0.0000	0.0000	0.0010	0.0000	0.0000	0.0015
III.2C	0.0000	0.0000	0.0000	0.0000	0.0000	0.0014	0.0000	0.0000	0.0020
III.7C	0.0000	0.0000	0.0000	0.0000	0.0000	0.0021	0.0000	0.0000	0.0024
III.8C	0.0000	0.0000	0.0000	0.0000	0.0000	0.0025	0.0000	0.0000	0.0030

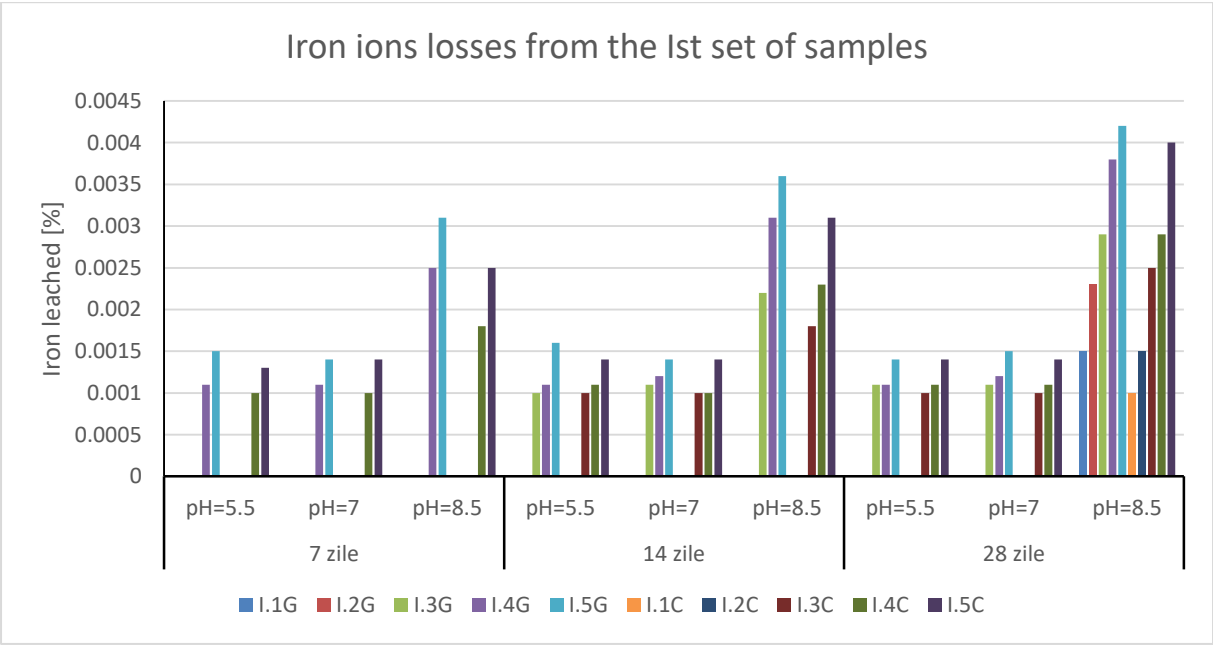
Iron ions losses from the Ist set of samples
Iron leached [%]
0.0045
0.004
0.0035
0.003
0.0025
0.002
0.0015
0.001
0.0005
0
pH=5.5
pH=7
pH=8.5
pH=5.5
pH=7
pH=8.5
pH=5.5
pH=7
pH=8.5
7 zile
14 zile
28 zile
I.1G
I.2G
I.3G
I.4G
I.5G
I.1C
I.2C
I.3C
I.4C
I.5C

a.

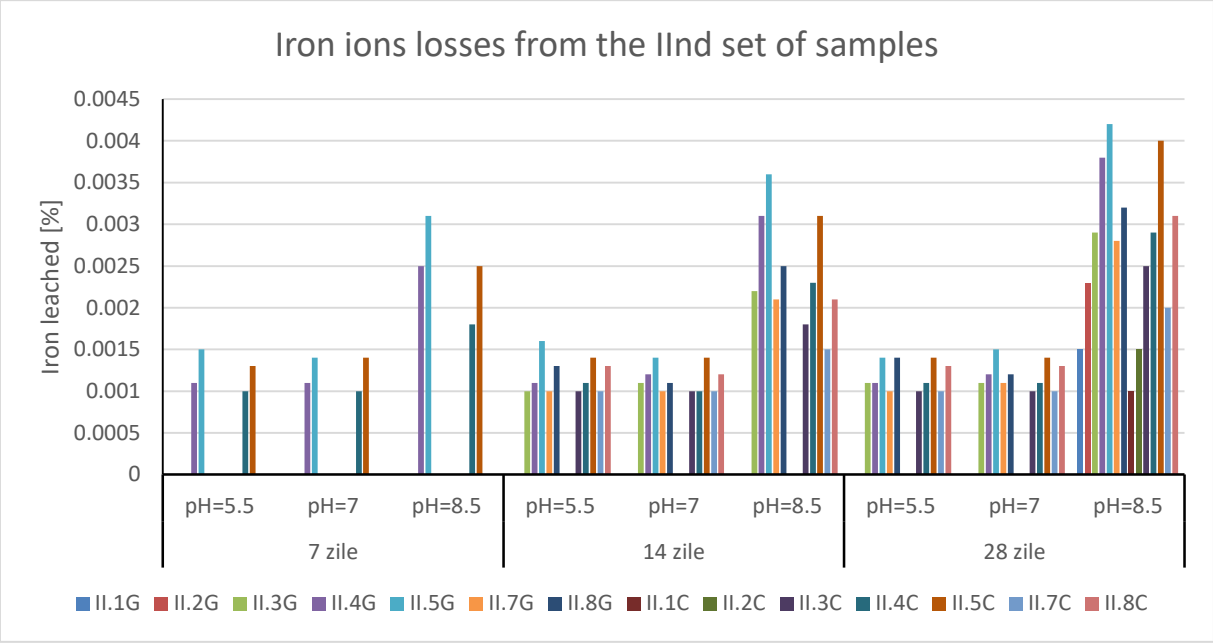
Iron ions losses from the IInd set of samples
Iron leached [%]
0.0045
0.004
0.0035
0.003
0.0025
0.002
0.0015
0.001
0.0005
0
pH=5.5
pH=7
pH=8.5
pH=5.5
pH=7
pH=8.5
pH=5.5
pH=7
pH=8.5
7 zile
14 zile
28 zile
II.1G
II.2G
II.3G
II.4G
II.5G
II.7G
II.8G
II.1C
II.2C
II.3C
II.4C
II.5C
II.7C
II.8C

b.

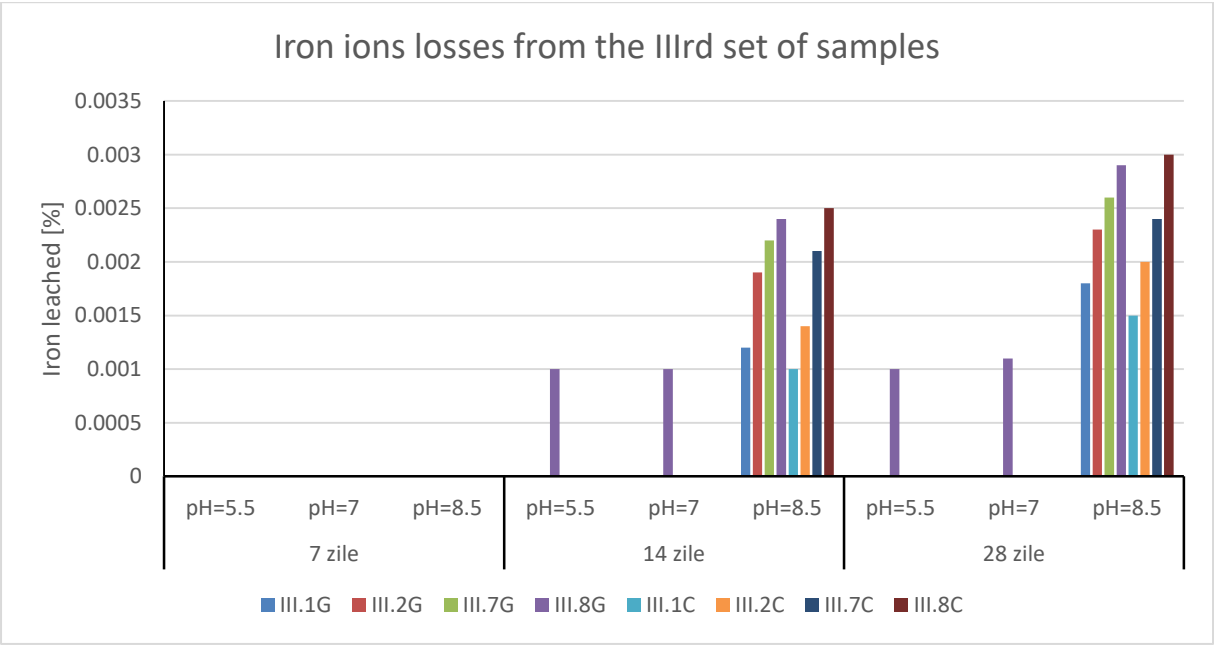

c.

Fig.41. Iron ions losses from the glasses containing exhausted reactive mixtures from: a - Ist set of columns; b - IInd set of columns; c - IIIrd set of columns.

The amount of iron ions leached from all the investigated glasses regardless the environment's pH and the considered time is very low, between 0-0.0042 % of the total iron brought by the exhausted reactive mixtures.

The samples I.1-I.5 and II.1-II.5 contain the same amount and granulometry of iron an therefore they have a similar behavior regarding the iron immobilization in the three chemically aggressive environments at all terms. For all the glasses from this sets, increasing the amount of iron and decreasing the amount of SiO_2 leads to a lesser encapsulation of the iron ions in the glass network and consequently generates a lower immobilization.

The use of a coarser iron particles generates a fragilization of the glass matrix as it is shown by the results for the glasses II.7 and II.8.

Using more fine iron particles in the third set leads to a better encapsulation of the iron ions in the glass matrix, generating the lowest values for the iron losses in this set compared to the previous two sets of glasses. The samples III.1-III.7 have no discernable iron losses in acidic and neutral environments for the three considered periods of time.

Similarly to the previous sets of samples, all glasses are more sensitive to the alkaline environment as it was explained before.

5.1.3 Conclusions

- The focus of this research is to immobilize the chromium and iron ions retained on exhausted reactive mixtures by vitrification together with two common glass wastes: window panes and cathode ray tubes.
- For economic reasons regarding the melting process the use of borax as a flux was necessary. Different ratios exhausted reactive mixture-glass wastes-borax was tested, the optimal value for the ration being established at 1-1-2.
- The obtained glasses were characterized from their capacity for immobilization of chromium and iron ions point of view.
- The hydrolytic stability of the studied glasses was measured. The majority of the glasses belong to HGB1 stability class, the best one according to ISO 719-1985. A

quasilinear dependence of the hydrolytic stability upon the amount of SiO_2 brought with the exhausted reactive mixture was established.

- The chemical stability of the glass samples was established by measuring the dissolution rate after 28 days in mediums having different pH. The low values recorded confirm the very good stability conferred by the glass matrix. The glasses present a high chemical stability towards the acidic and neutral environments, the recorded losses being between 0.013-0.059 μg/h. All the studied samples are more sensitive to the alkaline medium, the corresponding dissolution rates ranged from 0.143-0.492 μg/h. due to the absence of the passivation layer.
- The chromium ions leached in the three aggressive environments after 7, 14 and 28 days according to the American Extraction Procedure Toxicity Test were very low, ranging from 0-0.0148 % of the total chromium brought by the exhausted reactive mixtures.
- The amount of iron ions leached from all the investigated glasses regardless the environment's pH and the considered time is very low, between 0-0.0042 % of the total iron brought by the exhausted reactive mixtures.
- Decreasing the size of the iron particles leads to a better encapsulation of the iron ions in the glass matrix, generating the lowest values for the iron losses
- The higher amount of losses of both chromium and iron ions are generated by the alkaline environment that leach SiO_2 and B_2O_3, both network former oxides, generating a continuous aggressive attack on the vitreous matrix..
- The CRT glass generates at the synthesizing temperature more fluid melts comparing to window pane glass and therefore increase the chromium and iron ions immobilization.
- The obtained results confirm the viability of the suggested solution for immobilizing chromium contained in the exhausted reactive mixtures together with common glass wasted in order to obtain glasses having very high chemical stability with multiple economic advantages.

5.2. Immobilization of the retained chromium from exhausted reactive mixtures containing Fe(0) in ceramic matrices

The aim of this study was to immobilize the chromium ions retained in the exhausted reactive mixtures in ceramic matrices together with Bojidar kaolin.

5.2.1 Experimental procedure

The oxidic composition of the Bojidar kaolin is presented in table 16 (Goleanu et al., 2004).

Table 16. Oxidic composition of the Bojidar kaolin [%]

Oxide	Bojidar kaolin
SiO_2	49.29
Na_2O	0.14
K_2O	0.87
CaO	0.56
MgO	0.44
Al_2O_3	35.18
Fe_2O_3	0.78
TiO_2	0.43
P.C.	12.31

Three initial ratios exhausted reactive mixture:kaolin were tested: 2:1, 1:1 and 1:2. The homogenization process was realized by wet grinding using a Pulverisette laboratory mill. The mixture was dried at 120°C for 6h and then pressed into cylinders having the diameter and height around 35 mm using an uniaxial Greisinger Electronics M.P 150 D press using 6 tf.

The thermal treatment was conducted at 800, 900 and 1000°C for 90 minutes using a Nabertherm HTC08/16 electric furnace.

The ceramic samples obtained using the exhausted reactive mixture:kaolin ratio 2:1 present after the thermal treatment a large number of cracks extended in the whole volume being thereby unfit for further investigations.

5.2.2 Preliminary investigations

The following determinations were focused on the optimization of the initial compositions in order to achieve the highest chromium and iron immobilization in the ceramic matrices.

5.2.2.1 The apparent porosity of the ceramic samples

The apparent porosity represents the contribution of the open pores to the total porosity of a porous material being calculated as follows:

$$P_{ap} = \frac{\rho_a \cdot a}{\rho_0} \ [\%] \quad (21)$$

where: - ρ_a represents the apparent density of the material [g/cm^3];

- ρ_0 represents the density of the working fluid [g/cm^3];
- a represents the absorption capacity of the studied material.

The apparent porosity of the obtained ceramics was measured using the liquid saturation method under vacuum with water as working liquid.

The values of the apparent porosity for the samples obtained at 800, 900 and 1000°C are presented in the table 17 for the two exhausted reactive mixture:kaolin ratios 1:1 and 1:2.

Table 17. The apparent porosity (P_{ap}) of the obtained ceramic samples

Sample	**P_{ap}[%]**					
	exhausted reactive mixture:kaolin 1:1			**exhausted reactive mixture:kaolin 1:2**		
	800˚C	**900 ˚C**	**1000 ˚C**	**800˚C**	**900 ˚C**	**1000 ˚C**
I.1	29.65	25.45	18.75	35.45	33.15	30.75
I.2	33.55	27.25	21.15	41.95	37.10	35.45
I.3	38.85	35.35	33.15	44.35	41.20	39.15
I.4	41.15	37.25	35.45	47.23	44.85	42.75
I.5	44.15	42.85	40.15	50.75	48.15	45.25

5.2.2.2 The chromium ions immobilization in the initial ceramic samples

The high values of the apparent porosity presented in table 17 lead to the assumption that theses samples may have high chromium losses due to the large sample's specific surface exposed to the chemical aggression. Therefore the chromium dissolution from the initial samples was studied

according to the American Extraction Procedure Toxicity Test as it was previously presented in the chapter 5.1.2.4. The obtained results are presented in the tables 18 and 19.

Table 18 Chromium ions leached from the initial ceramics for the exhausted reactive mixture:kaolin ratio 1:1

Sample	Chromium ions leached [%]								
	800˚C			900 ˚C			1000 ˚C		
	pH=5.5	pH=7	pH=8.5	pH=5.5	pH=7	pH=8.5	pH=5.5	pH=7	pH=8.5
I.1	8.1554	8.1684	10.7514	7.5522	7.6115	9.0244	4.2323	4.2095	6.1115
I.2	8.8755	8.8268	12.6545	7.8015	7.7848	10.235	5.8955	5.9012	7.4868
I.3	9.3577	9.3281	14.4220	9.8710	9.8916	14.4248	8.7815	8.7909	12.4407
I.4	12.5545	12.4588	19.1055	11.0578	11.0611	17.4581	9.8515	9.8645	14.2841
I.5	15.9822	15.8875	21.1187	14.2365	14.2219	20.4408	12.5019	12.4899	18.9578

Table 19 Chromium ions leached from the initial ceramics for the exhausted reactive mixture:kaolin ratio 1:2

Sample	Chromium ions leached [%]								
	800˚C			900 ˚C			1000 ˚C		
	pH=5.5	pH=7	pH=8.5	pH=5.5	pH=7	pH=8.5	pH=5.5	pH=7	pH=8.5
I.1	9.8655	9.8702	14.5119	8.8489	8.8255	12.5945	8.1724	8.1695	10.8115
I.2	12.5815	12.5711	19.2341	11.0775	11.0805	17.5230	9.8715	9.8728	14.5425
I.3	16.0115	15.9489	21.255	12.4885	12.4915	19.1125	10.0515	10.0148	15.1585
I.4	18.9408	18.9387	23.8117	16.025	15.9925	21.1523	14.2518	14.2395	20.5105
I.5	20.5485	20.5512	25.755	19.2515	18.2482	23.9455	16.8972	16.8544	22.1775

The chromium ions losses for both considered ratios are high regardless the thermal treatment temperature, ranged from 4.23 - 25.75%.

Based on the previous data, the forwards investigations will focus on the reduction of the apparent porosity of the ceramic samples, knowing that the high specific surface associated to this porosity is the main cause for the low immobilization of chromium. Therefore common glass wastes such as window panes and cathode ray tubes were used together with the exhausted reactive mixture and the kaolin. The thermal treatment was conducted at 1000°C, considered optimal based on the previous data, in order to assure a fluid melt generated from the glass precursors, able to fill the pores in the ceramic matrix.

5.2.3 Synthesis of ceramic samples containing glass wastes

The two glass wastes used as precursors: window panes and cathode ray tubes (CRT) were grind and dried as described in the chapter 5.1.1. Together with the exhausted reactive mixtures and the kaolin they were homogenized using a Pulverisette laboratory mill. Two different ratios mixture:kaolin:glass were used: 1:1:1 and 1:1:2. The ceramic samples obtained using the last ratio after the thermal treatment presented important dimensional and shape deviations due to the high amount of liquid phase generated by the large glass quantity and therefore they are excluded from the further investigations. The compositions of the studied ceramics are summarized in the table 20.

Table 20. Ceramic samples composition (weight ratio)

Sample	Set-column	Bojidar Kaolin	Exhausted reactive mixture	Glass waste	
				Window pane	CRT
I.1G-C	I-1	1	1	1	-
I.2G-C	I-2	1	1	1	-
I.3G-C	I-3	1	1	1	-
I.4G-C	I-4	1	1	1	-
I.5G-C	I-5	1	1	1	-
I.1C-C	I-1	1	1	-	1
I.2C-C	I-2	1	1	-	1
I.3C-C	I-3	1	1	-	1
I.4C-C	I-4	1	1	-	1
I.5C-C	I-5	1	1	-	1
II.1G-C	II-1	1	1	1	-
II.2G-C	II-2	1	1	1	-
II.3G-C	II-3	1	1	1	-
II.4G-C	II-4	1	1	1	-
II.5G-C	II-5	1	1	1	-
II.7G-C	II-7	1	1	1	-
II.8G-C	II-8	1	1	1	-
II.1C-C	II-1	1	1	-	1
II.2C-C	II-2	1	1	-	1
II.3C-C	II-3	1	1	-	1
II.4C-C	II-4	1	1	-	1
II.5C-C	II-5	1	1	-	1
II.7C-C	II-7	1	1	-	1
II.8C-C	II-8	1	1	-	1
III.1G-C	III-1	1	1	1	-
III.2G-C	III-2	1	1	1	-
III.7G-C	III-7	1	1	1	-
III.8G-C	III-8	1	1	1	-
III.1C-C	III-1	1	1	-	1
III.2C-C	III-2	1	1	-	1
III.7C-C	III-7	1	1	-	1
III.8C-C	III-8	1	1	-	1

5.2.4 Properties of the ceramic samples containing glass

Considering the objective of this study – to immobilize the exhausted reactive mixtures containing chromium – the investigated properties for the obtained ceramics were the apparent porosity, the phase composition and the chemical resistance towards chemical aggression.

5.2.4.1 The apparent porosity of the obtained ceramics

The importance of this property that affect the chemical resistance of the ceramic samples was discussed in the chapter 5.2.2.2. The values of the apparent porosity for the samples obtained at 1000°C, measured using the liquid saturation method under vacuum with water as working liquid are presented in the table 21.

Table 21. Apparent porosity (P_{ap}) of the studied ceramics

Sample	P_{ap}[%]	Sample	P_{ap}[%]
I.1G-C	2.55	I.1C-C	2.20
I.2G-C	2.85	I.2C-C	2.70
I.3G-C	3.35	I.3C-C	3.15
I.4G-C	4.45	I.4C-C	4.05
I.5G-C	5.05	I.5C-C	4.65
II.1G-C	2.55	II.1C-C	2.20
II.2G-C	2.85	II.2C-C	2.70
II.3G-C	3.35	II.3C-C	3.15
II.4G-C	4.45	II.4C-C	4.05
II.5G-C	5.05	II.5C-C	4.65
II.7G-C	2.90	II.7C-C	2.55
II.8G-C	3.45	II.8C-C	3.25
III.1G-C	2.05	III.1C-C	1.98
III.2G-C	2.30	III.2C-C	2.15
III.7G-C	2.45	III.7C-C	2.35
III.8G-C	4.15	III.8C-C	3.75

The samples I.1-C - I.5-C and II.1-C - II.5-C contain the same amount and granulometry of sand and iron, differing only by the retained chromium. Since the quantity of chromium on the exhausted reactive mixtures is low compared to that of sand and iron, it's influence upon the apparent porosity is negligible, under the sensibility of the porosimeter.

The apparent porosity of all the synthesized ceramics are lower compared to those obtained without the glass wastes precursors, ranging from 1.98-5.05 %. This behavior is due to the liquid phase resulted by melting the glass wastes at 1000°C. The CRT glass, more fluid than the window panes glass wastes due to it's composition generates a lower porosity for the corresponding ceramic samples as it can be observed on the SEM images obtained using a Quanta FEG 250 microscope, presented in the figure 42 for two representative ceramic samples.

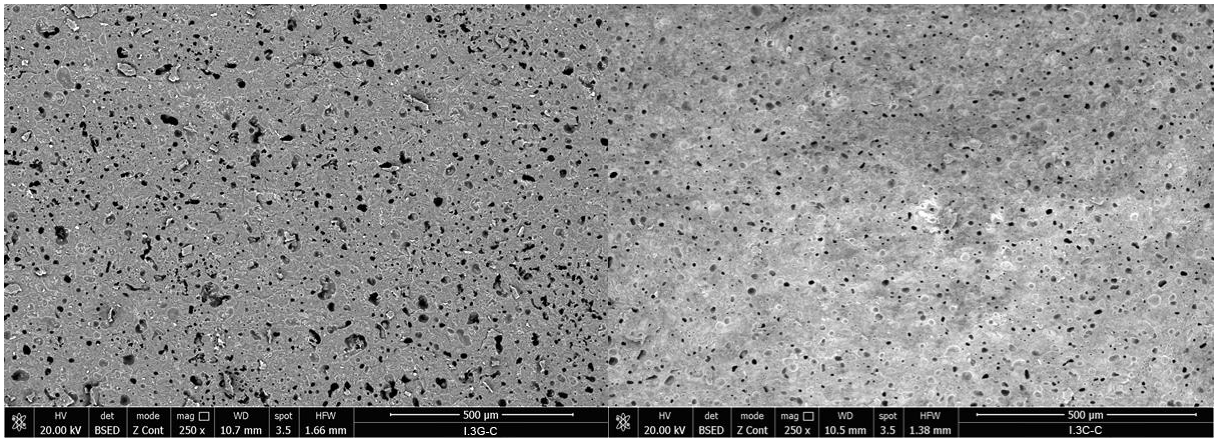

a. b.

Fig.42. The microporous structure of the samples: a - I.3G-C; b - I.3C-C.

Both samples present a microporous structure characterized by a relatively uniform distribution of the pores in the ceramic matrix with a narrow dimensional spectra, all pores having micrometric dimensions.

The influence of the sand upon the apparent porosity of the ceramic samples is presented in the figure 43.

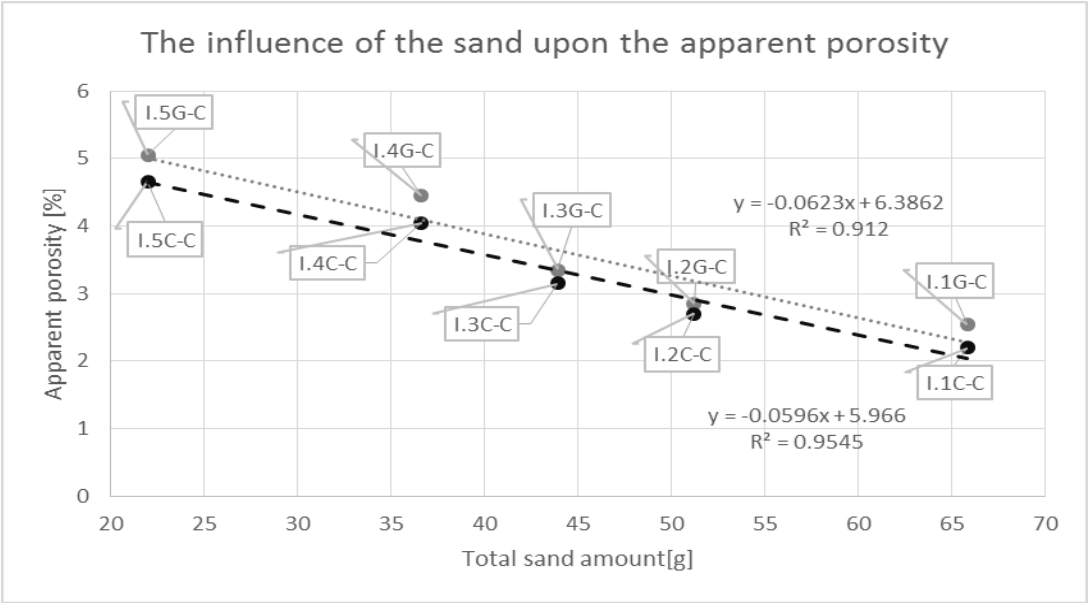

Fig.43. The influence of the sand brought by the exhausted reactive mixtures upon the apparent porosity of the ceramic samples I.1-C - I.5-C containing window panes and CRT glass wastes.

For both glass sets the apparent porosity decrease when the sand amount raise due to the replacement of a porogen material –the kaolin- by a non-porous one –the sand.

5.2.4.2 Phase composition of the studied ceramics

The phase composition of the ceramic samples was determined using a Rigaku Ultima 4 diffractometer.

The obtained results for the samples I.3G-C și I.3C-C containing window panes and CRT glass wastes respectively are presented in the figure 44.

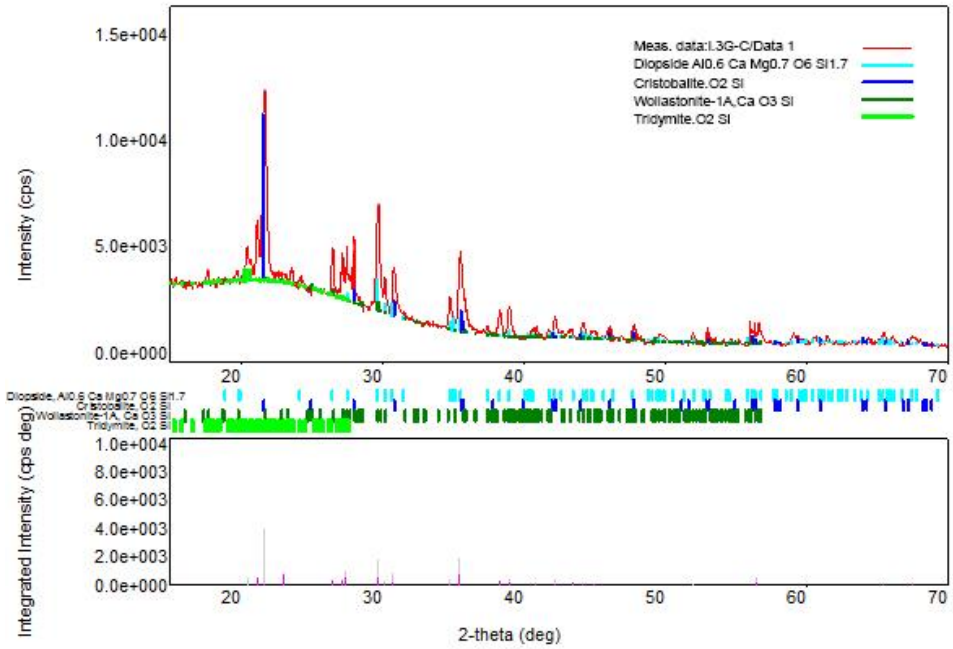

a.

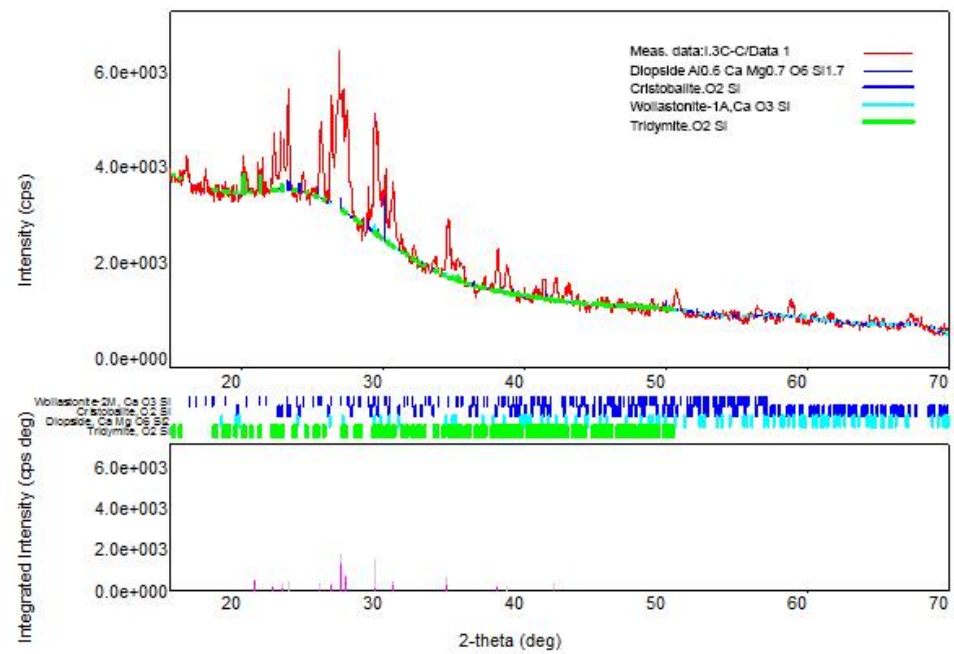

b.

Fig.44. Diffraction spectra of the samples: a - I.3G-C; b - I.3C-C.

The main crystalline phases in both samples, having different glass waste precursors, are wollastonite, tridymite, diopside and cristobalite. The presence of tridymite can be accounted for the sand that comes with the kaolin while the cristobalite is generated by the recrystallization process of the amorphous SiO_2 as it is presented by the reactions 22.

$$Al_2O_2 \cdot 2SiO_2 \cdot 2H_2O \xrightarrow{450-700°C} Al_2O_2 \cdot 2SiO_2 + 2H_2O_{(g)}$$

$$2(Al_2O_2 \cdot 2SiO_2) \xrightarrow{925-1050°C} 2Al_2O_2 \cdot 3SiO_2 + SiO_{2\,(amorf)} \qquad (22)$$

$$3(Al_2O_2 \cdot 3SiO_2) \xrightarrow{\geq 1050°C} 2(3Al_2O_2 \cdot 2SiO_2) + 5SiO_2$$

$$SiO_{2(amorf)} \xrightarrow{\geq 1200°C} SiO_{2(cristobalit)}$$

The diopside is generated by the reaction of the amorphous SiO_2 resulted from the thermal decomposition of the kaolinite with CaO and MgO from the glass melt.

The presence of the free SiO_2 in the ceramic matrix is confirmed by the SEM images and the EDAX analysis made punctually on the cristobalite crystals as it is presented in the figures 45 and 46.

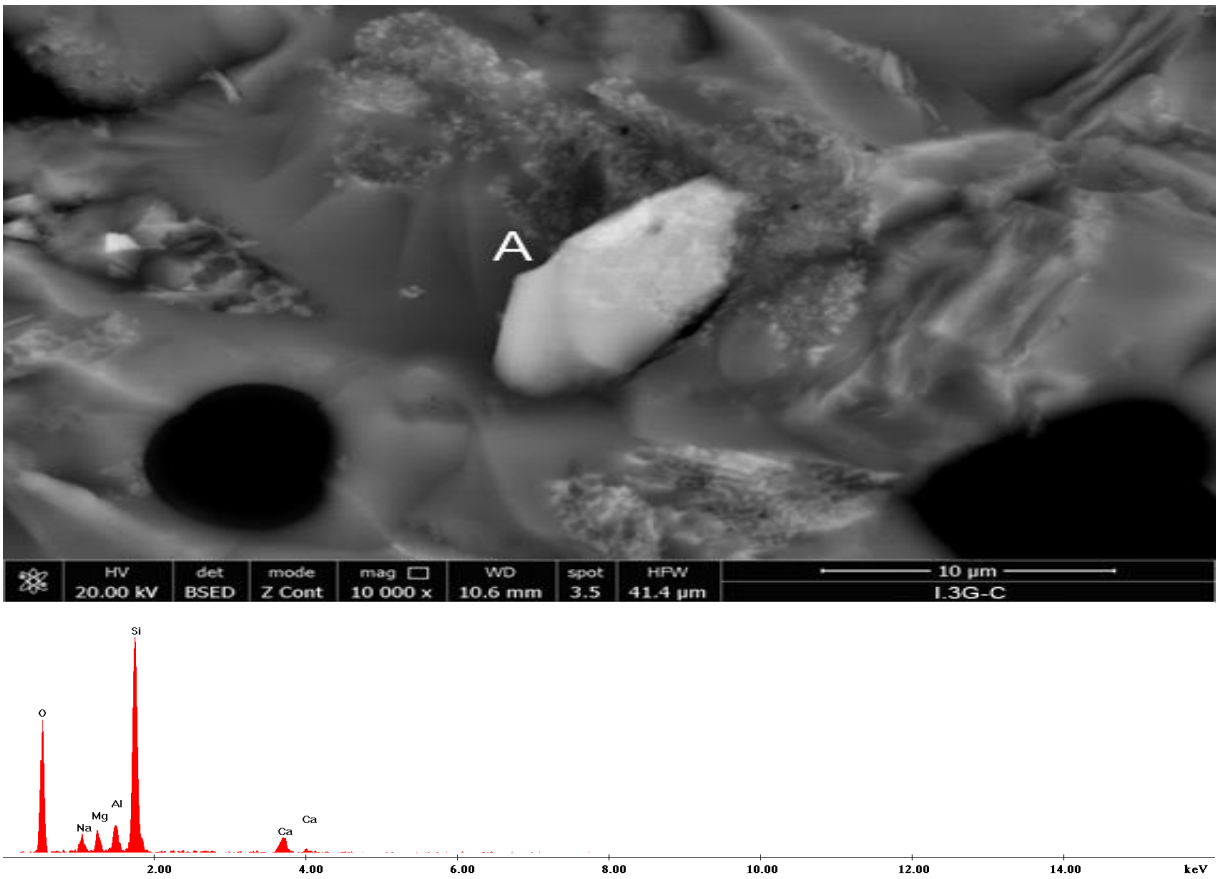

EDAX ZAF Quantification (Standardless)
Element Normalized

Elem	Wt %	At %
O K	53.62	66.33
NaK	4.51	3.88
MgK	4.01	3.27
AlK	4.55	3.34
SiK	31.95	22.51
CaK	1.36	0.67
Total	100.00	100.00

Fig. 45 SEM image and EDAX analysis of the crystalline phase (A) in the sample I.3G-C

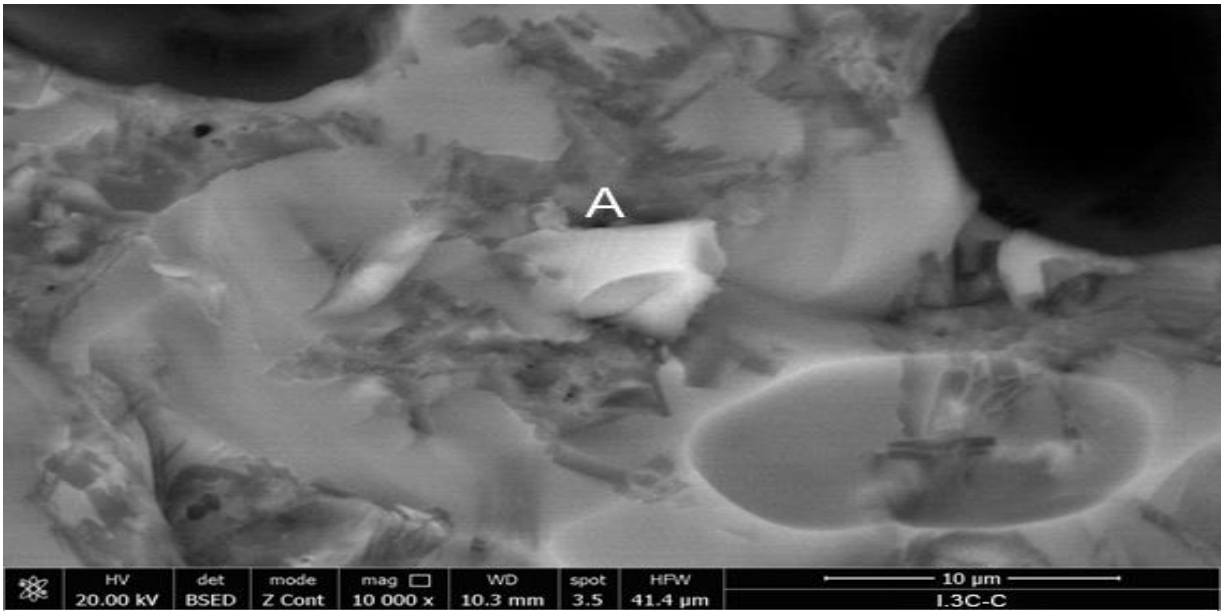

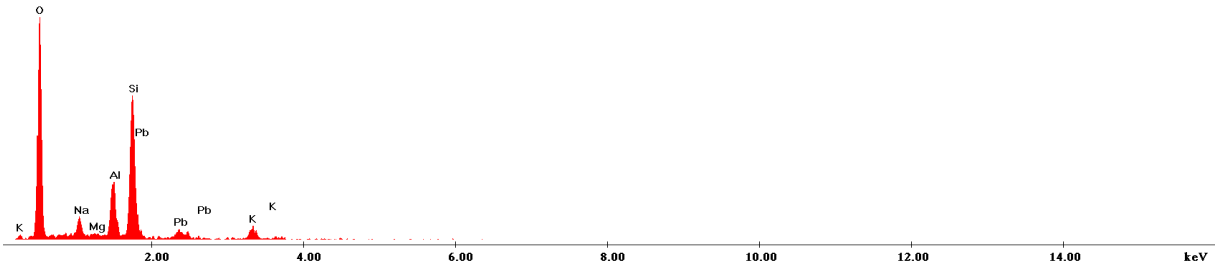

EDAX ZAF Quantification (Standardless)
Element Normalized

Elem	Wt %	At %
O K	57.72	72.04
NaK	4.63	4.02
MgK	0.55	0.46
AlK	8.26	6.11
SiK	22.44	15.95
PbM	4.47	0.43
K K	1.92	0.98
Total	100.00	100.00

Fig. 46 SEM image and EDAX analysis of the crystalline phase (A) in the sample I.3C-C

As the SEM images show, the cristobalite crystals are under 10 µm and are incorporated in the glass phase.

5.2.4.3. Chemical stability of the ceramic samples

The values for the chemical stability, measured by the samples' dissolution rate as it was presented in the chapter 5.1.2.3 are summarized in the table 22

Table 22. Dissolution rate values [μg/h] for the studied ceramic samples

Sample	Ceramic samples having windows panes glass wastes as precursor			Sample	Ceramic samples having CRT glass wastes as precursor		
	pH				pH		
	pH=5.5	pH=7	pH=8.5		pH=5.5	pH=7	pH=8.5
I.1G-C	0.144	0.138	0.425	I.1C-C	0.132	0.127	0.311
I.2G-C	0.151	0.148	0.468	I.2C-C	0.14	0.133	0.382
I.3G-C	0.162	0.158	0.521	I.3C-C	0.155	0.153	0.475
I.4G-C	0.172	0.172	0.665	I.4C-C	0.165	0.159	0.589
I.5G-C	0.189	0.185	0.778	I.5C-C	0.177	0.175	0.688
II.1G-C	0.144	0.138	0.425	II.1C-C	0.132	0.127	0.311
II.2G-C	0.151	0.148	0.468	II.2C-C	0.14	0.133	0.382
II.3G-C	0.162	0.158	0.521	II.3C-C	0.155	0.153	0.475
II.4G-C	0.172	0.172	0.665	II.4C-C	0.165	0.159	0.589
II.5G-C	0.189	0.185	0.778	II.5C-C	0.177	0.175	0.688
II.7G-C	0.144	0.141	0.395	II.7C-C	0.138	0.14	0.378
II.8G-C	0.169	0.164	0.543	II.8C-C	0.161	0.158	0.539
III.1G-C	0.118	0.121	0.311	III.1C-C	0.119	0.117	0.255
III.2G-C	0.125	0.122	0.324	III.2C-C	0.122	0.122	0.315
III.7G-C	0.133	0.132	0.375	III.7C-C	0.131	0.132	0.369
III.8G-C	0.161	0.158	0.615	III.8C-C	0.149	0.151	0.599

The influence of the apparent porosity upon the samples' chemical stability is presented in the figure 47 for the samples I.1G-C - I.5G-C and I.1C-C - I.5C-C.

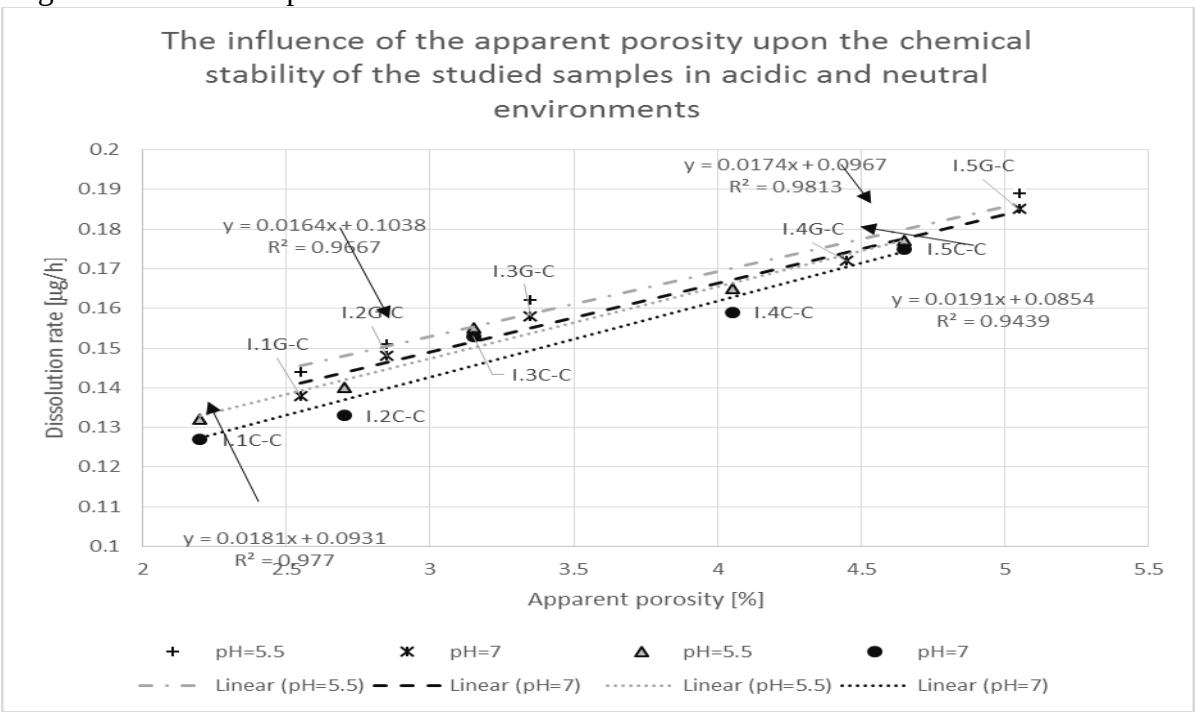

a.

b. 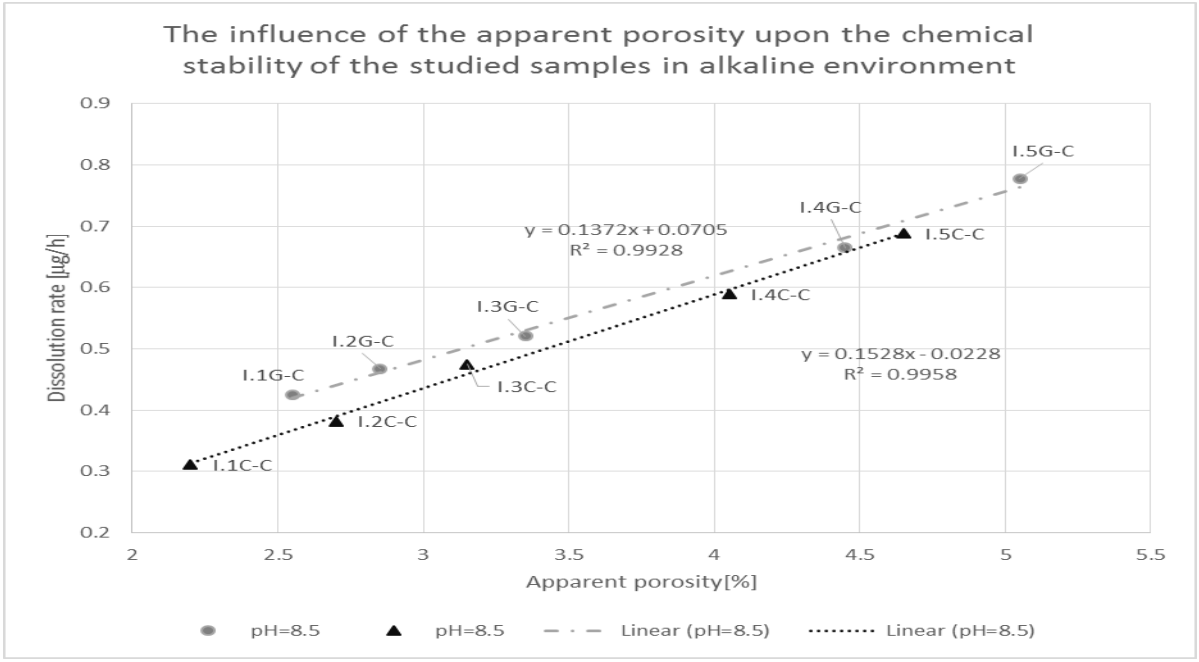

Fig.47. Apparent porosity influence upon the chemical stability of the ceramic samples containing window panes and CRT glass wastes measured at: a - pH = 5.5 and pH = 7.0; b - pH = 8.5.

The increasing of the apparent porosity leads to a rise of the dissolution rate values and a reduction of the chemical stability for all the investigated ceramic samples due to the higher specific surface exposed to the chemical aggression. As it can be observed in the figure 47, all the dependences are quasilinear, the correlation coefficient R^2 ranging from 0.9439 to 0.9958.

5.2.4.4. Chromium and iron ions immobilization in the ceramic matrices

The chromium and iron immobilization capacity of the studied ceramics were measured according to the American Extraction Procedure Toxicity Test as it was presented in the chapter 5.1.2.4.

The lixiviation values for chromium, calculated as percentage of chromium leached from the total chromium introduced by the exhausted reactive mixtures are presented in the table 23 and illustrated by the figure 48.

Table 23. Chromium ions losses from the investigated samples

Sample	Chromium ions leached [%]								
	7 days			14 days			28 days		
	pH=5.5	pH=7	pH=8.5	pH=5.5	pH=7	pH=8.5	pH=5.5	pH=7	pH=8.5
I.1G-C	0.0000	0.0000	0.0122	0.0281	0.0275	0.0711	0.0305	0.0290	0.0984
I.2G-C	0.0000	0.0000	0.0425	0.0335	0.0332	0.1018	0.0356	0.0348	0.1314
I.3G-C	0.0000	0.0000	0.0918	0.0466	0.0461	0.1414	0.0496	0.0468	0.1710
I.4G-C	0.0000	0.0000	0.1105	0.0511	0.0499	0.1782	0.0532	0.0525	0.1997
I.5G-C	0.0000	0.0000	0.1379	0.0589	0.0580	0.1922	0.0597	0.0591	0.2375
I.1C-C	0.0000	0.0000	0.0122	0.0235	0.0221	0.0681	0.0246	0.0242	0.0781
I.2C-C	0.0000	0.0000	0.0418	0.0279	0.0271	0.0685	0.0326	0.0332	0.0896
I.3C-C	0.0000	0.0000	0.0836	0.0389	0.0391	0.1104	0.0421	0.0421	0.1599

I.4C-C	0.0000	0.0000	0.1075	0.0475	0.0471	0.1655	0.0491	0.0489	0.1898
I.5C-C	0.0000	0.0000	0.1355	0.0554	0.0555	0.1819	0.0568	0.0566	0.2125
II.1G-C	0.0000	0.0000	0.0377	0.0334	0.0332	0.0954	0.0338	0.0338	0.1155
II.2G-C	0.0000	0.0000	0.0628	0.0399	0.0396	0.1132	0.0412	0.0411	0.1622
II.3G-C	0.0000	0.0000	0.1145	0.0549	0.0535	0.1719	0.0558	0.0560	0.1895
II.4G-C	0.0000	0.0000	0.1522	0.0628	0.0615	0.2121	0.0688	0.0681	0.2752
II.5G-C	0.0000	0.0000	0.1871	0.0751	0.0748	0.2753	0.0801	0.0795	0.3514
II.7G-C	0.0000	0.0000	0.1125	0.0524	0.0519	0.1775	0.0595	0.0059	0.1929
II.8G-C	0.0000	0.0000	0.0622	0.0406	0.0398	0.1088	0.0482	0.0482	0.1565
II.1C-C	0.0000	0.0000	0.0348	0.0329	0.0325	0.0908	0.0338	0.0336	0.1132
II.2C-C	0.0000	0.0000	0.0611	0.0383	0.0383	0.1115	0.0402	0.0401	0.1498
II.3C-C	0.0000	0.0000	0.1120	0.0522	0.0517	0.1665	0.0545	0.0544	0.1845
II.4C-C	0.0000	0.0000	0.1489	0.0608	0.0597	0.2050	0.0645	0.0648	0.2748
II.5C-C	0.0000	0.0000	0.1858	0.0724	0.0735	0.2711	0.0795	0.0788	0.3511
II.7C-C	0.0000	0.0000	0.1108	0.0521	0.0521	0.1698	0.0588	0.0585	0.1905
II.8C-C	0.0000	0.0000	0.0595	0.0381	0.0379	0.1108	0.0456	0.0451	0.1498
III.1G-C	0.0000	0.0000	0.0000	0.0000	0.0000	0.0000	0.0000	0.0000	0.0000
III.2G-C	0.0000	0.0000	0.0343	0.0145	0.0138	0.0555	0.0151	0.0150	0.0714
III.7G-C	0.0000	0.0000	0.0385	0.0188	0.0181	0.0612	0.0215	0.0211	0.1121
III.8G-C	0.0000	0.0000	0.0509	0.0275	0.0268	0.0811	0.0281	0.0288	0.1548
III.1C-C	0.0000	0.0000	0.0000	0.0000	0.0000	0.0000	0.0000	0.0000	0.0000
III.2C-C	0.0000	0.0000	0.0327	0.0132	0.0135	0.0518	0.0138	0.0139	0.0688
III.7C-C	0.0000	0.0000	0.0355	0.0175	0.0168	0.0595	0.0211	0.2080	0.1118
III.8C-C	0.0000	0.0000	0.0489	0.0255	0.0254	0.0788	0.0272	0.0272	0.1535

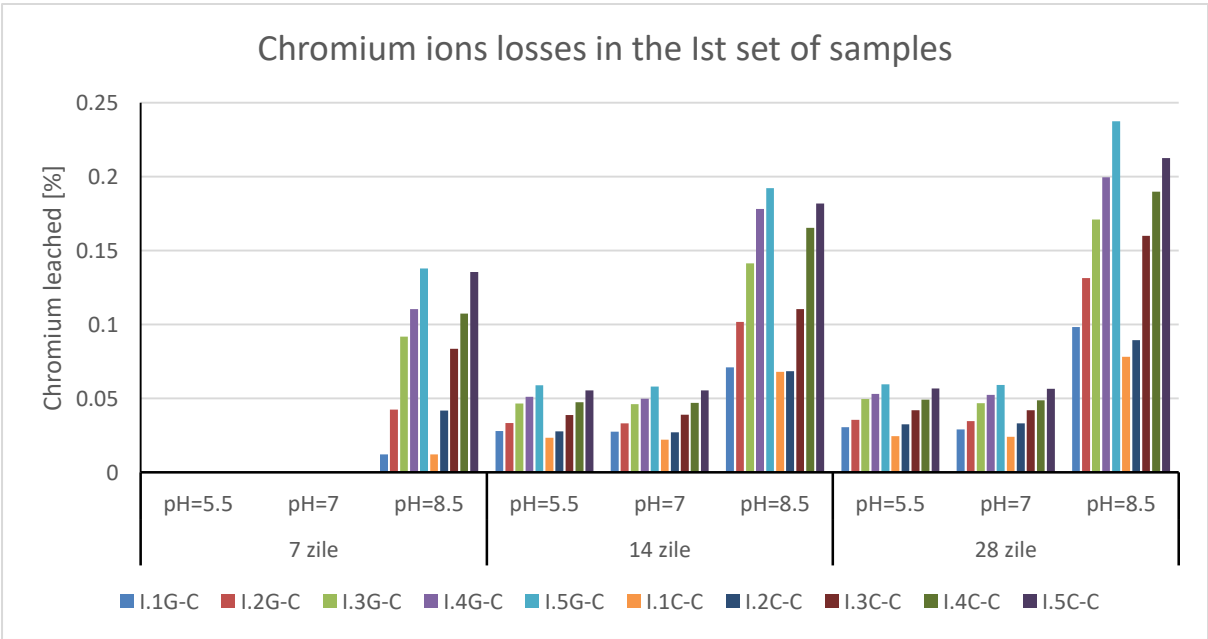

a.

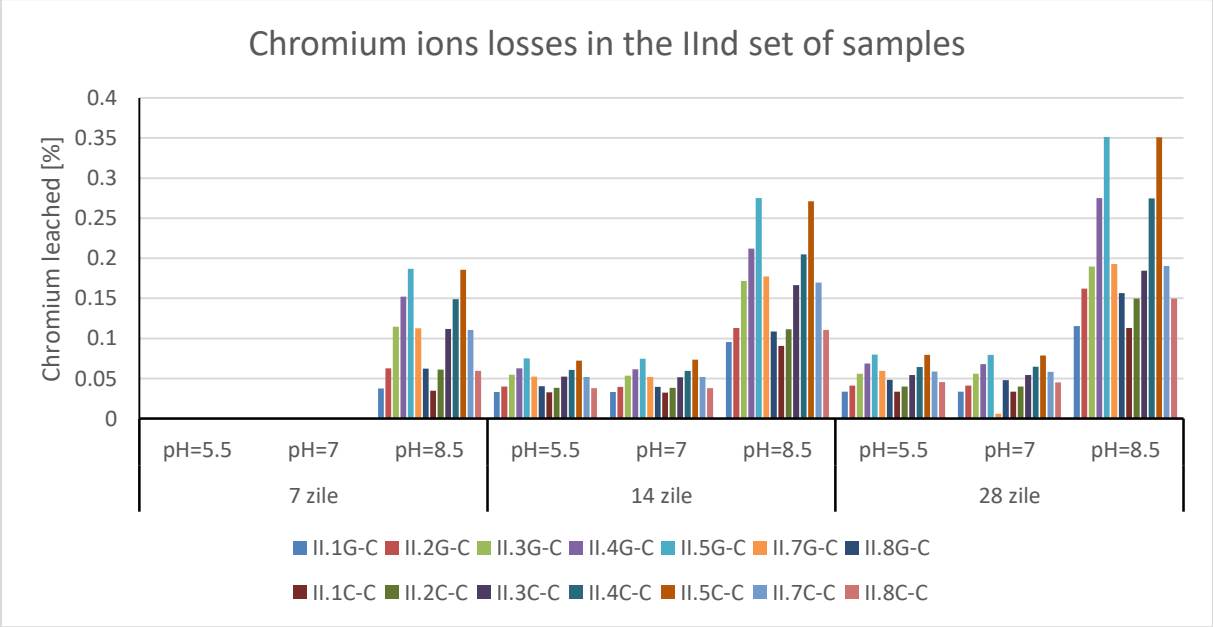

b.

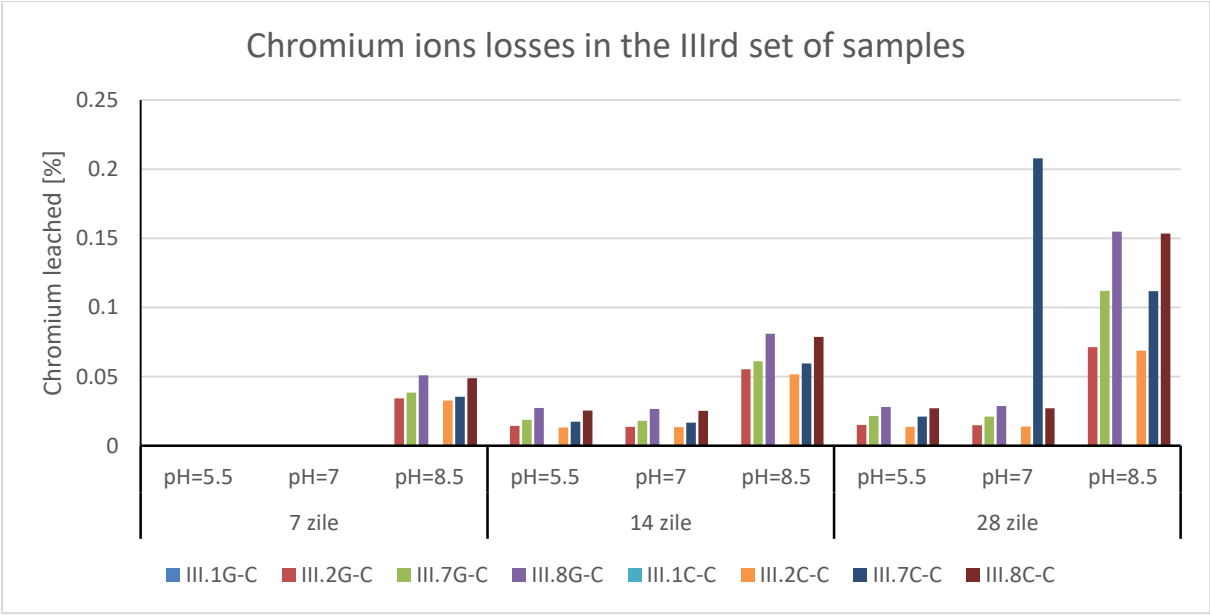

c.

Fig.48. Cromium ions losses from the ceramic containing exhausted reactive mixtures from: a - Ist set of columns; b - IInd set of columns; c - IIIrd set of columns.

The chromium ions lixiviation values from all the investigated ceramic samples regardless the environment's pH and the considered time are very low, ranging between 0-0.3514 % of the total chromium brought by the exhausted reactive mixtures.

The ceramics obtained based on the exhausted reactive mixtures from the first set of columns leads to samples having no discernable losses of chromium after 7 days, for acidic and neutral aggressive attacks. All the ceramic materials show low chromium losses in the alkaline medium, which increase by increasing the amount of chromium brought by the exhausted reactive mixture. The samples' apparent porosity play a key role in the chromium immobilization by increasing the specific surface exposed to the chemical attack. They were recorded low chromium losses for all samples after 14 and 28 days in the three used aggressive environments.

A similar behavior can be observed for the ceramic samples based on the second set of columns exhausted reactive mixtures. No discernable chromium ions losses were measured after 7 days for acidic and neutral aggressive attacks. Comparing to the previous set of samples, chromium losses are higher in the second set due to a higher amount of chromium introduced with the exhausted reactive mixtures. After 14 and 28 days, the losses in acidic and neutral mediums are comparable and both are lower than those recorded in alkaline environment.

The samples synthesized using exhausted reactive mixtures from the third set of columns don't present any discernable chromium losses after 7 days in acidic and neutral environments. The sample III.1-C has no chromium adsorbed in the column and therefore were no chromium losses. After 14 and 28 days, all the studied samples have chromium ions losses in the three considered mediums, higher in the alkaline environment comparing with acidic and neutral ones.

All the samples containing CRT glass wastes as precursors shows lower chromium losses due to lower porosity of the ceramics caused by the higher fluidity of these glass melt compared to the one generated by the windows panes wastes.

The described behavior for the chromium losses in all the ceramic samples suggests that the chromium ions are located in the glass phase, more sensible to the alkaline aggression comparing to the ceramic phases.

The lixiviation values for iron ions, calculated as percentage of iron leached from the total iron introduced by the exhausted reactive mixtures are presented in the table 24 and illustrated by the figure 49.

Table 24. Iron ions losses from the investigated samples

Sample	**Iron ions leached [%]**								
	7 days						**7 days**		
	pH=5.5	**pH=7**	**pH=8.5**	**pH=5.5**	**pH=7**	**pH=8.5**	**pH=5.5**	**pH=7**	**pH=8.5**
I.1G-C	0.0000	0.0000	0.0000	0.0320	0.0316	0.0864	0.0585	0.0581	0.1075
I.2G-C	0.0110	0.0000	0.0333	0.0391	0.0375	0.1055	0.0712	0.0708	0.1345
I.3G-C	0.0280	0.0220	0.0865	0.0478	0.0471	0.1465	0.0825	0.0823	0.1855
I.4G-C	0.0350	0.0348	0.1043	0.0684	0.0674	0.1828	0.1043	0.1045	0.2033
I.5G-C	0.0420	0.0405	0.1227	0.0828	0.0809	0.2075	0.1366	0.1358	0.2425
I.1C-C	0.0000	0.0000	0.0000	0.0298	0.0295	0.0771	0.0555	0.0538	0.1015
I.2C-C	0.0000	0.0000	0.0325	0.0385	0.0388	0.0985	0.0710	0.0701	0.1317
I.3C-C	0.0212	0.0198	0.0848	0.0472	0.0468	0.1152	0.0899	0.0895	0.1782
I.4C-C	0.0295	0.0307	0.1025	0.0550	0.0543	0.1543	0.1035	0.1032	0.2025
I.5C-C	0.0387	0.0379	0.1180	0.0678	0.0675	0.1848	0.1318	0.1315	0.2582
II.1G-C	0.0000	0.0000	0.0000	0.0320	0.0316	0.0864	0.0585	0.0581	0.1075
II.2G-C	0.0110	0.0000	0.0333	0.0391	0.0375	0.1055	0.0712	0.0708	0.1345
II.3G-C	0.0280	0.0220	0.0865	0.0478	0.0471	0.1465	0.0825	0.0823	0.1855
II.4G-C	0.0350	0.0348	0.1043	0.0684	0.0674	0.1828	0.1043	0.1045	0.2033
II.5G-C	0.0420	0.0405	0.1227	0.0828	0.0809	0.2075	0.1366	0.1358	0.2425
II.7G-C	0.0250	0.0220	0.0918	0.0498	0.0502	0.1215	0.0702	0.0699	0.1833
II.8G-C	0.0289	0.0278	0.1045	0.0512	0.0508	0.1209	0.0719	0.0716	0.1925
II.1C-C	0.0000	0.0000	0.0000	0.0298	0.0295	0.0771	0.0555	0.0538	0.1015

II.2C-C	0.0000	0.0000	0.0325	0.0385	0.0388	0.0985	0.0710	0.0701	0.1317
II.3C-C	0.0212	0.0198	0.0848	0.0472	0.0468	0.1152	0.0899	0.0895	0.1782
II.4C-C	0.0295	0.0307	0.1025	0.0550	0.0543	0.1543	0.1035	0.1032	0.2025
II.5C-C	0.0387	0.0379	0.1180	0.0678	0.0675	0.1848	0.1318	0.1315	0.2582
II.7C-C	0.0224	0.0220	0.0885	0.0498	0.0501	0.1186	0.0685	0.0688	0.1792
II.8C-C	0.0287	0.0285	0.0955	0.0507	0.0505	0.1195	0.0695	0.0692	0.1805
III.1G-C	0.0110	0.0102	0.0173	0.0242	0.0238	0.0326	0.0344	0.0351	0.0553
III.2G-C	0.0149	0.0150	0.0186	0.0286	0.0281	0.0685	0.0495	0.0489	0.0899
III.7G-C	0.0324	0.0319	0.0618	0.0354	0.0351	0.0915	0.0512	0.0512	0.1333
III.8G-C	0.0332	0.0327	0.0815	0.0521	0.0495	0.1025	0.0595	0.0591	0.1489
III.1C-C	0.0109	0.0105	0.0175	0.0245	0.0241	0.0318	0.0337	0.0332	0.0549
III.2C-C	0.0148	0.0152	0.0188	0.0288	0.0283	0.0677	0.0482	0.0478	0.0885
III.7C-C	0.0322	0.0320	0.0621	0.0358	0.0342	0.0928	0.0505	0.0502	0.1325
III.8C-C	0.0335	0.0331	0.0822	0.0401	0.0398	0.1137	0.0538	0.0532	0.1477

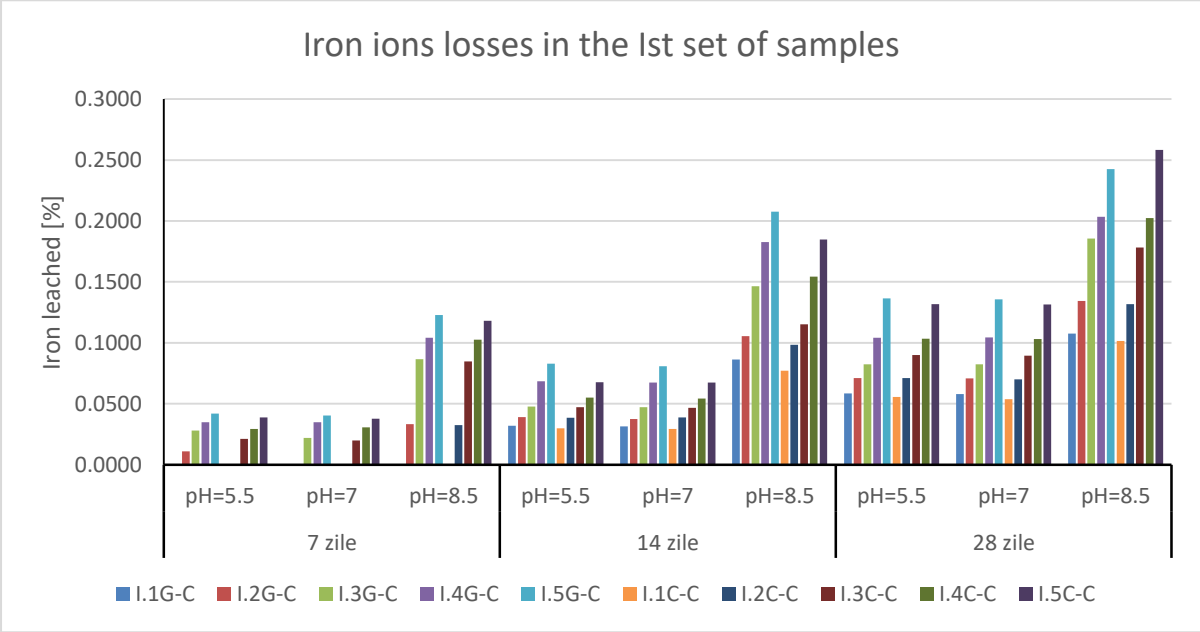

a.

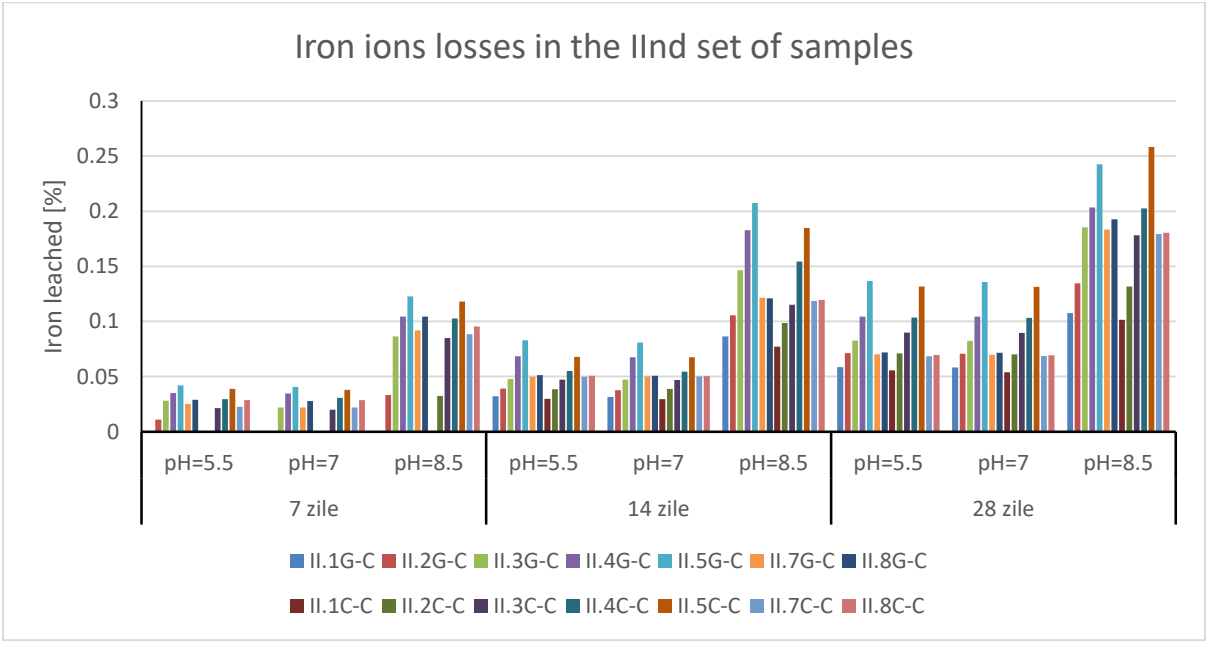

b.

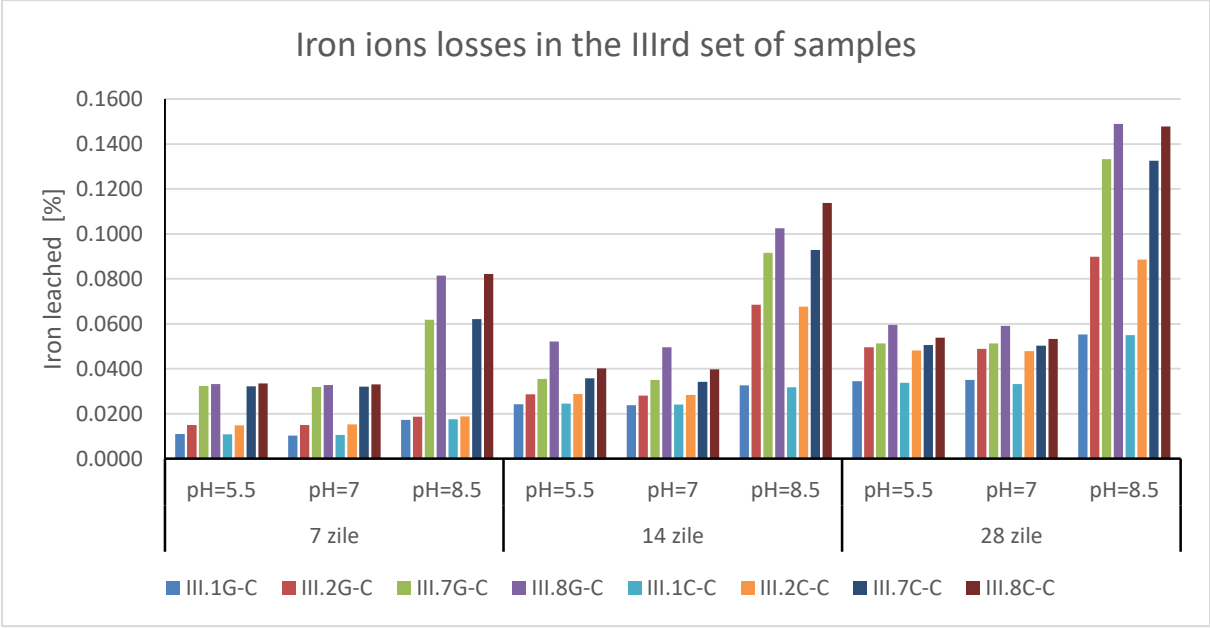

c.

Fig.49. Iron ions losses from the ceramic containing exhausted reactive mixtures from: a - Ist set of columns; b - IInd set of columns; c - IIIrd set of columns.

The iron ions losses from all the investigated ceramic samples regardless the environment's pH and the considered time are very low, ranging between 0-0.2582 % of the total iron brought by the exhausted reactive mixtures.

The samples I.1-C - I.5-C and II.1-C - II.5-C contain the same amount and granulometry of iron, differing only by the retained chromium and therefore present a similar behavior regarding the iron leached by the three considered aggressive environments. Only the sample I.1G realize a perfect immobilization of the iron ions after 7 days in acidic and neutral mediums. Increasing the iron content and simultaneously decreasing the sand amount in the exhausted reactive mixtures leads

to a lower iron immobilization in the ceramic matrices. The iron ions losses increase after 14 and 28 days, being higher in acidic and neutral aggressive environments for all the studied samples.

The decrease of the granulometry of the iron particles in the exhausted reactive mixture from the 3rd set of columns generates higher iron ions losses in the three aggressive environments even after 7 days comparing to the samples containing coarse iron particles. These samples show a similar behavior as it was presented for the first sets of ceramics, having higher losses in the acidic and neutral environments compared to the losses recorded in the alkaline one.

The described behavior for the iron losses in all the ceramic samples suggests that the iron ions are located prevalently in the ceramic matrix, and therefore being more sensible at the acidic and neutral aggression. The increase of the iron particles fineness leads to an increase of the specific surface exposed to the chemical attack and therefore a higher iron lixiviation.

5.2.5 Conclusions

- The aim of this study was to immobilize the chromium and iron ions from the exhausted reactive mixtures in ceramic matrices together with Bojidar kaolin.
- Three different weight ratios exhausted reactive mixture-kaolin were tested: 2:1, 1:1 and 1:2. First set of samples generates after the heat treatment fragile and fractured ceramics, unfit for further investigations. The last two groups of samples had high apparent porosities, ranged between 18.75-50.75% that lead to massive chromium losses, up to 25.75%. Those lixiviation values are too high to validate the proposed method as an alternative for chromium immobilization.
- The next experiments were focused on the porosity reduction in the ceramic samples, knowing that this is responsible for the chromium losses. Therefore windows panes and cathode ray tubes glass wastes were used together with the exhausted reactive mixtures and the kaolin. At the optimal heat treatment temperature, considered based on the previous tests to be 1000°C, the two glass wastes generate liquid phase by melting, that is able to fill the open pores in the ceramic matrix and therefore to reduce the chromium losses.
- The apparent porosity for the ceramics containing glass wastes range between 2.05-5.05%, ten times lower than those based only on exhausted reactive mixture and kaolin, reflecting therefore the positive effect of using the glass wastes.
- The main crystalline phases the studied ceramics having different glass waste precursors, are wollastonite, tridymite, diopside and cristobalite.
- The chemical stability of the glass samples was established by measuring the dissolution rate after 28 days in mediums having different pH. The low values recorded confirm the very good stability conferred by the glass matrix. All the ceramic samples have higher chemical stability towards acidic and neutral aggression measured by dissolution rates of 0.013-0.059 μg/h than towards alkaline aggression where the mass losses range between 0.143-0.492 μg/h. That behavior support the conclusion that the glass phase is mainly affected by the chemical aggression compared to the more stable ceramic phases.
- The chromium ions leached in the three aggressive environments after 7, 14 and 28 days according to the American Extraction Procedure Toxicity Test were low, ranging between 0-0.3514 % of the total chromium brought by the exhausted reactive mixtures.

- The behavior for the chromium losses in all the ceramic samples suggests that the chromium ions are located in the glass phase, more sensible to the alkaline aggression comparing to the ceramic phases.
- The amount of iron ions leached from all the investigated ceramic samples is very low, ranging between 0-0.2582% of the total iron brought by the exhausted reactive mixtures.
- The behavior for the iron losses in all the ceramic samples suggests that the iron ions are located prevalently in the ceramic matrix, and therefore are more sensible at the acidic and neutral aggression. The increase of the iron particles fineness leads to an increase of the specific surface exposed to the chemical attack and therefore a higher iron lixiviation.
- The obtained results confirm the viability of the suggested solution for immobilizing chromium contained in the exhausted reactive mixtures together with common glass wasted and kaolin as ceramics having very high chemical stability with multiple economic advantages.

Objective 6. Dissemination of the obtained results
Activities: Analysis and interpretation of experimental data. Writing of scientific articles

The experimental data was analyzed, interpreted and disseminated, as following:

M. Gheju, I. Balcu, C. Vancea, An investigation of Cr(VI) removal with metallic iron in the co-presence of sand and/or MnO_2, Journal of Environmental Management, 170, 2016, 145-151.

M. Gheju, I. Balcu, G. Mosoarca, Removal of Cr(VI) from aqueous solutions by adsorption on MnO_2, Journal of Hazardous Materials, 310, 2016, 270-277.

M. Gheju, I. Balcu, Characteristics of hexavalent chromium removal in H_2O-Fe(0) system, Proceedings of the 11th Conference on Sustainable Development of Energy, Water and Environment Systems, p. 196.1-196.16, 4-9 September 2016, Lisbon, ISSN 1847-7178.

M. Gheju, I. Balcu, Impact of anionic amendments on green remediation of Cr(VI) pollution, Proceedings of the 11th Conference on Sustainable Development of Energy, Water and Environment Systems, p. 198.1-198.17, 4-9 September 2016, Lisbon, ISSN 1847-7178.

M. Gheju, Treatment of water by means of metallic iron. A lost and recovered technology. „Quality for results" round table organized by Aquatim Company and The General Association of the Engineers in Romania, within the frame of the 16th "Quality Week", 9 November, Timișoara, 2016.

Objective 7. Project self-evaluation
Activities: Analysis of the achievement degree of the 2016 stage objectives

The degree of achievement of objectives for the 2016 stage was analyzed. It was concluded that all the proposed objectives were fully achieved, so there was no need to make any corrective action.

References

APHA, AWWA, WEF, 1995. Standard methods for the examination of water and wastewater, 19th edition. United Book Press, Inc., Baltimore.

Bafghi M.S., Zakeri A., Ghasemi Z., Adeli M., Reductive dissolution of manganese ore in sulfuric acid in the presence of iron metal, Hydrometallurgy, 90, 2008207-212.

Flury B., Eggenberger U., Mader U., First results of operating and monitoring an innovative design of a permeable reactive barrier for the remediaton of chromate contaminated groundwater, J. Appl. Geochem., 24, 2009, 687-697.

Gheju M., Iovi A., Kinetics of hexavalent chromium reduction by scrap iron, J. Hazard. Mater., B135 (1-3), 2006, 66-73.

Gheju M., 2011. Hexavalent chromium reduction with zero-valent iron (ZVI) in aquatic systems, Water Air Soil Pollut., 222(1-4), 103-148.

Goleanu A., Lazău I., Apetri C., Lazău R.I., Corelatii între caracteristicile fizico-mineralogice şi proprietătile tehnologice ale unor caolinuri utilizate în industria portelanului, Revista Română de Materiale, 34 (3), 2004, 163.

ISO 719-1985, Glass - Hydrolytic resistance of glass grains at 98 degrees C - Method of test and classification.

Lazău I., Vancea C., New vitreous Matrix for the Chromium Wastes immobilization, Cent. Eur. J. Chem., 12(7), 2014, 763-768.

Noubactep C., Btatkeu K.B.D., Tchatchueng J.B., Impact of MnO_2 on the efficiency of metallic iron for the removal of dissolved Cr^{VI}, Cu^{II}, Mo^{VI}, SbV, U^{VI} and Zn^{II}, Chem. Eng. J. 178, 201178-84.

Noubactep C., Caré S., Btatkeu K.B.D., Peguy N.N.C., Enhancing the sustainability of household Fe^0/sand filters by using bimetallics and MnO_2, Clean - Soil Air Water, 40(1), 2012, 100-109.

Noubactep C., Metallic iron for environmental remediation: a review of reviews, Water Res. 85, 2015, 114-123.

Postma D., Appelo C.A.J.,. Reduction of Mn-oxides by ferrous iron in a flow system: column experiment and reactive transport modeling, Geochim. Cosmochim. Acta 64(7), 2000, 1237-1247.

SR ISO 6333/1996, Water quality. Determination of manganese. Formaldoxime spectrometric method.

US EPA, Extraction procedure toxicity test, in: Stabilization/Solidification of CERCLA and RCRAWastes. US EPA625/6-89/022, US EPA, Cincinnati, Ohio, 1986.

Wilkin R.T., Su C., Ford R.G., Paul C.J., Chromium-removal processes during groundwater remediation by a zerovalent iron permeable reactive barrier, Environ. Sci. Technol., 39(12), 2005, 4599-4605.